$5

QEX

July/August 2012
www.arrl.org

A Forum for Communications Experimenters

Issue No. 273

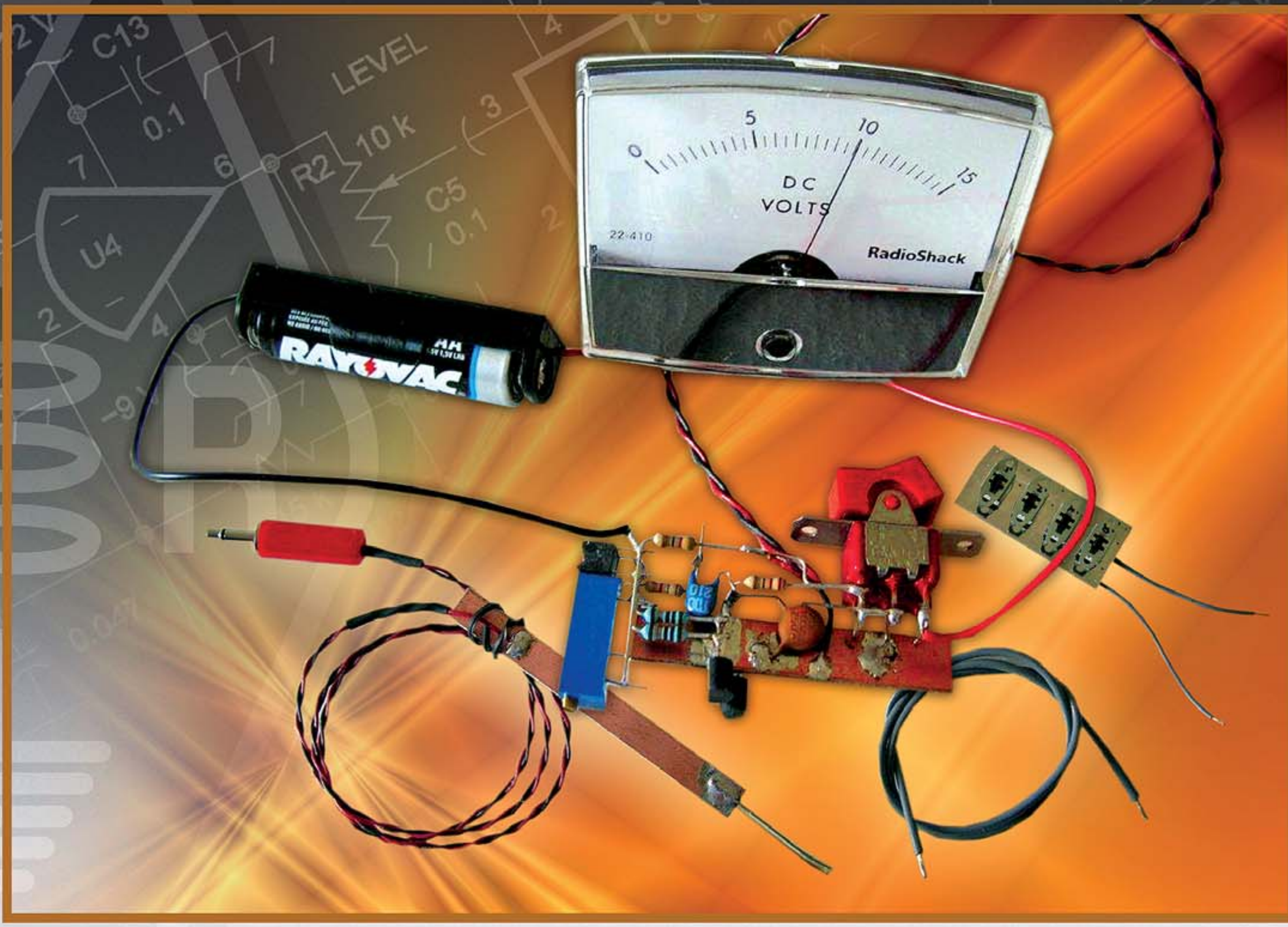

N2PON describes the construction of A Linear Scale Milliohm Meter. Along with construction details, he offers a number of testing and troubleshooting tips for using the meter.

ARRL The national association for AMATEUR RADIO™
225 Main Street
Newington, CT USA 06111-1494

KENWOOD

Rising to the Occasion

Kenwood's new TS-990S raises the bar on the HF performance and DX operating ease in more ways than one. The dual display and dual watch function will give you the edge in DX contesting.

TS-990S

Dual TFT Display & Dual Receiver
HF / 50 MHz Transceiver

- Frequency Range: HF+50MHz
- Output Power: 5W - 200W
- Mode: SSB, CW, FSK, PSK, FM, AM
- Built-in Switching Power Supply
- Built-in Antenna Tuner
- COM port, USB A/B port & LAN port

http://www.kenwoodusa.com

ADS#21712

QEX (ISSN: 0886-8093) is published bimonthly in January, March, May, July, September, and November by the American Radio Relay League, 225 Main Street, Newington, CT 06111-1494. Periodicals postage paid at Hartford, CT and at additional mailing offices.

POSTMASTER: Send address changes to: QEX, 225 Main St, Newington, CT 06111-1494
Issue No 273

Harold Kramer, WJ1B
Publisher

Larry Wolfgang, WR1B
Editor

Lori Weinberg, KB1EIB
Assistant Editor

Zack Lau, W1VT
Ray Mack, W5IFS
Contributing Editors

Production Department

Steve Ford, WB8IMY
Publications Manager

Michelle Bloom, WB1ENT
Production Supervisor

Sue Fagan, KB1OKW
Graphic Design Supervisor

David Pingree, N1NAS
Senior Technical Illustrator

Carol Michaud, KB1QAW
Technical Illustrator

Advertising Information Contact:

Janet L. Rocco, W1JLR
Business Services
860-594-0203 – Direct
800-243-7768 – ARRL
860-594-4285 – Fax

Circulation Department

Cathy Stepina, *QEX Circulation*

Offices

225 Main St, Newington, CT 06111-1494 USA
Telephone: 860-594-0200
Fax: 860-594-0259 (24 hour direct line)
e-mail: **qex@arrl.org**

Subscription rate for 6 issues:

In the US: ARRL Member $24, nonmember $36;

US by First Class Mail: ARRL member $37, nonmember $49;

International and Canada by Airmail: ARRL member $31, nonmember $43;

Members are asked to include their membership control number or a label from their QST when applying.

In order to ensure prompt delivery, we ask that you periodically check the address information on your mailing label. If you find any inaccuracies, please contact the Circulation Department immediately. Thank you for your assistance.

About the Cover

Steve Whiteside, N2PON, describes the design and construction of A Linear Scale Milliohm Meter. This meter is temperature stabilized over normal operating temperatures, and includes compensation for battery voltage variations with age. Steve describes a number of practical applications for a milliohm meter when troubleshooting various electrical and electronics equipment.

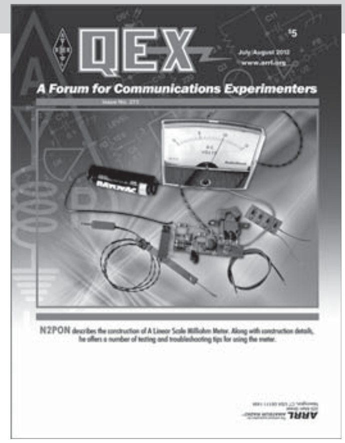

In This Issue

Features

Index of Advertisers

The American Radio Relay League

The American Radio Relay League, Inc, is a noncommercial association of radio amateurs, organized for the promotion of interest in Amateur Radio communication and experimentation, for the establishment of networks to provide communications in the event of disasters or other emergencies, for the advancement of the radio art and of the public welfare, for the representation of the radio amateur in legislative matters, and for the maintenance of fraternalism and a high standard of conduct.

ARRL is an incorporated association without capital stock chartered under the laws of the state of Connecticut, and is an exempt organization under Section 501(c)(3) of the Internal Revenue Code of 1986. Its affairs are governed by a Board of Directors, whose voting members are elected every three years by the general membership. The officers are elected or appointed by the Directors. The League is noncommercial, and no one who could gain financially from the shaping of its affairs is eligible for membership on its Board.

"Of, by, and for the radio amateur," ARRL numbers within its ranks the vast majority of active amateurs in the nation and has a proud history of achievement as the standard-bearer in amateur affairs.

A *bona fide* interest in Amateur Radio is the only essential qualification of membership; an Amateur Radio license is not a prerequisite, although full voting membership is granted only to licensed amateurs in the US.

Membership inquiries and general correspondence should be addressed to the administrative headquarters:

ARRL
225 Main Street
Newington, CT 06111 USA
Telephone: 860-594-0200
FAX: 860-594-0259 (24-hour direct line)

Officers

President: KAY C. CRAIGIE, N3KN
570 Brush Mountain Rd, Blacksburg, VA 24060

Chief Executive Officer: DAVID SUMNER, K1ZZ

The purpose of *QEX* is to:

1) provide a medium for the exchange of ideas and information among Amateur Radio experimenters,

2) document advanced technical work in the Amateur Radio field, and

3) support efforts to advance the state of the Amateur Radio art.

All correspondence concerning *QEX* should be addressed to the American Radio Relay League, 225 Main Street, Newington, CT 06111 USA. Envelopes containing manuscripts and letters for publication in *QEX* should be marked Editor, *QEX*.

Both theoretical and practical technical articles are welcomed. Manuscripts should be submitted in word-processor format, if possible. We can redraw any figures as long as their content is clear.
Photos should be glossy, color or black-and-white prints of at least the size they are to appear in *QEX* or high-resolution digital images (300 dots per inch or higher at the printed size). Further information for authors can be found on the Web at **www.arrl.org/qex/** or by e-mail to **qex@arrl.org**.

Larry Wolfgang, WR1B

lwolfgang@arrl.org

Empirical Outlook

Web Update

It has been a few issues since I last mentioned progress on replacing the files from past issues of *QEX* onto the ARRL website. It has been a time-consuming process, but I am pleased to tell you that I now have all of the files posted, back through the 1994 issues. I only have a few files from 1993 to add, and you will have access to all of the files from past issues. I wish it had not taken so long to restore the files, but soon you will be able to download any of the files that we "lost" in the transition to the new ARRL website. Check it out at **www.arrl.org/qexfiles**.

Many readers have asked about plans to make *QEX* available as a digital edition, or have asked about making the *QEX* archive files available for download in a manner similar to the availability of past *QST* articles. With the recent unveiling of digital *QST*, the number of such questions has increased quite a bit. Digital *QST* seems to be quite popular! Along with the announcement of the availability of digital *QST* there was an announcement that all previous *QST* articles on the ARRL Periodicals Archive and Search website would be available for download. This has also caused some confusion, with some believing that also meant that the *QEX* articles in that archive would be available. Unfortunately, that is not the case. Don't throw away your paper copies just yet! The only format for obtaining digital copies of *QEX* articles at this time is to purchase the *ARRL Annual Periodical CDs*. These go back to 1995, although several years are out of stock and discontinued, so there is no plan to make more copies of those CDs. Go to **www.arrl.org/shop** and search for "Periodicals CD" for the complete listing.

Will we ever have a digital edition of *QEX*? Probably. There has been some limited discussion, but no specific plans. The technical content of *QEX* presents a number of challenges when it comes to converting it to the various digital publication formats. I imagine all of those issues can be solved, but there are costs involved with the conversion of the files, and the *QEX* subscriber base is relatively small. There are also some challenges with regard to controlling access, although those can also be solved. In the case of *QST*, it is fairly easy to use ARRL Membership Numbers and the secure website log-on procedure to control access to the copyrighted material. It is a bit more difficult with *QEX*, since there is no one-to-one correlation between Members and *QEX* readers.

None of these issues should be major problems, but together they present some challenges to be overcome. ARRL is just beginning to learn the ins and outs of digital publication of copyrighted material. With digital *QST*, we are learning about the process as well as the advantages and any disadvantages. With more experience, we will be better able to extend the techniques we've learned to *QEX* and other publications. Please be patient with us.

Summer Activities

Do you spend more of your leisure hours away from your radio shack in the summer? I know I do. There are so many reasons to head outside, whether it is for a few hours, a few days or an extended vacation. What part does ham radio play in your summer activities? Do you enjoy a bit of portable operation during your vacation time? Perhaps a vertical and a radio on the beach, or a small QRP rig and a dipole or other wire to toss into the trees for some mountain-top operating?

Tradition has it that any antenna works better when it has been put up or repaired during the worst weather possible, so waiting for winter to come back may be a good idea for that antenna upgrade you have been dreaming about. Even so, it is more pleasant to be outside on a warm summer day than in the middle of a winter blizzard, at least when it comes to most antenna work. This is a good time to check all those coax connections and even the feed line itself. If something needs to be replaced before a busy Fall/Winter operating season gets underway, summer days present an excellent opportunity. The most important thing is to have fun!

George Works, KJ6VW; Shelley Works, KG4SRS

Pleasures Estate, St. Eustatius, Dutch Caribbean; **kj6vw@arrl.net**

Confirmation Measurements of Vector Potential Waves

More vector potential communications experiments.

After measurements with multiple antennas and plasma tubes, we confirmed the observations that led Robert Zimmerman and Dr. Natalia Nikolova to announce the detection of vector potential waves.[1] We found another possible explanation for these observations, however, based entirely upon conventional electromagnetic theory and not involving vector potential waves.

We read with considerable interest Robert Zimmerman and Natalia Nikolova's announcements[1, 2, 3] that they had detected and communicated with vector potential (VP) waves, and set out to confirm this discovery. Our approach was twofold. First, we set up an antenna test range for 1296.1 MHz and measured pairs of transmitting and receiving antennas including folded dipoles, a monopole, Zimmerman's waveguide transmit antenna, Zimmerman's plasma tube-in-a-waveguide receiving antenna, a plasma tube in a quart jar, a geometrically similar copper tube in a quart jar and a plasma tube with the cathodes outside the RF path. Second, we modeled these antennas using *EZNEC Pro/2* in ground wave mode to compute the drive impedances and patterns, as an aid to interpreting our measurements. Our experiments began in September 2011 and continued into April 2012. We collected over 500 measurements on the test range.

[1]Notes appear on page 7.

Test Range

Our test range, illustrated in Figure 1, consists of antenna mounts 1.52 m above ground on two telephone poles 15.2 m apart in a goat pasture. The mounts are aligned to bore sight with a tight string. Short lines and wooden clothes pins hold the antennas in position during tests. An isolator at the transmit mount provides low SWR on the transmit feed line. Buried LMR-400 feed lines from the two antenna mounts lead into our shack, where the signals are generated and measurements made.

In the shack, a custom *Java* program digitally generates transmit audio at 1.8 kHz, which is up-converted to 28.1 MHz by a

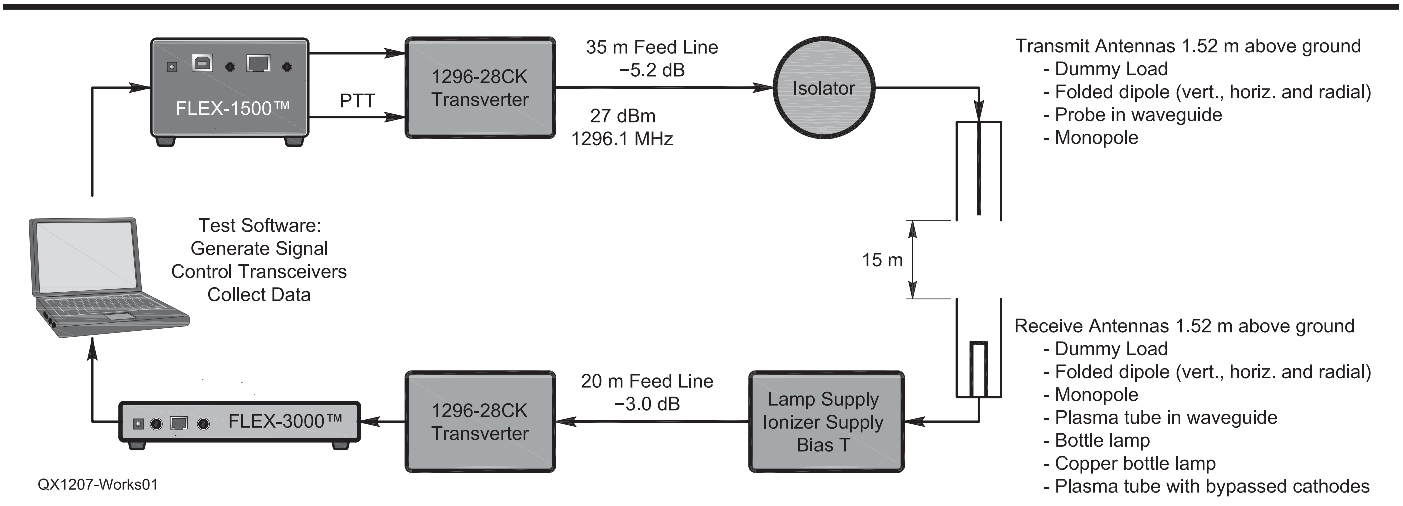

Figure 1 — This diagram illustrates the 1296 MHz antenna test range and equipment set up used for these measurements.

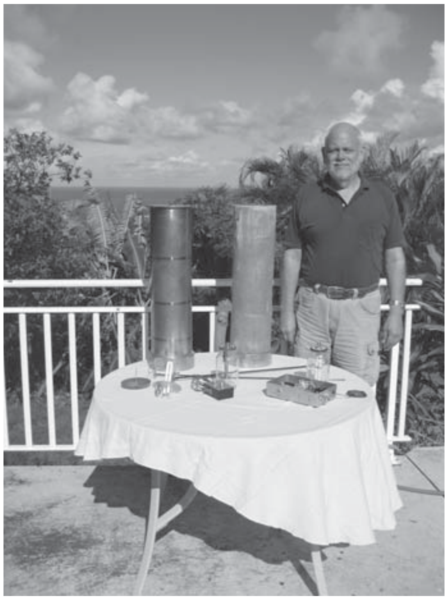

Figure 2 — The author shows the antennas used in these experiments.

Flex-1500 transceiver in USB mode. The transceiver drives a Down East Microwave 1296-28 transverter for further up-conversion to 1296.1 MHz. A second identical transverter feeding a Flex-3000 transceiver, also controlled by the *Java* program, receives the signals. The Flex-3000 receive bandwidth is set to 500 Hz, DSP buffer size to 4096, S-meter averaging to 1.0 s, AGC threshold to 90 and AGC speed to slow. Approximately 21.6 dBm transmit power is available at the transmit antenna. The receive gain is presently uncalibrated, but appears to be constant from day to day.

While George changes antennas on the test range Shelley operates the equipment in the shack. For each test, Shelley informs George of the required transmit and receive antenna types as specified in the test description. George installs the correct antennas and confirms this by cell phone. Shelley starts the test, confirms that the Flex-1500 transmit output is correct, tunes the Flex-3000 to center the received CW signal in the passband, and clicks the "Take Measurement" button on the computer screen. The test software records a file with the date, time, test description, receive frequency and averaged S-meter reading for each measurement. Each measurement set includes receiver noise, cable crosstalk and two folded dipole-to-folded dipole measurements to validate that all is working correctly. Setting up, collecting a full set of measurements, and taking down the equipment in the pasture requires about one hour for each run. Tropical showers and inquisitive goats make it inadvisable to leave equipment set up between runs.

Antennas

Figure 2 shows the assortment of antennas and the plasma tube power supply that we use in our experiments. We fabricated transmit and receive waveguide antennas based on Zimmerman's designs, with 178 mm diameter waveguides 690 mm long. The transmit waveguide is made of sheet brass rather than a stovepipe, and the receive waveguide is made of copper screen wrapped with fiberglass-epoxy. We added waveguide chokes to both antennas to reduce electromagnetic radiation. Folded dipoles are from a design in *The ARRL UHF/Microwave Experimenter's Manual*.[4] The monopole is a quarter wave probe mounted on an N connector centered on a quarter wave radius brass plate.

We used widely available Sylvania Dulux S compact fluorescent lamps, part number CF9DS/78, which look identical to the lamp in Zimmerman's photos. These are "low mercury" lamps, which is the only type now sold in the US. Zimmerman's lamp was apparently not a "low mercury" lamp. We removed the plasma tubes from their bases, which contain lamp starters. The two leads from one end of the plasma tube are soldered directly to the center pin of an N connector, and the two leads from the other end are soldered to a ground lug. Figure 3 shows a fluorescent lamp as received, a lamp with its base removed, and a plasma tube installed on a brass plate ready for mounting on the receive waveguide. A thin piece of Kapton tubing supports the plasma tube.

In addition to the plasma tube in the receive waveguide we installed a second plasma tube in a quart jar with an N connector mounted on the lid, in the same folded monopole configuration used in the waveguide. The tube in a bottle proved to be about 4 dB less sensitive than the plasma tube in the waveguide, but was considerably more convenient to carry around.

We powered our plasma tubes on direct current, like Zimmerman's original design, using a custom-built dc-dc converter and bias-T. The dc-dc converter delivers 260 V dc to an un-ionized lamp, but this drops to about 65 V dc across the lamp after the lamp ionizes. Ionizing these lamps requires about 1600 V dc, which is generated by an accessory cold cathode fluorescent lamp inverter with an added voltage doubler rectifier circuit, also mounted in the lamp supply box. A momentary switch activates the ionizing supply to start the lamp. A bias polarity switch on the supply box allows testing the plasma tube with either positive or negative bias current.

Modeling

We used *EZNEC Pro/2* to model each

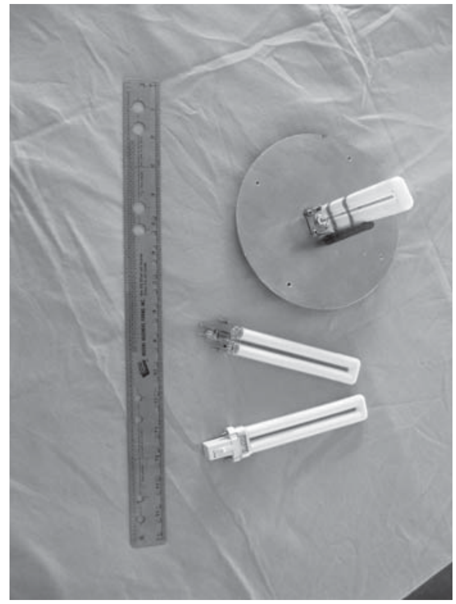

Figure 3 — From the right, here is a lamp, a plasma tube with the base removed and a plasma antenna mounted to a disk to fit in the end of the waveguide.

antenna, with the most complex models, the mesh models for the waveguides, having over 9,000 wires. Computed azimuth patterns for each antenna were constructed in ground wave mode using the actual transmitter power, antenna heights and separations on the test range. Figure 4A shows the mesh model for Zimmerman's transmit antenna, and Figure 4B shows the computed vertical, horizontal and total field patterns including ground wave. No antenna had a total field null deeper than about 20 dB, modeled over real ground, which measurements confirmed.

Evidence for Vector Potential Waves

If there were an antenna that had, over real ground, very deep nulls in its horizontal, vertical and radial fields at the same azimuth angle, then we could declare that any signal we detected with a plasma tube in this near-perfect null was probably due to vector potential waves. We have not discovered such an antenna, either through modeling or measurements, but we found less direct evidence that might suggest vector potential waves.

Nikolova and Zimmerman[3] and later Zimmerman[2] argue that if vector potential waves exist physically and are detectable by a plasma tube, they will modify the momentum of electrons in a plasma that travel at velocities greater than a critical threshold. The phase of the current resulting from the modified momentum depends on the direction of the average current. Reversing

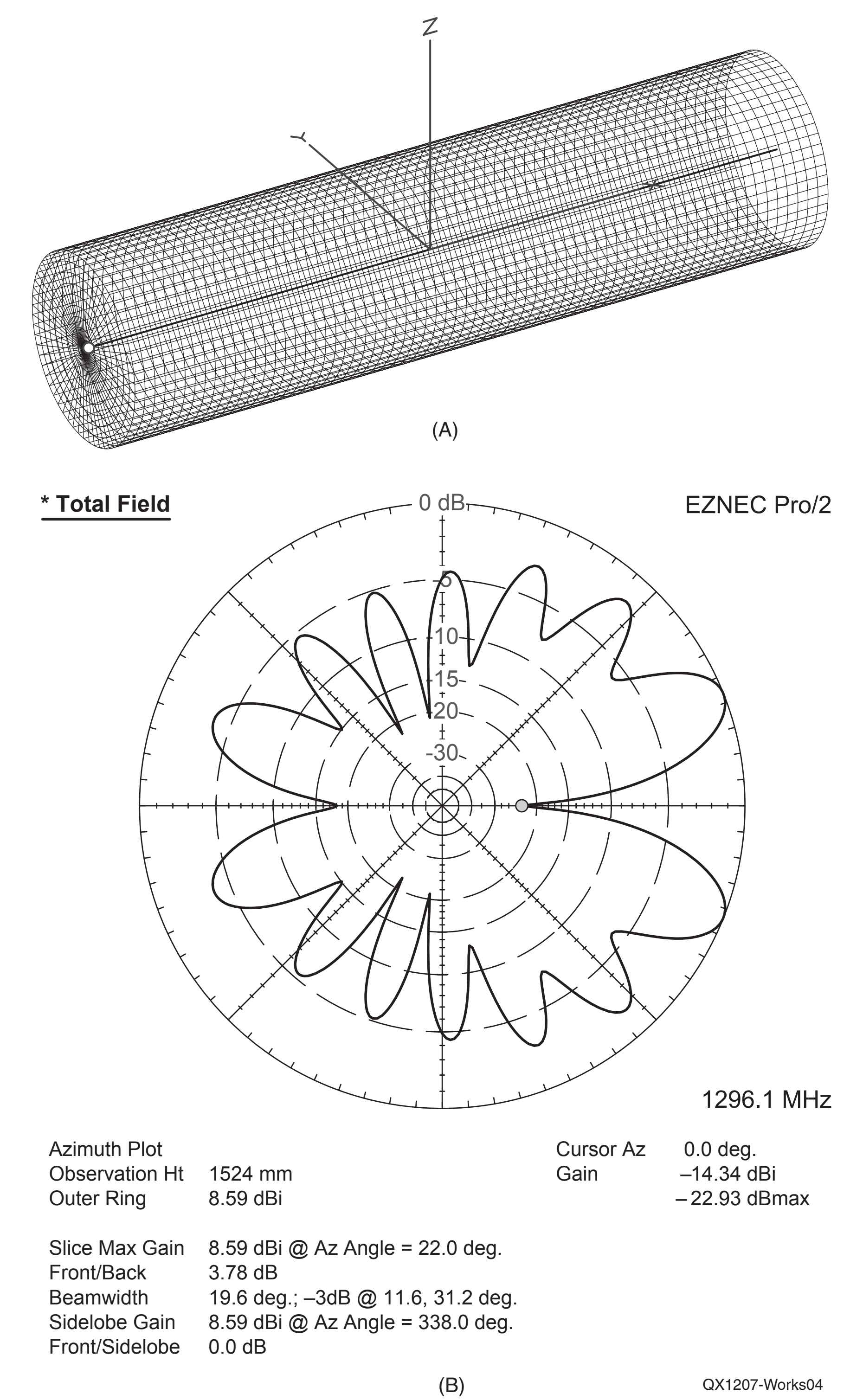

Figure 4 — Part A shows an *EZNEC* mesh model of our (and Zimmerman's) transmit antenna, and Part B is the computed antenna pattern plots.

the bias current reverses the average electron velocity and so reverses the phase of any received vector potential signal. The response of a plasma antenna to electromagnetic waves, however, doesn't depend on the direction of the bias current but only on the plasma's high conductivity. So they expect any signal generated by vector potential effects to add to, or subtract from, the signal due to the electric field.

In particular, they expect to see a greater signal with negative bias than with positive bias if vector potential waves are being detected because the two signals add in phase with negative bias, and out of phase with positive bias. Conversely, if vector potential were not involved, the signal measured with either negative or positive bias should be about equal and it would be equally likely that either one would be the larger. Nikolova and Zimmerman observed these signal differences with bias reversal experimentally using U-shaped plasma tubes similar to ours, with dc bias, and that was key experimental evidence that led them to conclude that they had observed vector potential waves.

We measured signal levels with both negative bias and positive bias on two different U shaped plasma tubes, with five different transmitting antennas, on 89 occasions. In every case the negative bias signal exceeded the positive bias signal as Nikolova and Zimmerman had reported. The probability of that happening due to random chance is less than 2×10^{-27}, which is very unlikely indeed. It seems reasonably certain that something is causing the negative bias signal to be greater but vector potential waves are not the only possible cause. Before we can conclude that we have confirmed the detection of vector potential waves with plasma tubes, we must rule out any other plausible causes for our observations.

Other Possible Causes

Possible sources of asymmetry in our system are the plasma tube structure, the power supply for the plasma tube, the bias T and changes in the plasma shape and fields in the plasma tube associated with the bias polarity. Structural asymmetry in the plasma tube might develop if the tube were operated for an extended period with one dc bias polarity, causing one of the cathodes to be damaged by ion bombardment, or if the mercury relocated to one end of the tube. To explore this possibility we made 10 pairs of measurements on the "bottle lamp" with alternating bias polarity, unsoldered and reversed the plasma tube, and repeated the measurements. The transmitter was a monopole in all cases. For the original configuration, the mean signal difference was 7.2 dB, with a standard deviation of 1.0 dB. For the reversed configuration, the mean signal difference was 6.2 dB, with a standard deviation 0.6 dB. In all 20 cases the negative bias signal was stronger. It appears that any structural asymmetry in this tube is much too small to account for the signal difference.

Asymmetry in our tube power supply might lead to different positive and negative bias currents. Using the bottle lamp load, we measured the bias current 22 times each for positive and for negative bias, alternating the measurements. The mean (of 22) bias cur-

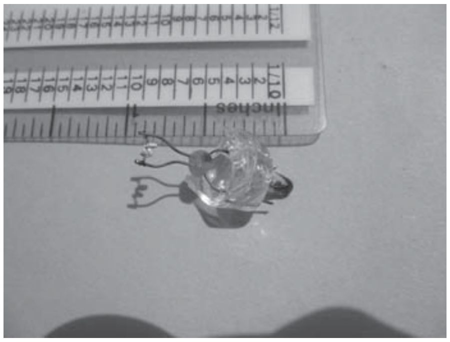

Figure 5 — This photo shows the cathode structure in a CF9DS/78 plasma tube.

rent measurements was 146.4 mA, with a standard deviation of 3.7 mA, and the mean bias current difference (positive – negative) was –2.6 mA with a standard deviation of 3.5 mA. It appears that there is no significant asymmetry in the lamp supply.

Our original bias T design included a pair of 1N4148 diodes shunting the N connector to the transverter as protection against transient voltages from the plasma tube. Large tube noise or coupling capacitor leakage could possibly bias one of the diodes on and attenuate the received signal asymmetrically with bias. We replaced the diodes with a shorted quarter wave stub across the N connector to eliminate this possibility and made 10 pairs of measurements on the "bottle lamp" with alternating bias polarity. The transmitter antenna was a monopole in all cases. The mean signal difference between positive and negative bias readings was 5.3 dB with a standard deviation of 0.8 dB. In all cases the negative bias signal was stronger. Bias T asymmetry does not appear to have caused the bias-dependent signal levels.

Cathode Shift

Ray Cross, WKØO, suggested that an asymmetry may be associated with the cathode location, which shifts from the N connector end to the ground end of the plasma tube depending on bias polarity.[5] He argues that the fields and the shape of the plasma in the tube might be affected by the cathode position, so we investigated the plausibility of this through modeling and direct observation. Modeling can't prove or disprove that these effects actually occur, but it can show whether cathode shift is a plausible explanation for our results that requires experimental investigation.

It seemed possible that at the cathode end, the plasma begins at a "hot spot" on the cathode wire and expands out to nearly the diameter of the tube over a few millimeters. The hot spot would be expected because the higher the temperature of a spot on the cathode wire, the higher the electron emis-

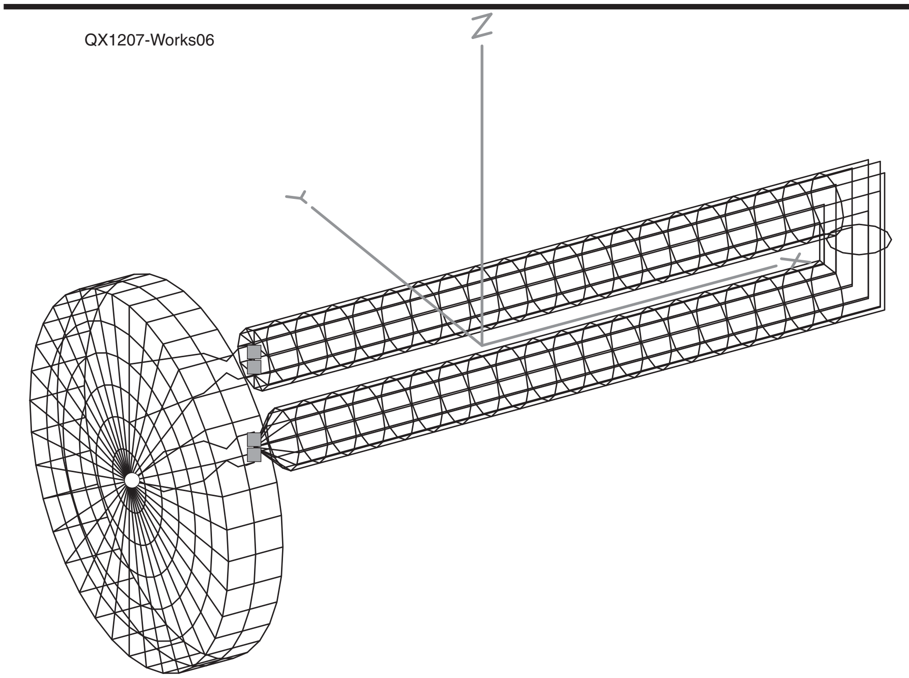

Figure 6 — Here is the bottle lamp *EZNEC Pro* model, with negative bias.

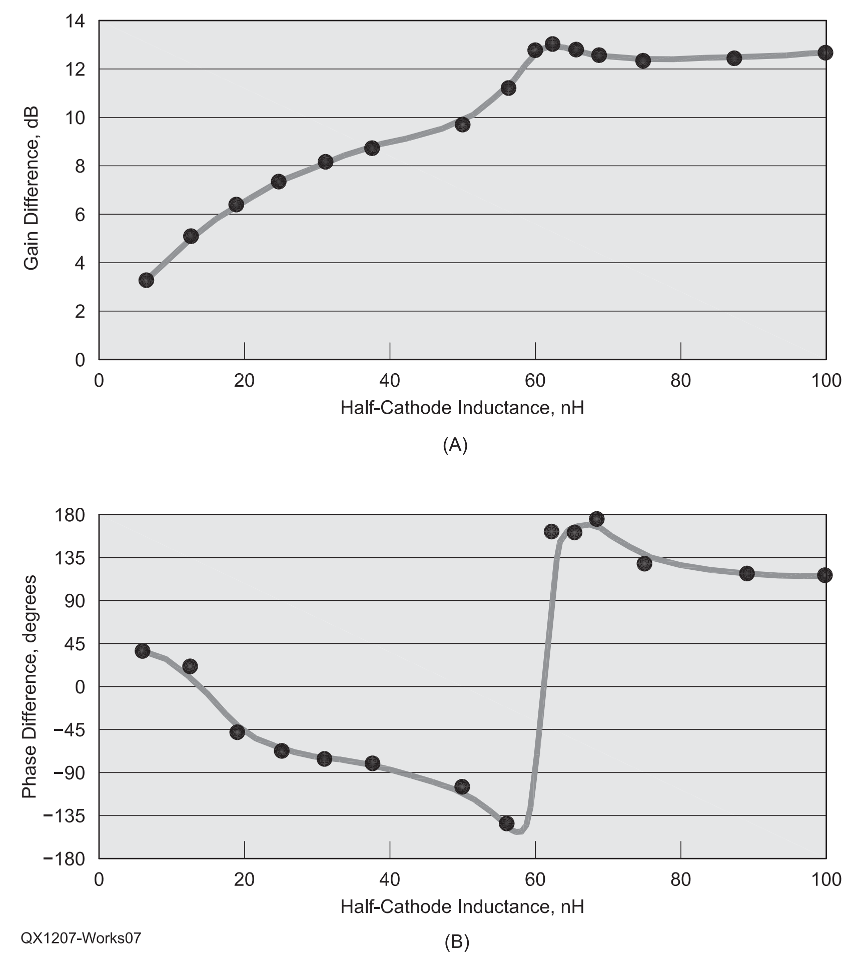

Figure 7 — Part A shows the modeled gain change of the bottle lamp antenna with bias polarity reversal as a function of cathode inductance. Part B shows the modeled phase change of the bottle lamp antenna with bias polarity reversal as a function of cathode inductance.

sion. Higher electron emission means more current, and therefore a higher temperature. But at the anode end electron emission is irrelevant so the plasma might well extend past the electrode wire into the area of the support wires, shorting out the inductance of the electrode wire.

Figure 5 shows a cathode and support wires from one of the CF9DS/78 tubes that we used in our experiments. The cathode is coated with a white electron-emitting material and consists of a coil of very fine wire, coiled into larger coil, and this is coiled into a still larger two-turn coil supported by two horizontal support wires. We measured the inductance of this cathode with an L-C meter at 600 ± 30 nH between the two support wires. If the plasma attached to a hot spot at the center of this wire, it could place the inductance of the two halves of the cathode, paralleled, in series with the plasma tube at the cathode end. This series inductance could be as much as 75 nH.

We modeled the cathode structure and plasma in the bottle lamp, with the plasma beginning at a hot spot in the center of the cathode and ending at the support wires at the anode. Figure 6 shows the mesh model with negative bias. We represented the cathode inductance as a lumped inductance in each half of the cathode, and varied this half inductance while recording the gain and phase of the bottle lamp antenna for each bias polarity. Figure 7A shows the antenna gain difference and Figure 7B shows the received signal phase difference between positive and negative bias as a function of inductance. A cathode half inductance in the range of 15 to 40 nH would be consistent with the 5 to 8 dB gain differences that we measured on the test range. Although we did not measure phase difference, Nikolova and Zimmerman did, and the phase difference that they measured also appears consistent with this model.

There remained the question of whether the cathode hot spot actually occurs in these tubes. We obtained some transparent 9 watt U-shaped tubes without phosphor coating, made for ultraviolet sterilizers, part number PLS9W/TUV, and constructed a second bottle lamp with one of these tubes. Using a digital microscope and optical filter sheets, we were able to photograph the cathode and anode while the tube was ionized. [6] Figure 8A shows the anode and Figure 8B shows the cathode, with different filters required for each image to avoid saturating the digital microscope. The cathode in these sterilizer tubes has a three-turn outer coil instead of the two-turn coil in the tubes that we used in the test range but we would not expect this to affect the presence or absence of a cathode hot spot.

Figure 8A shows that the plasma at the anode end does in fact surround the coiled electrode wire and its supporting wires, and fairly uniformly heats the wire along its length. Figure 8B shows that the plasma attaches to the cathode at a single very bright hot spot. When the tube is first ionized the cathode glows uniformly, and over a period of about one second the glow coalesces into the single hot spot. The exact position of the hot spot varies as the tube is repeatedly turned off and on.

(A)

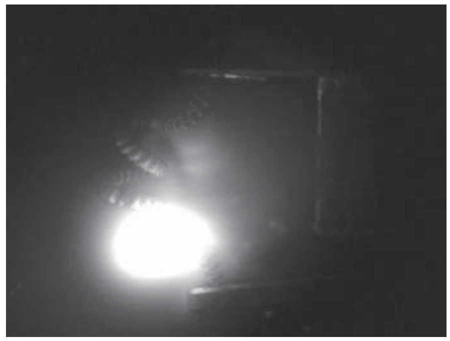

(B)

Figure 8 — Part A shows an image of the anode and plasma in an ionized 9 W U-shaped tube. Part B is an image of the cathode, showing a hot spot in an ionized 9 W U-shaped tube.

Conclusions

We confirmed Nikolova and Zimmerman's observations that a 9 W U-shaped plasma tube, connected as a folded monopole in front of a ground plane, receives a stronger signal with negative dc bias than with positive bias. This effect seems to be completely explained by conventional electromagnetic theory and the construction of U-shaped fluorescent tubes, however, without any need to assume vector potential waves. This does not prove that vector potential waves do not exist physically. They may exist and be detectable by other means, but their existence cannot be inferred from our experiments.

Our test data, antenna models and design details are available by email request to KJ6VW@ARRL.net.

George Works, KJ6VW, was first licensed in 1961 as WA2PAY. He enjoyed experimentation and constructing his own equipment and served as a volunteer civil defense radio operator. He received a BSEE from MIT in 1966 and held engineering and management positions at several companies before retiring in 2005. George is a private pilot and has captained a sailboat around the Pacific and around the Caribbean where he operated maritime mobile. He now raises goats, cows and chickens on a small farm on the island of St. Eustatius, Dutch Caribbean. He operates a very active Winlink station serving the Caribbean and many maritime mobiles, installs satellite terminals and consults as a volunteer on information technology, solar energy and similar projects on the island.

Shelley Works, KG4SRS, was first licensed in 2002. She received a BS degree in mathematics from Salisbury State in 1976 and worked as a software engineer and engineering manager before retiring in 2005. Shelley is also a private pilot, a sailor and an avid gardener, raising a variety of fruits and vegetables in her extensive garden. She enjoys reading novels in Dutch, which she has learned since retiring. She developed the records and billing software and website for the St. Eustatius Animal Welfare Foundation, and websites for several other island organizations.

Shelley and George discovered St. Eustatius while sailing on their boat in the Caribbean and decided on the spot to buy a house and retire there. St. Eustatius is a tiny Dutch island of 3000 inhabitants with few street numbers and no postal codes. They live on the side of a dormant volcano 700 feet above sea level, overlooking the Caribbean.

Notes

[1] Robert K. Zimmerman, NP4B, "Transmission and Reception of Longitudinally-Polarized Momentum Waves," *QEX,* July/August 2011, Issue 267, pp 31-35.

[2] Robert K. Zimmerman, "Macroscopic Aharonov-Bohm Effect at L-Band Microwave Frequencies," *Modern Physics Letters B,* Vol. 25, No. 9 (2011), pp 649-662.

[3] Natalia K. Nikolova and Robert K. Zimmerman, *Detection of the Time-dependent Electromagnetic Potential at 1.3 GHz*, McMaster University, Research Report CEM-R-46, November 2007.

[4] *The ARRL UHF/Microwave Experimenter's Manual*, The American Radio Relay League Inc, 1990, p 9-7.

[5] Ray L Cross, WKØO, unpublished e-mail correspondence, dated 12 March 2012.

[6] If you plan to observe one of these sterilizer tubes in operation, remember that the very bright UV light can damage your eye as well as saturate an image detector. To be safe, either cover the tube with an opaque shield during operation or wear a pair of UV safety goggles.

QEX

Glenn Elmore, N6GN

446 Halter Ct, Santa Rosa, CA 95401; **n6gn@sonic.net**

A New Antenna Model

Think you know how an antenna radiates a signal? This article may give you some new insight.

This article is intended to provide a useful interpretive model for understanding how antennas operate. While many amateurs are likely to have good practical knowledge of antennas, how to construct them, how to match to them, the use of baluns, wave polarization and so on, when it comes to having a picture of how and why an antenna generates a wave that can be received far away or why the feed point has a particular impedance value, things may not be so clear. A precise closed form alternative to the equations presently used for antenna analysis won't be provided here. Instead of that, this article is intended to give a reasonably complete and accurate intuitive way to view simple antennas that most amateurs commonly use.

Antennas have been important for more than a century and the analytical theory to describe them, derived from electromagnetic theory by James Clerk Maxwell, Heaviside and others, has been developed for a long time as well. This theory may leave most of us without an intuitive understanding — without a useful mental picture. To help change this it is useful to first look at what analytical theory, measurement and computer modeling does tell us. We can then go on to form a new understanding that may be easier to picture.

Antennas such as dipoles are usually analyzed by applying Maxwell's equations to the current within infinitesimal segments of a longer conductor and then computing the resulting fields and impedances. A common approach is to start with a description of the fields produced by current in an infinitesimal section of a dipole, as shown in Figure 1. A dipole can be modeled as a collection of a very large number of these elements laid end to end. The currents in each of the elements are assumed to follow something close to a sinusoidal distribution along the length of the dipole, and to be opposite in the two dipole halves. At the dipole tips, where the element ends, the current is assumed to be zero. An interesting consequence of solving analytically in this way is that both the radiation pattern and the feed point impedance are obtained.

Solutions of the traditional field theory are much more approachable these days because of the availability of the numerical electromagnetics code (*NEC*) modeling tool and its derivatives. These computer programs can quickly solve the equations and display both antenna impedance and pattern. For the discussion that follows, let's look at what classic Maxwellian field theory — with the help of modern computer tools — tells us about a thin, perfectly conducting one meter long center-fed dipole. This is an antenna that, if we had thin, perfectly conducting material from which to make it, would be a fine dipole for 2 meters.

Antenna Pattern

Figure 2 displays the far field pattern of a one meter long center-fed dipole as calculated by *4NEC2*.[1] For these displays, the dipole may be imagined as located at the center of the plot with its elements running vertically, above and below center. This analysis is of a vertically polarized dipole far from any ground, conductors, dielectrics and anything else, so the antenna is said to be located in "free space."

Plots for 150 MHz, 300 MHz and 570 MHz are shown. These three plots corespond to different wave sizes. That is, at 150 MHz this dipole is a conventional center fed half-wave dipole, at 300 MHz it is a full-wave dipole and at 570 MHz the length is about 1.9 wavelengths, all of these measured from tip to tip.

Note particularly that to an observer located to the right or left of center, the half wave and the full wave dipoles each have a maximum. This is the broadside direction of the antenna. You can see about 2 and 4 dB indicated gain for the half and full wavelength dipoles, respectively. If the observer were located at the top or bottom of the plot, it would be found that there was no signal at all coming off the side, that is, from the element ends.

This is what most of us expect from a dipole. Note what happens, however, when the antenna length is about 1.9 wavelengths.

[1]Notes appear on page 18.

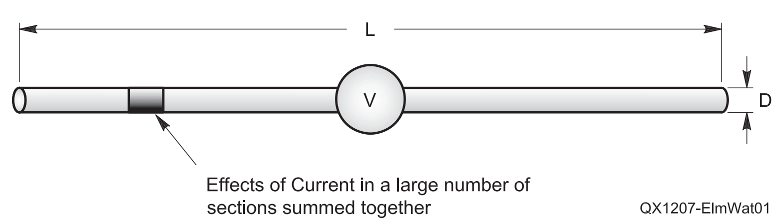

Figure 1 — The individual effects of currents in a very large number of small elements laid end-end can be summed to model the operation of a center fed dipole of length L. These elements are presumed to be perfectly conducting and very much thinner than their length, D << L.

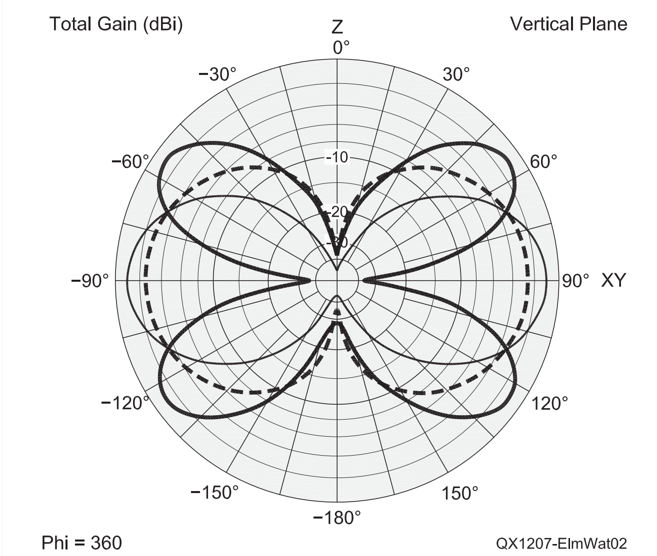

Figure 2 — Far field radiation pattern of a half-wave (dashed line) and full wave (thin line) and 1.9 wave (bold line) center-fed dipoles. Notice the broadside nulls at 1.9 wavelengths.

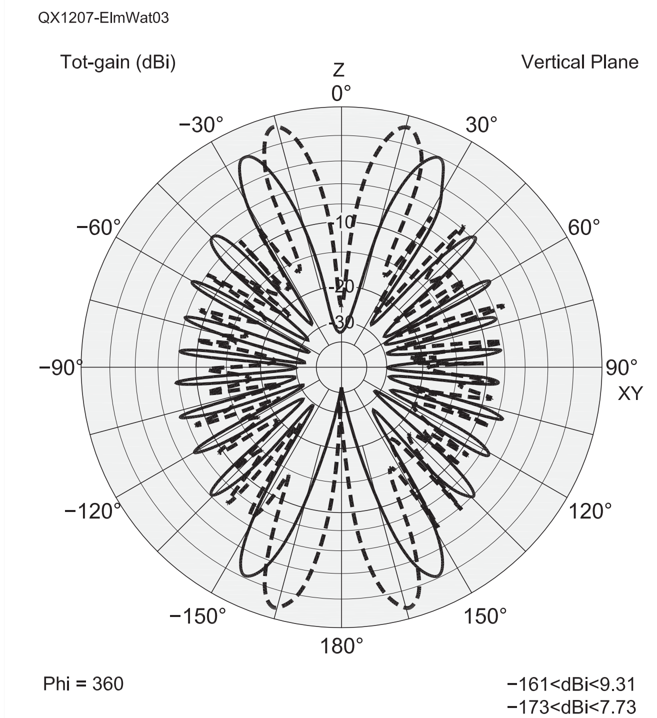

Figure 3 — When a dipole gets electrically long, it can be said to have a large wave size. Here the patterns of two such antennas are plotted, one that is 10 wavelengths long (dashed line) and a second that is 10.5 wavelengths. For these antennas, the direction of the maximum lobe splits into two major beams each side of the broadside direction and the direction of these maximum signals gets closer to the longitudinal direction of the dipole element. Note that there may also be a null in the broadside direction.

Instead of a broadside maximum with nulls off the sides, a dipole of this electrical length produces two peaks, around 35° above and below the broadside direction and a null off the ends. Perhaps surprisingly, at the same time there is also a null in the broadside direction where the other dipole lengths gave a maximum.

Figure 3 shows the patterns from the same center-fed dipole again placed vertically at the center in open space with no nearby ground. But in this case the two plots show the patterns when the frequency has been increased to around 3000 MHz, where the overall lengths are 10 and 10.5 wavelengths. By keeping the dipole physical size the same, but changing the frequency (wavelength) we are examining a dipole of varying *wavesize*. The plots show what happens to the radiation pattern as the dipole gets considerably longer than the common half-wave variety many of us use at our stations. The direction of maximum gain, the main lobe, is split and points more along the axis in the direction of the ends. Just as we saw in Figure 2 with shorter dipoles, as the antenna length is increased, there is a continuous alternation of peaks and nulls in the broadside direction. If you think about this, it may seem surprising that a dipole can have any broadside nulls at all.

Antenna Feed Point

Now let's turn our attention to what we measure at the center feed point of this dipole and what happens when we change frequency. Figure 4A plots the reactance against the *logarithm* of the resistance as frequency and with it, wavesize, are increased. This is the form of the plot shown in the *ARRL Antenna Book*. This plot doesn't explicitly show frequency or length but the various resonances associated with a dipole as wave size is varied are easy to spot. A very short dipole starts with a very small resistive component but high capacitive reactance. This is a point down on the lower left of the plot and is the sort of impedance that a 160 m mobile whip might present to a loading coil or tuner. As the length approaches a half wave, the reactance drops to zero and the antenna reaches its first resonance and shows a value for the logarithm of resistance of about 1.86. This corresponds to $10^{1.86}$ or about 72 Ω. This is the common operating length and impedance for many dipoles used in Amateur Radio. As the length increases further, the reactance becomes inductive and the resistance increases to a much higher value. When the antenna reaches one full wavelength, at about 300 MHz in this example, the reactance again drops to zero and the feed-point resistance reaches its maximum of around 8 kΩ at this first "high impedance resonance."

As the length continues to increase, a sequence of low impedance resonance followed by high impedance resonance continues with the reactive component looking alternately inductive and capacitive in between.

Figures 4B, C and D plot this same behavior versus frequency in different ways.

Figure 4B shows the resistance and reactance separately but on the same linear scale. Figure 4C shows them combined into an equivalent impedance magnitude. Figure 4D shows the effects this impedance has on the SWR when fed from a 50 Ω transmission line. For all of these, the repetitive nature of the low impedance resonances is clearly visible. These occur at about 3/2, 5/2, 7/2 wavelengths and so on. This is the same phenomenon that also allows us to easily use a 7 MHz half wave dipole at 21 MHz — the third harmonic of its half wave resonance.

Beyond 50 Ω

An interesting thing seems to have happened within Amateur Radio sometime around the end of World War II. Amateur antennas, which had previously been fed with single or balanced wires, were increasingly fed with 50 Ω coaxial cable. Then a bit later, in the 1970s, our transmitters, which had often included pi-network output net-

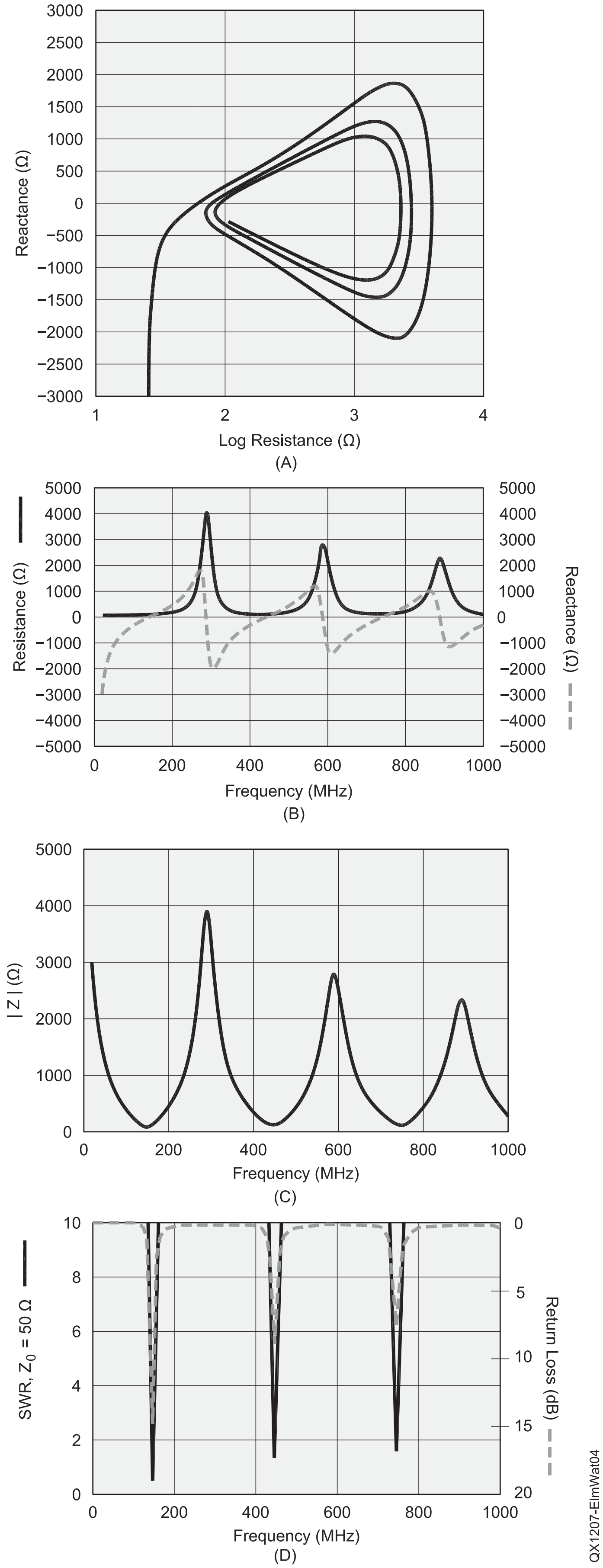

Figure 4 — Four different representations of the feed point characteristics of a center fed dipole. These show resistance, reactance, impedance SWR and return loss for the same very thin, perfectly conducting 1 meter long center-fed dipole. Examination of these different views reveals the low-impedance resonances at odd half-wave lengths as well as the high impedances ones near even half-wave lengths.

works capable of matching these high impedance antennas, increasingly became solid state and were designed to only drive loads of 50 Ω or something close to this. More recently, 50 Ω reference SWR bridges for use with 50 Ω coax have been included right inside amateur transceivers.

Coaxial cable has certainly been of great benefit, and most of us have spent considerable time trying to assure ourselves that the SWR we measure on our 50 Ω coax using a 50 Ω reference SWR meter was low enough. From the point of view of antenna physics or the way an antenna fundamentally operates, however, there is really nothing special about a 50 Ω reference impedance.

The rectangular graph of Figure 5B, shows a plot of the SWR of a dipole in a 50 Ω system, as before, along with a second plot of the SWR that would be measured if you were using a much higher impedance reference. Note the nature of the high impedance resonance you see when viewing SWR from a 6 kΩ perspective for this antenna. This second resonance, the high impedance one located between the low impedance resonances we normally use, actually has lower SWR over a wider bandwidth. The precise value computed by modeling tools for this high impedance may vary somewhat depending upon the tool and the dipole dimensions, just as it does for low impedance resonances.

Figures 5A and 5C plot these same feedpoint characteristics in terms of impedance when plotted on a Smith chart. If you aren't too comfortable with Smith charts, don't let this format put you off. It's only another method to simultaneously display both resistance and reactance. You can think of it as a sort of "warped grid" for plotting the same information you saw in Figure 4A. This method has some nice features, however, when it comes to considering how to match to a load, whether you're using lumped elements or transmission lines.

In Figure 5A the Smith chart has a reference impedance of 50 Ω. This means that a 50 Ω resistive load with no capacitive or inductive reactance component will plot as a point right at the center. In fact, on a Smith chart of any reference impedance, a load of that impedance would be perfectly matched,

Figure 5 — Here the characteristics of a dipole are shown from the point of view of different reference impedances. The SWR plot shows the same dipole viewed from 50 Ω and 6 kΩ viewpoints. The Smith charts show the data plotted against a chart impedance of 50 and 754 Ω. A circle around Smith Chart center is characteristic of a mismatched transmission line, $Z_0 = Z_{ref} \neq Z_{load}$.

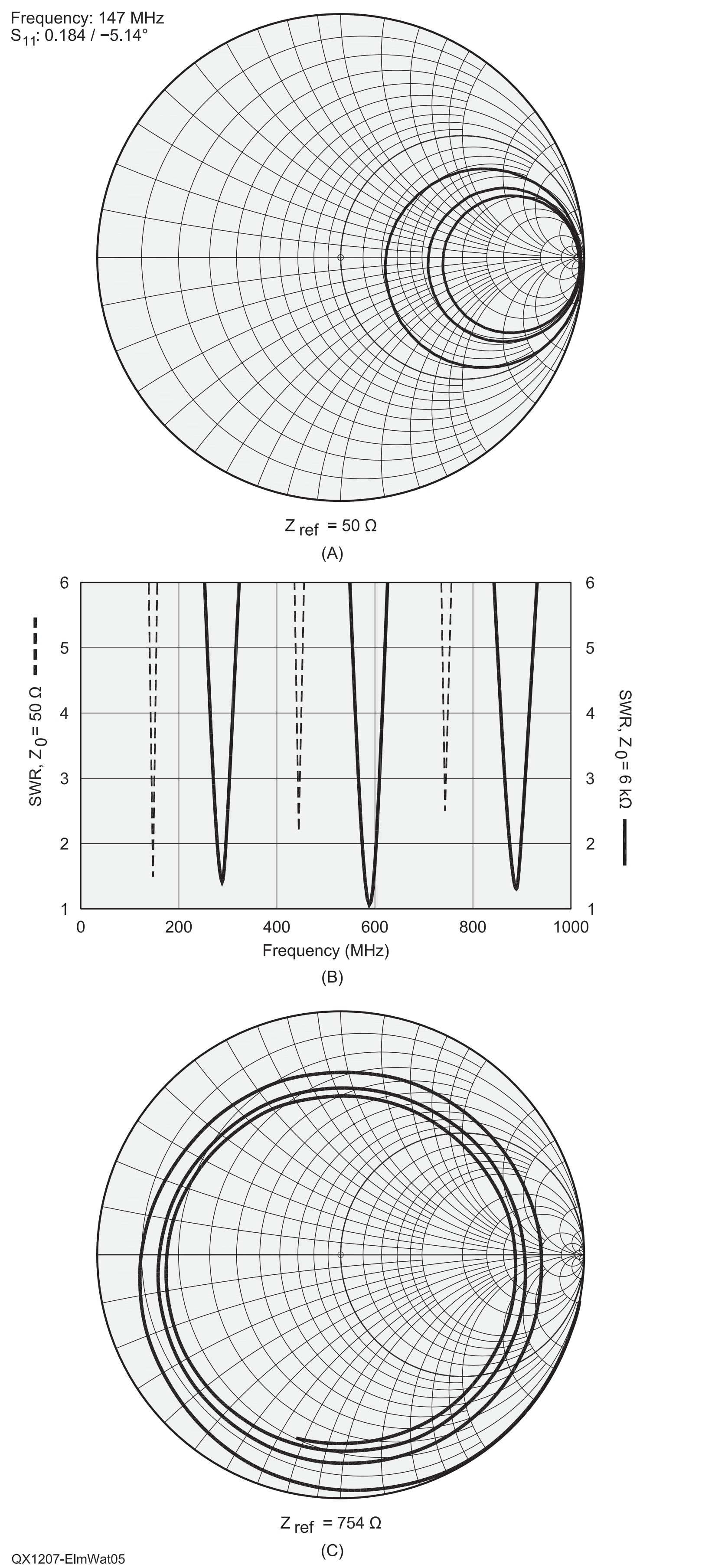

would plot at the chart center and the SWR for that would be 1:1. Also notice the circles on both of the Smith charts. If you are familiar with Smith charts, you may recognize them as "SWR circles" and know that a circle around the center of a Smith chart is a characteristic of a mismatched transmission line. Recognizing that a dipole operates like a transmission line with SWR is a benefit we get from looking at the data using the Smith chart.

In Figure 5C the reference impedance of the Smith chart has been changed to 754 Ω. At this value the circles that describe the dipole impedance are nearly centered on the Smith chart.

In Figure 6 the impedance of a thin, one meter long dipole is again plotted, but the frequency goes all the way to 3.1 GHz, where the dipole is 10.5 wavelengths long. Here again, with a chart reference impedance of 754 Ω, a dipole looks an awful lot like a mismatched transmission line and the size of the circle indicates that the SWR on that line is about 8:1.

If you are wondering about the choice of this particular reference impedance, it might help to realize that 754 Ω is twice 377 Ω, which is the impedance of an electromagnetic wave in free space, and that a center-fed dipole has two elements going in opposite directions from the center. This may make more sense when we consider a possible schematic model of a dipole.

A Simple Circuit Model of a Dipole

These observations show us that for the calculated data provided, a dipole behaves a lot like a pair of mismatched transmission lines, each operating with an SWR of about 8:1. It is as though each of the dipole elements was a 377 Ω transmission line and each was terminated with a resistor of about 3 kΩ.

All this invites us to use a rather simple circuit model for a dipole. Figure 7 portrays this schematically. In this schematic, the transmitter's 50 Ω output impedance is connected through a length of 50 Ω coaxial cable to an antenna tuner or matching network of some sort. This tuner may include provision for converting the unbalanced coaxial feed to a balanced load like a dipole or Yagi or the balun may be built into the matching struc-

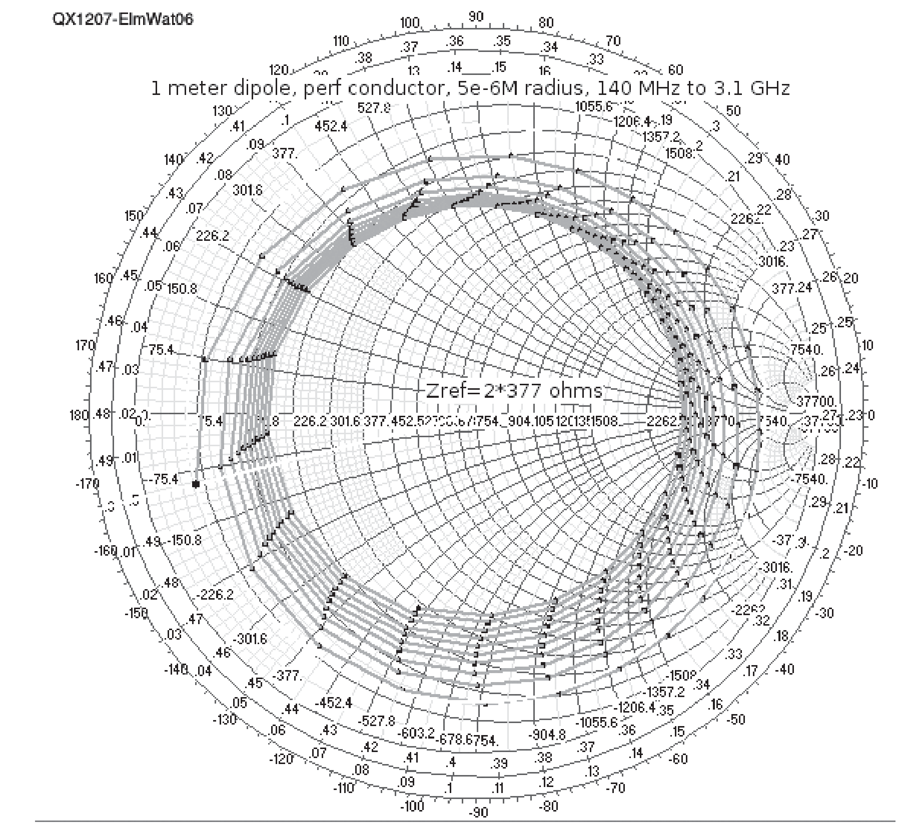

Figure 6 — Feed point impedance (from *4NEC2*) of a thin 1 meter dipole plotted on a Smith chart having a reference impedance of 754 Ω, This value is approximately twice the impedance of a wave in free space. For this plot, frequency is swept from just below the 2 m amateur band to above 3 GHz so the antenna wave size is changing from one half wavelength to over ten wavelengths. Notice that as the antenna gets electrically long, successive circles have nearly the same center and radius.

ture at the antenna itself. For a radio communications system designer, the goal is usually to transfer as much of the transmitter power into the radiation resistance as possible.

Sometimes both the balun and any required matching is built into an antenna. A ground plane fed directly with coaxial cable is an example of this. For an antenna that uses a ground plane, a perfect ground system, we can say that there is an "image plane" that acts like a mirror to reflect the image of the actual antenna element to create an "inverted twin." Imagine looking into a mirror that has only one element of a dipole placed so that it stands on the reflecting surface. If you looked at both the element and the mirror you would see a full size dipole but only half of it would be real, the other half would be a reflected image. This effect is present in a ground plane antenna and produces the effects — the radiation polarity and pattern — of a full-size dipole but with only a single element. The feed-point impedance is one half that of the dipole because for the same voltage there is twice the current, the original current in the element plus the equal image current due to the image element in the ground plane. Because of this relationship, the circuit model we create for a balanced dipole can easily be adapted to work for a single-ended antenna as well.

The resulting circuit model for the dipole has two mismatched transmission lines between the feed point at the center and the radiation resistors at the tips. The feed point impedance acts like each of these lines is terminated with a resistance of 2 to 3 kΩ. For a thicker dipole, the termination resistance will be lower. For shorter dipoles, say less than a wavelength or two, there is also a little bit of shunt capacitance between the ends of the lines — that is, between the tips of the dipole — that affects the impedance slightly. The terminating resistance and this shunt capacitance vary somewhat with dipole length, element thickness and taper, but overall this model is pretty good.

When we build transmitters and tuners, our goal is usually to transfer as much transmitter power, often coming from a 50 Ω transmitter, to these radiating termination resistors at the ends of the lines. This circuit model can give us some insight of how to do this effectively.

Near-Field Characteristics

Now that we have examined both the far field pattern and the feed characteristics let's turn to see what sorts of fields are present very close to the elements of this dipole. We call this region close to the antenna the "near field." Figure 8 shows four different near field plots produced by *4NEC2*, solving Maxwell's equations. For these plots the vertical dipole is centered on the left edge of the plot and color is used to indicate field intensity. [Since

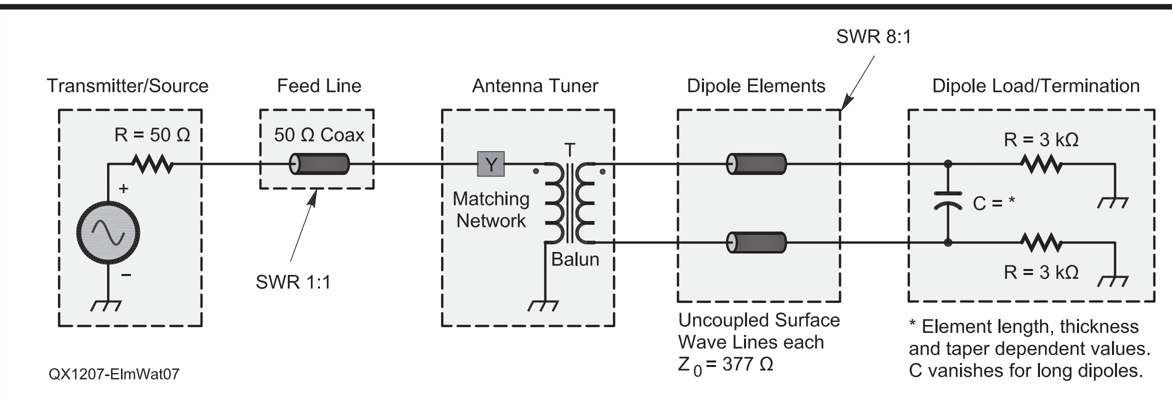

Figure 7 — A simple schematic model for matching a center-fed dipole to a radio receiver or transmitter.

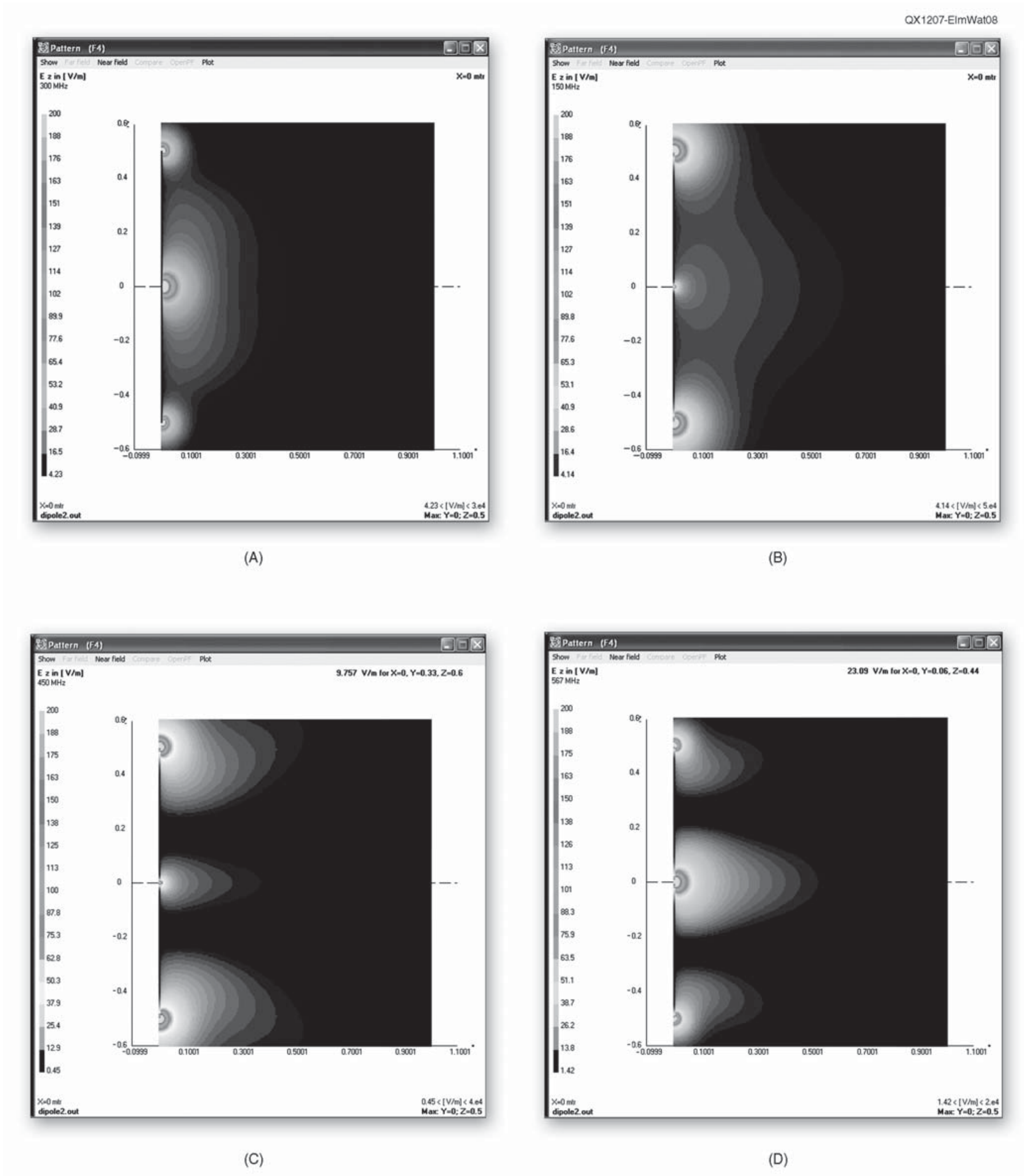

Figure 8 — Longitudinal electric field strength in the vicinity of a center-fed dipole. Various antenna sizes (in wavelengths) are shown here. The antenna is located at the left edge of each plot and color is used to represent field strength. Notice that the only significant "hot spots" are at the tips of the dipole and, for some lengths, at the center.

we can't print color in *QEX*, it will appear as gray shading here. I will put the original color screen captures on the ARRL *QEX* files website. Go to **www.arrl.org/qexfiles** and look for the file **7x12_Elmore.zip**. — *Ed.*][2] Only the electric field parallel to the dipole conductor is shown for this center fed dipole driven at different frequencies. We're calling this field direction the E_z direction. This is not the total electric field. There are other components coming away from the dipole at right angles to the elements, the E_x and E_y directions. We can, however, take advantage of something we know from the analytical solution mentioned at the beginning. In the far field, due to symmetry and cancellation, E_x and E_y each become zero and may be ignored. Both common experience and analytical theory tell us that at great distance a vertical antenna radiates only a vertically polarized signal. This simplifies the display and allows us to see something else of interest — significant E_z components are present only at the element ends and (sometimes) at the center of the dipole.

Putting It Together — A New Interpretive Model

As a result of these observations about the patterns, impedances and fields associated with a dipole it is possible to form a new interpretive model of how an antenna acts when it is fed, and how it radiates. Since there is a central plane of symmetry, this model can also be applied to a monopole having an image plane, a vertical working against an infinite ground plane.

The Antenna as a Wave Device

We saw from the impedance information plotted on a Smith chart that the dipole acted like a transmission line with a relatively high SWR, that is, with forward and reflected waves. Figure 9 fills out this description. In it, two oppositely directed and opposite phase waves flow from the feed point at the center toward the tips. A wave model is just an alternative to using voltages and currents for considering power flow. Here, the feed is shown as a voltage source split into two equal parts to emphasize the plane of symmetry that exists at the center. At this point, now switching to the wave model, waves begin and continue along the antenna elements, which act just like transmission lines. When the waves reach the mismatch at the element end some power is coupled into the radiating Tip region, where the radiation resistance is located, but most of the wave is reflected back toward the center. By recognizing that the dipole is symmetric and that the waves in the two halves are opposite, both in phase and direction, it is easy to see that the regions of radiation at the tips are equal in both phase and magnitude.

Depending upon element length, at the center of the dipole the reflected waves may or may not be phased so as to add with the source wave to produce a third radiating field. For a half wave dipole, or actually any dipole that is an odd number of half waves long, the returning waves exhibit about 180° of phase reversal and mostly cancel with the outgoing waves produced by the voltage sources at the center. I say "mostly" because the reflected wave is slightly smaller than the outbound one, some of the power in the outbound wave was radiated away at the element tip. It is the phasing of these reflected waves, determined by the element length that produce the alternating low and high impedance resonances that are so familiar to us. For the half wave dipole the radiation source at the center produces only a small contribution to the far field pattern, as shown in Figure 8A and 8C. For other antenna lengths there can be significant contribution to the far field pattern from this central electric field source. At an antenna size of about 1.9 wavelengths, in the broadside direction the phase and magnitude of this central source just cancel the combined sources at the tips. It is this cancellation that produces the broadside nulls and beam splitting shown in Figures 2 and 3.

Surprisingly, the antenna element conductors themselves act like 377 Ω transmission lines that don't radiate at all! This type of line is called a surface wave transmission line (SWTL) and construction and use of practical lines of this type for amateur purposes has been described, as has been a more theoretical and historical description.[3, 4] The antenna elements can be thought of as transmission line matching elements, transformers or "resonators" that exhibit significant *Q*.

The areas producing the radiation are located in the space just beyond the ends of the SWTL, the dipole tips, and sometimes at the center of the dipole. This "wave model" of a dipole helps to make clear how and why the harmonic characteristics of a dipole are produced.

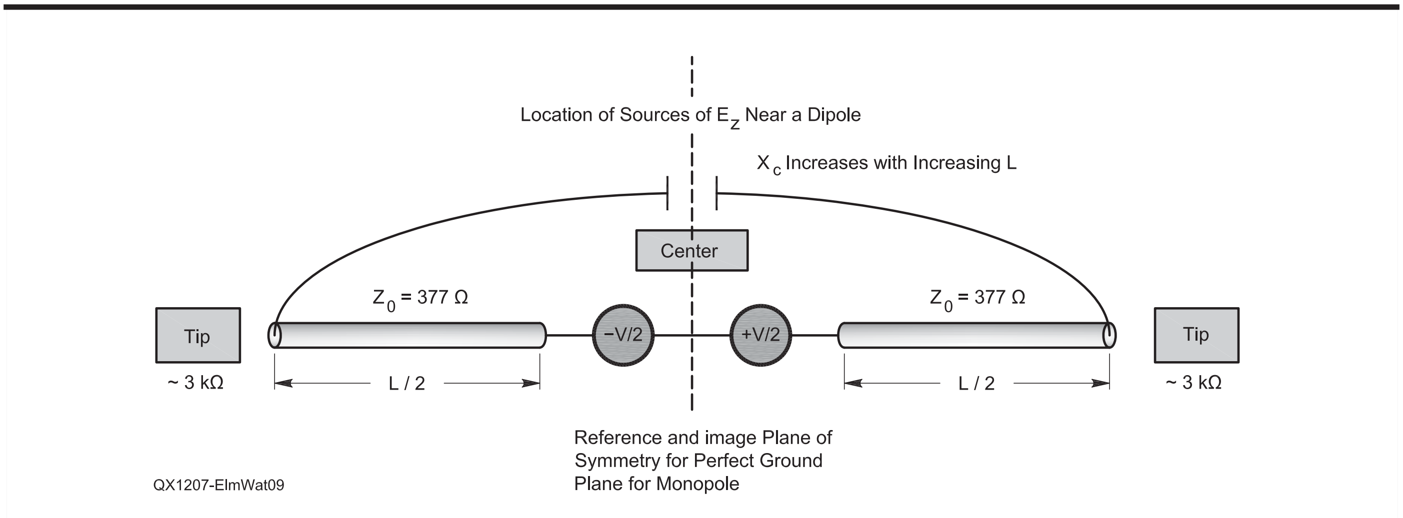

Figure 9 — Considering both the feed-point characteristics and the far field radiation pattern, a thin center-fed dipole can be modeled as a simple structure. The dipole elements themselves do not radiate but act as 377 Ω surface wave transmission lines. Radiation occurs near the element tips and, depending upon the element electrical length, sometimes near the center as well. The feed-point impedance is the same as if the transmission lines were connected to approximately 3 kΩ loads and each operating with an SWR of 8:1. For short dipoles, generally those under a wavelength in length, there is an additional capacitive load that appears between the element tips. This effect becomes small as the dipole gets electrically large.

Waves on a SWTL produce a longitudinal electric field; longitudinal electric lines of force that begin and terminate on the conductor itself. This wave is said to have transverse magnetic (TM) fields. Compare this to conventional coaxial cable, which operates mostly in transverse electromagnetic (TEM) mode and has both electric and magnetic fields that are transverse to the direction of propagation. TM mode has components of the electric field in the direction of propagation but magnetic fields are only transverse. To fully support a wave in this mode requires a line at least one half wave long. In practice, some extra length is often required to properly start (launch) the process. This condition is not fully met for short dipoles so they show a mixture of modes. Rather than all the electric field produced by the source going into generating a surface wave, some of the field lines terminate back on their "twin" in the other element of the dipole.

That a long thin antenna also behaves somewhat like a transmission line and resonator is hardly news, but that a dipole can behave like a 377 Ω mismatched surface wave transmission line terminated with two ~3 kΩ loads may be something that you haven't heard before.[5]

The far field radiation pattern and the impedance of a center-fed dipole (or monopole) can be modeled as due to sources of longitudinal electric field at the ends and feed point. At the tips, these regions act as the mismatched loads to non-radiating surface wave transmission lines. For short dipoles, the lines are slightly coupled and the feed impedance is modified somewhat by a shunt coupling capacitance.

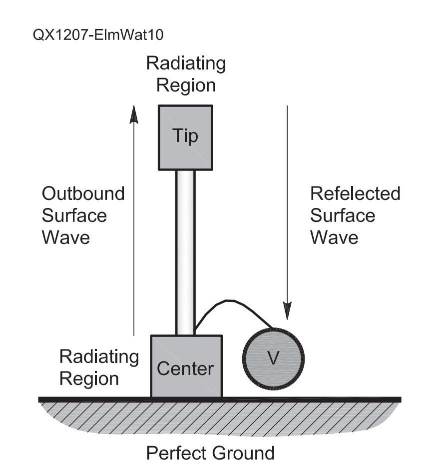

Figure 10 — The model shown in Figure 9 applies well to a monopole antenna operating over a good ground system. Since a plane of symmetry exists down the center of the structure, the resulting pattern for a monopole like this (a ground plane antenna) is the same and because there is twice as much current for the same feed-point voltage, the impedance is one half that of the dipole.

Wrapping It Up

While Figure 9 shows a new model that describes a dipole in an intuitive way, if you're like me, something simpler, with fewer pieces, may be easier to picture and remember. Toward that end, Figure 10 shows only one half of the dipole but includes the perfect ground plane already mentioned. It really is just Figure 9 laid on its side with only the top element and ground plane remaining. Because of the symmetry and function of the image plane, this is fair to do. What we have is simply a vertical antenna, fed from the bottom against a perfect ground. As shown, power from the source propagates in a wave along the element without radiating. When the wave reaches the top, some of it is coupled into a region of radiation having a relatively high radiation resistance compared to the impedance of the line. The majority of the wave reflects off of this mismatch and returns toward the feed point. At the feed-point, the forward wave and the slightly diminished reflected wave add together and, depending upon the phasing produced by the out-and-back travel, may add together to either nearly cancel or else produce another significant source of radiation similar to the one at the top.

If you can remember this model for a monopole with its image plane, you also have the model for a dipole by just "looking in the mirror".

If you've read this far but you're still wondering "Why do we need another model?" read a bit more and perhaps you will find that this new model provides an intuitive way to understand familiar antennas and to get some new insight into how to best use them.

A Practical Application – A Very Broadband Vertical

Hopefully this new antenna model provides an intuitive way for understanding the

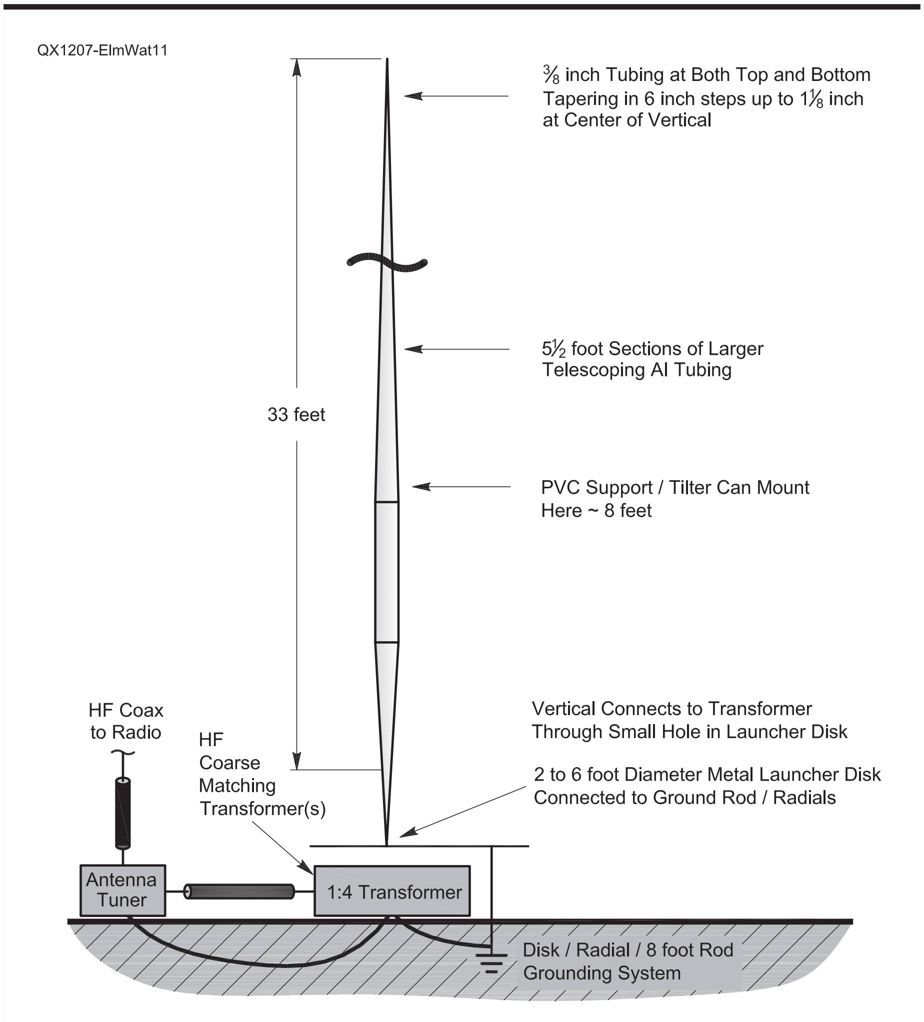

Figure 11 — A practical application of the new antenna model makes a general coverage, 7 MHz to 432+ MHz vertical antenna possible.

feed-point impedance and the radiation characteristics of a very thin, perfectly conducting center-fed dipole or monopole. To help this model be a bit more practical, let's look at a real vertical monopole antenna that you can easily build. This vertical can be used at any frequency between 7 MHz and 432 MHz and even beyond, to produce a good match and radiation performance.

The antenna shown in Figure 11 is approximately 33 feet high and made from 6 foot long aluminum tubing sections that can "nest" together. It's quite similar to the usual quarter wave 40 m vertical. One slight difference is that these sections vary in diameter from ⅜ inch at the top and bottom to 1⅛ inch near the middle. The larger middle sections overlap only about 6 inches and provide most of the length. The remainder of the length is made up by tapering down quickly near the ends with smaller tubing in 6 inch steps. Because these ends are not very strong, the whole structure is supported by an insulator made from 2 inch PVC pipe fittings located about 8 feet from the ground end. For grounding, an 8 foot ground rod is used, and in addition to this ground rod, immediately under this vertical antenna, there is a 2 foot diameter metal foil disk. For the measurement shown, this was simply a plywood disk covered with aluminum foil. This measurement was made by connecting a vector network analyzer to an SMA connector mounted at the center of the foil disk. The center pin of this connector attached to the bottom of the vertical and the disk and ground rod were connected together with a short piece of wire.

Figure 12 shows the measured feed impedance, displayed as S_{11} on a Smith chart having a reference impedance of 200 Ω. The plotted data shows measurement from 0.3 MHz to 250 MHz. The characteristic circles like those previously shown for the *4NEC2* model of the 1 meter dipole are obvious, but there is additional information present here too. Below approximately 50 MHz, the circles are not centered as nicely, they are a little ragged and they are shifted slightly to the right in the direction of higher impedance. Above this frequency they look cleaner, have nearly a common center and lie nicely on top of one another.

Figure 13 shows this same data displayed as the SWR that would be produced if the antenna was fed by a 200 Ω transmission line. As a practical matter, this "strange" impedance can be transformed with a 4:1 transformer to achieve the same results with 50 Ω coax and a 50 Ω SWR meter. Above about 6 MHz, where the antenna is not quite a quarter wave long, the SWR is around 6:1 or better. Above 90 MHz, where the disk apart from the ground and ground rod provides a better image plane, the SWR is always less than 4:1. This relatively small degree of mismatch can be easily handled by most antenna tuners. The 50 to 200 Ω transformer should have a minimum of stray reactance at the operating frequency. For very broadband usage, it may be necessary to use several different 4:1 transformers in order to get sufficient coverage. Both toroidal and transmission line transformers are good candidates, depending upon the frequency of operation.

This arrangement produces an antenna usable over most of the HF and even VHF amateur bands. For frequencies below

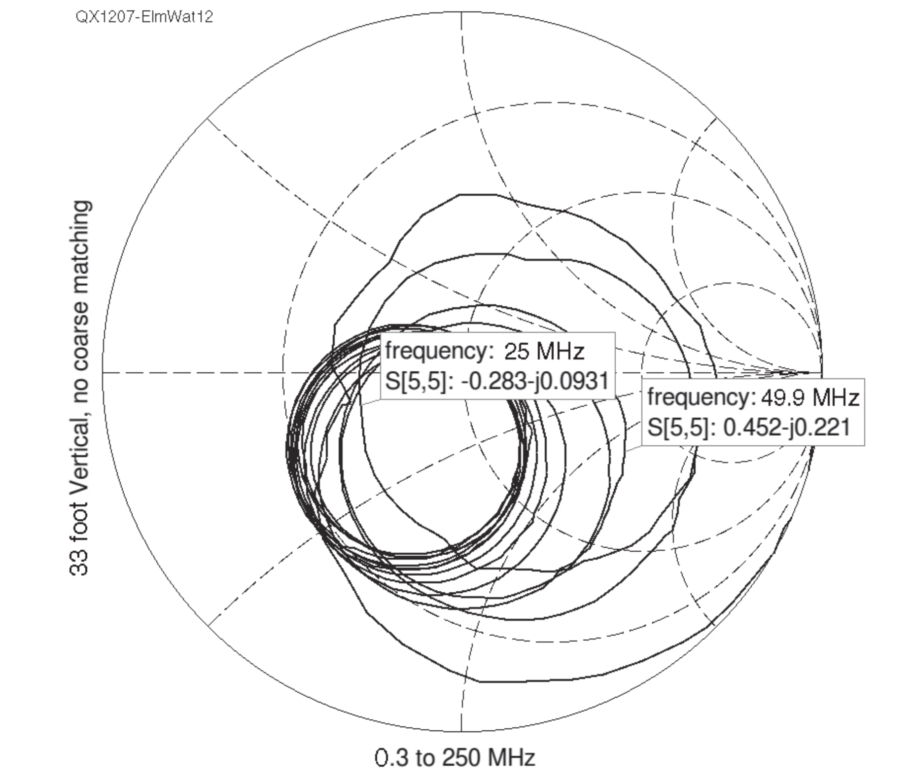

Figure 12 — Measured S_{11} parameters of a 33 foot monopole having tapered end sections. The monopole is mounted at ground level directly above an additional 2 foot diameter metal ground disk (launcher).

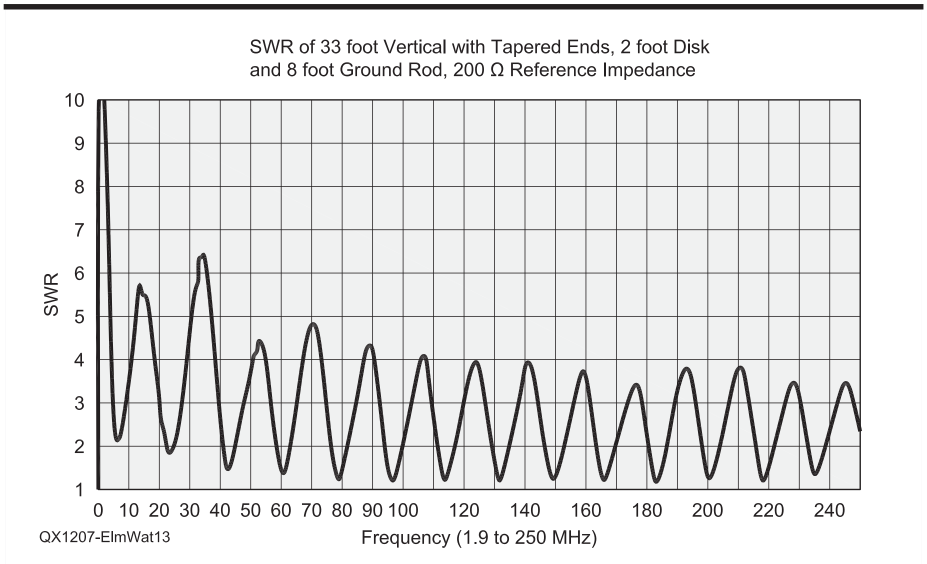

Figure 13 — Measured SWR of a 33 foot vertical with tapered ends with a reference impedance of 200 Ω. A 2 foot diameter ground launcher is used in conjunction with an 8 foot ground rod.

6 MHz, the impedance is capacitive and additional inductance may need to be added in order to get within the matching range of some antenna tuners. Even so, with relatively simple matching circuits and equipment, this simple vertical can effectively operate over a much larger frequency range than might be commonly thought.

The circumstances described here are those that amateurs encounter with any simple vertical, quarter wave or otherwise, with regard to ground rods, radials and counterpoises, but we are considering these from the viewpoint of the new model. We are also considering use over a much wider frequency range than you might have thought appropriate for a 40 m vertical.

By viewing this vertical as a length of mismatched surface wave transmission line, the ground, ground rod, and the metal disk combination can be thought of as a planar surface wave launcher. Launchers are devices that convert a different mode, in this case the TEM mode in the coaxial cable at the SMA connector, to the TM mode on a SWTL.[3] Here, that launcher is the combination of the ground, the ground rod and the disk. The disk portion has much higher conductivity, however, and is a better defined plane than the ground rod and the sod under and around the antenna. Above about 90 MHz, this 2 foot disk is completely sufficient to effectively launch a surface wave. Below that, the ground beyond the 1 foot radius limits of the disk becomes involved and, because it is not so good, the impedance seen at the feed point rises due to ground losses and the effective ground depth. A larger disk, perhaps 6 feet in diameter could make things better from about the 20 meter band and higher.

This model also lets us see how to match to this vertical everywhere, not just near a resonance and it gives us a better understanding of the radiation pattern we should expect at any frequency.

Thinking of the antenna element as a SWTL also gives some practical insight into mounting an antenna at a typical QTH. SWTL theory indicates that the vast majority of the power propagated along the line is very near the surface, within a few conductor diameters of the line. Combined with what we saw about regions of radiation, we have a good indication that a thin vertical antenna at a low-impedance resonance might actually be operated very successfully as long as only the immediate space around it is kept clear and the tip can stick up above absorbers and clutter. It may not be necessary to have a large flat open space to get good results.

Remember that a trade-off with low-impedance operation is that a better ground system is required. A vertical operated at the high-impedance resonance with a lot of foliage near the bottom and the top clear might lose significant efficiency because of absorption of the energy radiating from the bottom.

By using this new model we have found a way to match and use a conventional vertical antenna over a very broad range of frequencies rather than only at a resonance. The model has shown us a way to couple transmitter power to the radiating regions of space near the antenna itself without requiring a particular length of element. It has also shown us an easier way to provide a reference ground point from which to feed it. While common wisdom has suggested that a quarter wave grounding system is important, you can see that at least for matching purposes, a good planar ground much smaller than a quarter wave, on the order of 5 to 10% of a wavelength radius, can actually be quite adequate. Note that we are only talking about feeding and effectively matching. By using a very good but smaller plane, ground losses can be avoided but this does not necessarily mean that the far field pattern of a vertical will be good at all take off angles. Particularly for low angles, the qualities of the ground quite far from the antenna base may be important. Our model is only addressing the problem of coupling power to the radiating part of the antenna structure. Far field radiation pattern and take off angle may be strongly affected by ground characteristics at much larger distances, where we have no access or ability to modify the ground.

An antenna of this sort can provide excellent performance over most of the amateur HF and VHF bands. At HF it works particularly well when operation near one of the familiar low-impedance resonances is avoided. Operating at higher impedance points reduces the antenna current and the equal image current in the ground system. This reduces the I^2R loss in the grounding system. At the 33 foot length shown here, only 40 m and 12 m are very close to a low-impedance resonance. Because this antenna does not depend upon a resonance to operate, however, you are free to adjust the length to accommodate different requirements.

For higher HF and VHF operation there is a trade-off here. Although the efficiency of feeding the antenna is better at the high-impedance resonance because of reduced ground losses, at these wave sizes the lower radiation point shown in Figure 13 is very significant — there is a lot of electric field at ground level. For many amateur locations, this can mean that more transmitter power is lost to foliage, buildings and other ground clutter. This is in contrast to the benefit of the radiation region at the top, which is likely to be furthest away from these absorbers and up where the signal is more likely to be radiated away. At antenna wave sizes that produce a low impedance feed point, this top point is dominant, but it may be possible to "have your cake and eat it too" in some situations. A length may be found that lets you set one of the low-impedance resonances on higher bands, say, 10, 6 or 2 m at the same time you achieve a high impedance resonance near 20 m. When used with a relatively small disk, of perhaps 2 to 3 foot radius, radiation on the higher band will occur primarily from the top while at 20 m the ground losses will still be quite low.

Obviously there are a lot of possibilities and an impedance measurement like that shown in Figure 12 should give you good guidance as to what lengths will or won't work the best. The markers placed at the 12 and 6 m bands illustrate this. An impedance bridge or vector network analyzer is probably required to do the best job of selecting the exact length. Of course, an alternative is to slightly adjust the length of the antenna between band changes to select a high impedance resonance for HF and a low impedance resonance for higher bands.

This antenna can perform well from 10 m through 450 MHz and even beyond, since it gets the radiation point well up in the air and away from absorbers. Measurements at N6GN show on the order of 10 dB better performance at 432 MHz as compared to a dipole or ground plane mounted at 10 feet. The "height gain" makes it work as well as a medium sized Yagi would if placed only at roof level. The biggest challenge to VHF operation seems to be providing a 4:1 transformer and low loss antenna tuner this high. Transmission line transformers are probably good candidates.

A related version of this antenna that can operate over an even broader frequency range by also using the HF vertical conductor as a SWTL having a bottom launcher to feed a top-mounted discone antenna with integrated launcher was presented at ARRL Pacificon in 2011, and will be published in *QEX* in an upcoming issue.[7]

Models

This article is meant to provide a model that is helpful for understanding how and why an antenna operates without requiring a thorough understanding of Maxwell's equations. George Box, an expert in quality control and modeling, once wrote "All models are wrong — but some are useful." Models are at the heart of the scientific method. In all scientific endeavors, it is important to remember that we are only using models. Remembering this helps keep us humble, keeps us from thinking we know all the answers and keeps us looking for better models.

Sometimes we use more than one model, even overlapping and potentially conflicting models, to describe our world. The two different models for describing light, the wave model and the particle model, are an example of this. While they seem at odds with one another, each is extremely useful for describing certain aspects of measurement and observation in situations where the other doesn't work so well.

A good model should be useful to:

1) Describe the Known — A good model accurately describes what we already know and experience. It fits our observations.

The antenna model described here does a good job at explaining what we already know about the radiation pattern and the feed-point characteristics of a common center-fed dipole. It provides a method for intuitively grasping what an antenna does.

2) Point to New Possibilities — A good model should provide something previous models don't. It should enable new understandings and indicate new applications.

This model has already pointed to some new possibilities. Hopefully the SWTL previously described and the All Band antenna to be presented in a future issue of *QEX* will prove useful to radio amateurs. It may be that this new model may also be useful for better understanding how other antennas, such as the Beverage or "Wave Antenna" work. Recognizing that this antenna is a slightly unbalanced, terminated SWTL and that it acts very much like a directional coupler to an incoming sky wave signal might lead to new ways of using this old favorite for efficient transmit as well as receive.[6]

3) Make Us Ask Questions that Lead to Better Models — A good model should cause us to seek even better models. It should raise questions or raise possibilities that point us to explore further and better. A good model can provide the seeds of its own replacement.

This model also makes us ask questions. For example, Maxwellian field theory provides us with the tools to examine the effects due to the moving charge (current) in an antenna. This theory only deals with the charge of an electron and not the mass. Recognizing that a long dipole acts as a wave device with little or no coupling between the halves invites a question.

We know from other areas of physics that the charge and mass of an electron are inseparable, the presence of a "current column" due to moving charge on a dipole would seem to be associated with the presence of a "momentum column" due to the moving mass of the electron carriers. From physics we believe that in any closed system, momentum is always conserved. Since we see that the electron current at the ends of a dipole is zero and that for a long dipole there is insignificant coupling between the elements, isn't the wave on each element in a closed system? If the displacement field and displacement current provided by Maxwell are necessary to provide continuity of the magnetic field, is there not a need for a parallel device — a "displacement field for momentum" to account for conservation of momentum on an antenna? Is there an associated "momentum field" or "momentum wave" emanating from the tip of a dipole?

Whether there is a simple answer to this from classical mechanics, a vector potential analysis, one from quantum electrodynamics that explains an antenna as a quantum device, or whether some other explanation is required, hopefully the process of discovering the answer will prove to be useful to generate new applications.[8] Maybe this model of a dipole as a surface wave device will even prove to be useful enough to be replaced by a better one.

Glenn Elmore, N6GN, has been a licensed Radio Amateur for the past 50 years, and has held call signs of WV6STS, WA6STS and now N6GN. He has held an Amateur Extra class license since 1972. For most of his working career, Glenn has been an electrical engineer involved with the design of RF and microwave test and measurement equipment, notably scalar, vector network and spectrum analyzers.

Glenn's Amateur Radio interests have included weak signal VHF/microwave operation including meteor scatter, EME, terrestrial DX as well as higher speed Amateur TCP/IP radios and networks. He has recently been active on WSPR, the weak signal reporting network. Glenn is an ARRL Member.

Notes

[1]You can download a copy of 4NEC2 at **http://home.ict.nl/~arivoors/Home.htm**.

[2]The color plots for Figure 8 are available for download from the ARRL QEX files website. Go to **www.arrl.org/qexfiles** and look for the file **7x12_Elmore.zip**.

[3]Glenn Elmore, N6GN, John Watrous, K6PZB, "A Surface Wave Transmission Line," May/Jun 2012 *QEX*. pp 3-9.

[4]Glenn Elmore, N6GN, *Introduction to the Propagating Wave on a Single Conductor*, 2009, **www.corridorsystems.com/FullArticle.pdf**.

[5]John Kraus, W8JK, *Antennas*, McGraw-Hill 1950, Chapter 1. "Thus, a single device, in this case the dipole, exhibits simultaneously properties characteristic of an antenna, a transmission line, and a resonator."

[6]Beverage, Kellogg, Rice, "The Wave Antenna," *Transactions of the AIEE*, Feb 1923, p 215.

[7]Glenn Elmore, N6GN, John Watrous K6PZB, "*An All-Band Antenna*," ARRL Pacificon, 2011.

[8]Natalia Nikolova and Robert Zimmerman, *Detection of the TIme-Dependant Electromagnetic Potential at 1.3 GHz*, II.A. McMaster University, CEM-R-46, Nov 2007.

Sivan Toledo, 4X6IZ

School of Computer Science, Tel-Aviv University, Tel-Aviv 69978, Israel; **stoledo@tau.ac.il**

A High-Performance Sound-Card AX.25 Modem

The author leads us through the process of fixing several known problems with AX.25 modems, leading to a new software modem.

I had been running an APRS RF-to-internet gateway (an iGate) for a few months using a sound-card modem by Thomas Sailer, HB9JNX/AE4WA, (soundmodem).[1] The software modem caused various problems and I have not found a suitable replacement. Eventually, I decided to try to implement my own sound-card-based software modem. The results have been very good, in spite of the fact that I do not have much background in digital signal processing.

This article describes the problems with current AX.25 software modems, the design methodology I followed in implementing the new modem, and of course, the resulting software. The methodology is particularly important; it has allowed me to design and implement a high-performance modem with little background in digital processing and absolutely no background or experience in designing digital decoders.

Figure 1 — This graph shows a piece of the audio I recorded from an AX.25 packet I received from a nearby station. The 2200 Hz tone amplitude is much lower than the 1200 Hz tone amplitude. Various software modems that I tried were unable to decode these packets.

Existing AX.25 Modems: Some Software, Some Hardware

VHF APRS uses AX.25 packets with 1200 baud audio frequency shift keying (AFSK) modulation. Binary ones are represented by a continuous tune, either 1200 or 2200 Hz, and zeros are represented by a switch from one of these tones to the other. This modulation scheme is based on the Bell 202 telephone modem standard from around 1980.

Three types of modems are in wide use in APRS systems today. One type uses a dedicated modem integrated circuit (IC), the mx614.[2] There is not a wide selection of 1200 baud modem ICs in production today. The IC is only responsible for generating the tones and for deciding which tone is present at any given time. In mx614-based modems, such as John Hansen's X-TNC and the OpenTracker series, the modem IC is connected to a microcontroller that determines the symbol timing, extracts the packet bit stream, and checks the packet for integrity. In many APRS systems the same microcontroller also performs other functions, such as converting GPS sentences to APRS messages.

In the second type of modem, the microcontroller is also used for modulation and demodulation, using its built-in analog-to-digital converter and a resistor-network digital-to-analog converter. Bob Ball's TNC, Byon Garrabrant's TinyTrak series, Scott Miller's OpenTracker series, and Robert Marshall's Arduino-based TNC all belong to this group.[3, 4, 5]

Modems in the third group run on a PC and rely on a sound card to transfer audio between the radio and the computer: Thomas Sailer's soundmodem and multimon, George Rossopoylos's AGWPE, Frank Perkins' AX.25-SCS, and Andrei Kopanchuk's recent modem (which I was not aware of when I started this project).[6, 7, 8, 9, 10]

Decoding and Interfacing Problems with Existing Software Modems

I faced two types of problems with the sound-card-based software modems that I tried. I started with AGWPE, connected through a homebrewed computer/radio interface to a Yaesu FT-857D. The software generated packets that nearby stations

[1]Notes appear on page 25.

were able to decode, but it could not decode packets from the same stations. I switched to AX.25-SCS, but the results were similar. I recorded the audio of several packets from stations that the modems could not decode and discovered that the amplitude of the 2200 Hz tone was much lower than the amplitude of the 1200 Hz tone, as you can see in Figure 1.

This turned out to be what caused difficulties to both AGWPE and AX.25-SCS. I switched to a different sound-card interface, which apparently does not attenuate high-frequencies as much, and both modems were able to decode many more packets. You may say that the first sound-card interface is simply not good enough, but AX.25 is modulated using *frequency* shift keying, so in theory, the demodulator should not be sensitive to amplitude variations.

It appears that soundmodem suffers from similar problems. When fed by an old Kenwood TR-2500, it decoded packets just fine, but when I switch to a Motorola radio (a PageTrac, in which the radio is the same as in the more common MaxTrac radios), it failed to decode most packets.

All of these modems need to interface to both a sound card and an AX.25 or APRS program. I also faced problems in this area. AX.25-SCS does not allow you to select a sound card, so I could not use it with an external high-quality sound card. Both of these programs, as well as the new UZ7HO modem, are *Windows*-only programs, so I could not use them in my *Linux*-based APRS iGate. Soundmodem does work under *Linux*, but interfacing it to Pete Loveall's *javAPRSSrvr* proved challenging.[11] I initially tried to interface the two programs using a virtual serial port, but *javAPRSSrvr* kept complaining that soundmodem was closing the serial port. I then interfaced them using the *Linux* kernel's support for AX.25 networking; this approach is somewhat more complicated, but it did work reliably. Either way, soundmodem must be started before *javAPRSSrvr*, otherwise *javAPRSSrvr* fails to find the virtual serial port or the AX.25 kernel interface.

In spite of these problems, I was able to find a working reliable configuration. A Kenwood TR-2500 fed soundmodem, which fed *javAPRSSrvr* through the *Linux* kernel's AX.25 support. This setup worked fine for a few months, but when I switched to the Motorola PageTrac and discovered that soundmodem would not decode packets received by it, I decided to try to design and implement a better AX.25 sound-card modem. I did not have much experience in digital-signal processing (DSP), but I decided to learn the necessary tools and to try to implement a good modem.

Pre-Emphasis and De-Emphasis

Before describing the modem and how I designed it, it is worth explaining why the amplitudes of the 1200 Hz and 2200 Hz tones in received packets often vary significantly. In FM voice communication, the transmitter pre-emphasizes high tones by 6 dB per octave. That is, it amplifies high audio frequencies more than it amplifies low frequencies, which results in wider deviation for high tones. To compensate, the receiver de-emphasizes the received audio by the same amount, to make the audio sound natural. This scheme originated in the use of phase modulators rather than frequency modulators, but it is still useful today because the de-emphasis in the receiver cuts down annoying high-frequency noise (hiss).

If all transmitters and receivers adhered precisely to the 6 dB/octave curve, and if all AX.25 modems were interfaced to the pre/de-emphasized audio path, we would not see any amplitude variations between the two tones. But some radios do not adhere precisely to the 6 dB/octave curve, and some radios interface the AX.25 modem directly to the modulator and/or discriminator, bypassing the pre/de-emphasis circuits. To make things even more complicated, some modems pre/de-emphasize the audio too, in an attempt to compensate for the radio.

The outcome of all of this is that no matter what you do at the receiving end, your AX.25 demodulator is going to see packets with amplitude variations between the tones. It is, therefore, important for the demodulator to be able to cope with such variations.

A Design and Evaluation Methodology

To design the modem and to evaluate how well it works, I used a methodology that is somewhat different from the methodology used in many other amateur projects.

One aspect of the methodology is the use of *Matlab* to do much of the design. I intended to write the modem in *Java* or *C* (I settled on *Java*), but for the initial prototyping I used *Matlab*, an interactive technical computing environment with excellent support for plotting graphs, for DSP, and for reading wav files (sound recordings). *Matlab* has other features, of course, but these three were important in this project.

I started by recording packets off the air, some from stations that I knew are hard to decode and some from stations that I knew were easy to decode. I recorded segments of about 5 minutes that I knew were likely to contain beacon packets (digipeaters tend to beacon at fixed intervals) and trimmed the audio using *Audacity*, a free cross-platform sound editor.[12]

I then started to develop the DSP algorithm, testing it on the recorded packets after every modification. The behavior of the code on the recorded packets helped me understand the DSP techniques that are used in modems, and it eventually showed that my demodulator was working. The ability to plot signals that are derived within the algorithm from the input audio, in particular, was crucial; it really helped me understand what works and what does not work. You will see some of these plots below, and I hope that you will agree that they do indeed provide insight as to how the algorithm works. The plots shown below are static; you cannot zoom in and out, select which time series appear on each plot, and so on. In *Matlab*, the plots are interactive, and hence even more useful.

My experience with AGWPE, AX.25-SCS, and soundmodem taught me that a modem that can decode a few packets from particular transmitter/receiver combinations can still fail on other transmitter/receiver combinations.

This brings us to the second aspect of the methodology: the use of Stephen Smith's APRS test CD.[13] This CD consists of several recordings of APRS traffic. The first two tracks on the CD are the most useful ones for evaluating modems. The first track is a recording of about 40 minutes of APRS traffic in Los Angeles, consisting of more than 900 packets from many different radios and modems. This track is a recording of the discriminator output of a radio, with no de-emphasis. The second track contains the same audio, but it is accurately de-emphasized by 6 dB/octave. If a modem works well on both tracks, it is likely to work well with most radios.

The test CD has been critical in optimizing the ability of my modem to decode packets. I ran the entire first two tracks through variations of my modem many times. From each such run, I would note the number of decoded packets from each track. This allowed me to test different filters and algorithms and to understand how different parameters of the algorithm affect its performance.

Using a real-world workload (sometimes called a benchmark) to monitor the evolution of a system as it is being optimized, and to compare systems is not new, of course. Stephen Smith made the test CD available precisely for this purpose. I learned of the CD from the website of Robert Marshall, who used it to compare his microcontroller-based AX.25 modem to several existing modems (his results, while perhaps not completely scientific, show that AGWPE and soundmodem indeed perform quite poorly).[14] The fact that the methodology is not new does not mean that it is widely used. It is not, usually because a suitable large and representative workload is not available. For example, Bob Ball, who designed his AX.25 modem before the test CD was available, described the performance of his modem in the following way: "My units routinely decode packets that are less than 1 S unit on my 2 meter radio from stations over 75 miles away." This is useful information, but quantitative information on a standard workload is much more informative.

The Design of the Modem

An AX.25 modem consists of a transmit path and a receive path that are almost unrelated (apart from decisions as to when to transmit, which are based on whether a packet is correctly being received). The transmit path currently consistists of an *encoder*, which encodes an AX.25 packet into a bit stream, and a *modulator*, which turns the bit stream into audio samples at a particular sample rate. Similarly, the receive part consist of a *demodulator* that transforms audio samples into bits, and a *decoder* that transforms the bits into packets (or drops them, if the packet was not received correctly in its entirety).

The encoder and decoder algorithms are completely described by the AX.25 specifications and they have been explained in many articles, so I will not describe them here. All that is important here is that the bit sequence that makes up a packet is *bit-stuffed*; if five ones appear in a row, a zero is inserted by the encoder (and dropped by the decoder) in order to ensure that zeros are not too rare. Another important piece of information is that *flag* bytes (hexadecimal 7E) surround each packet, and they are not bit stuffed, which means that if the decoder sees six ones in a row, it must be either a flag or just noise.

The modulator transforms the bit-stuffed sequence into audio. This is done using a *phase-continuous digital resonator* that runs at either 1200 Hz or 2200 Hz. The resonator has one state variable, an angle (between 0 and 2π). To produce a sample at 1200 Hz, the resonator outputs sin (α) and advances α by $2\pi / (f_S / 1200)$, where f_S is the sampling frequency. To produce a sample at 2200 Hz, the resonator outputs sin (α) and advances α by $2\pi / (f_S / 2200)$. This is pretty simple. The demodulator is more interesting.

Time-Domain Filtering and Emphasizing

The processing of incoming signal samples starts with a filter that filters out some of the energy in frequencies outside the 1200 to 2200 Hz range. The same filter can also emphasize the 2200 Hz tone by 6 dB relative to the 1200 Hz tone; this is an option that the modem uses sometimes, but not always; more on that later.

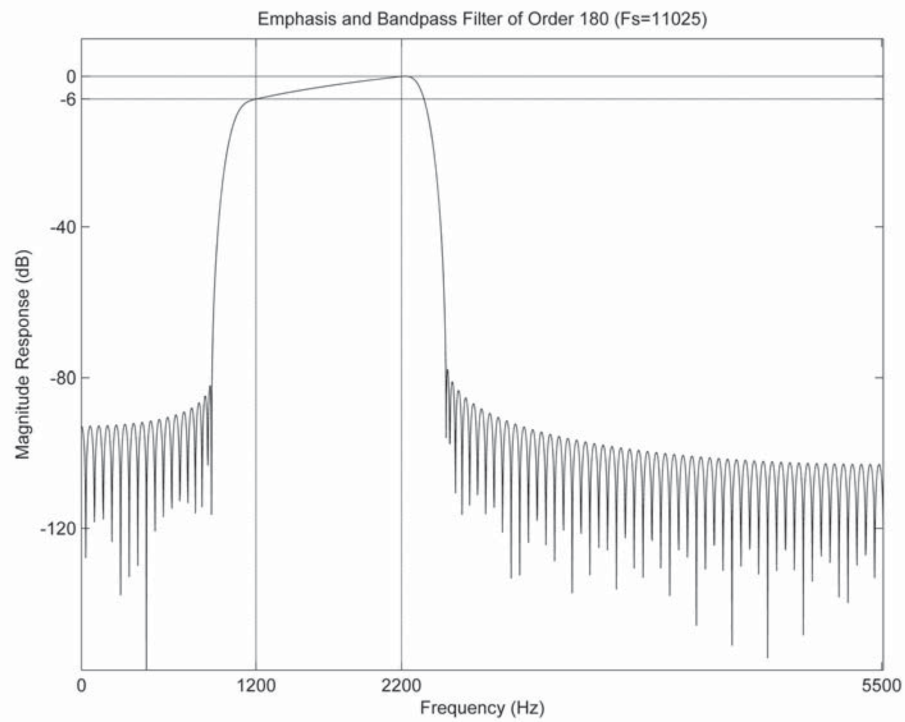

Figure 2 — Here is the response of the 900 to 2500 Hz high order (180) bandpass filter I created in *Matlab*. Note the 6 dB ramp up of the response across the passband, so there is no gain or attenuation at 2200 Hz.

Filtering out frequencies below 1200 Hz and above 2200 Hz is theoretically useless. I say theoretically because the filter is useless only if received noise obeys certain theoretical assumptions. But this filtering is cheap, harmless (even theoretically), and was found to be useful in some hardware-based modems, so I included it anyway.

We must not filter away energy in between 1200 Hz and 2200 Hz. During transitions from one tone to the other the signal contains energy in intermediate frequencies. If we filter these in-between frequencies, the filtered signal won't be able to switch from one tone to the other and will get stuck in one of the tones. I was initially not aware of this and learned this lesson the hard way: I produced a filter that essentially passed only 1200 Hz and 2200 Hz, and discovered that it strips away all the information in the signal!

The filter is an FIR filter that the modem applies in the time domain, by convolving the filter coefficients with incoming samples. I construct the filter in *Matlab* using the firls function, which constructs a filter whose frequency response matches a given response as well as possible given the filter order. The specification I have firls called for a complete attenuation of frequencies below 900 Hz and above 2500 Hz, with a 6 dB ramp-up from 1200 Hz to 2200 Hz, with no attenuation and no gain at 2200 Hz. Figure 2 shows what the frequency response of the filter looks like when we specify a high-order filter.

Applying high-order filters is expensive, however, and experiments showed that going to very high-orders does not improve the demodulator's performance (this is probably an outcome of the theoretical result I mentioned earlier). In practice, the demodulator uses filters whose order is twice the number of samples per symbol (that is, per $1/1200$ samples). The graph of Figure 3 shows the response of the actual filter that we use at f_S = 11,025. Compared to the order-180 filter, it looks fairly crude, but it still works well, as we'll see below. The response has a significant variation within the 1200 to 2200 Hz passband, but it still emphasizes the high tone by about 6 dB relative to the low tone.

Figure 4 shows a signal recorded off the air before and after this filtering. The sampling rate here is 48,000 samples per second, to give a high resolution. What we see is the flag (0×7E byte) just before the packet and the first data bits of the packet itself. In this case the original signal is fairly clean, so the filtered version is pretty close to the original, except for some attenuation and the elimination of dc. The filtering introduces a time delay.

Detecting the Tones Using Correlations

After filtering the signal, we try to detect which of the two tones was transmitted at every sample point. We do this by correlating the received samples with synthetic signals that the demodulator generates at the two tone frequencies over a period of one symbol.

Let us examine this computation in some more details. The demodulator generates f_S / 1200 samples of a sine and f_S / 1200 samples of a cosine, and stores them in two arrays, s and c. When processing a new received sample, the demodulator puts it in an array together with the previous (f_S / 1200) – 1 samples, in increasing time order. This is done efficiently by using the array as a cyclic buffer. Now the demodulator loops over the f_S / 1200 input samples and multiplies each one by the corresponding sine sample and the corresponding cosine sample. The products for the sine are added up and the products for the cosine are added up, the two sums are squared, the squares are added, and finally the square root of that sum is taken. This is the correlation value for the sample just received.

Formally, the correlation is an inner product of the received signal with a complex exponential function, but there is an easy way to understand why the correlation detects tones without resorting to complex numbers. If the incoming signal is at the frequency we correlate with and at the same phase as our synthetic sine, the sum of squares for the sine products will give a high value and the cosine will give a zero. If the phase corresponds to the cosine, the situation will be reversed, but the sum of the two sums of squares will be large either way. If the incoming signal's phase is somewhere in between, both the sine and the cosine will contribute to the correlation, and the correlation will still be high. The use of both a sine and a cosine essentially compensates for the fact that we have no idea what the phase of the received signal is. If the received signal's frequency does not match closely that of the sine and the cosine, the sample-by-sample products will produce both positive and negative numbers that will tend to cancel out; the overall correlation will be low. Figure 5 shows the two correlation signals for the signal shown in Figure 4. The correlation with 1200 Hz tends to be high when the 1200 Hz tone is present and low otherwise, and the correlation with 2200 Hz behaves just the opposite. They appear quite noisy, but nonetheless they contain very useful information.

Decision Making: Which Tone is More Dominant?

To decode the AX.25 bit stream, we need to find transitions between the two tones. This requires us to decide which tone is more dominant at every sample. As we can see from the computed correlations displayed in Figure 5, the correlation signal can be quite noisy; it is not easy to decide whether a particular tone is present or not. (The noisiness

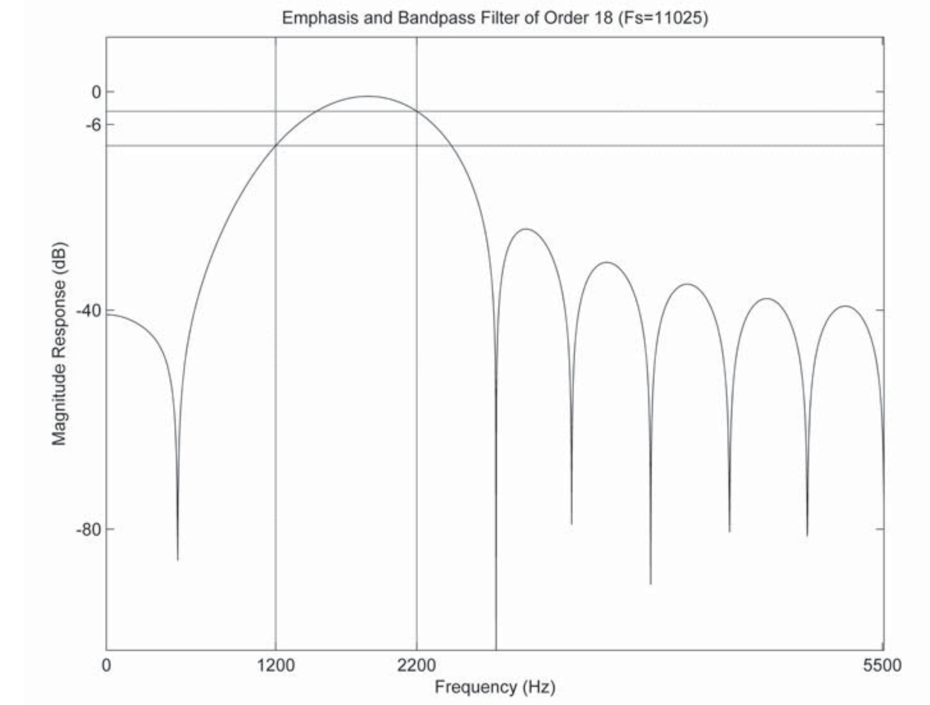

Figure 3 — This graph shows the response of a more practical low order (18) bandpass filter. It does not look nearly as good as the 180 order filter, and has a significant variation across the passband, it still emphasizes the high tone by about 6 dB.

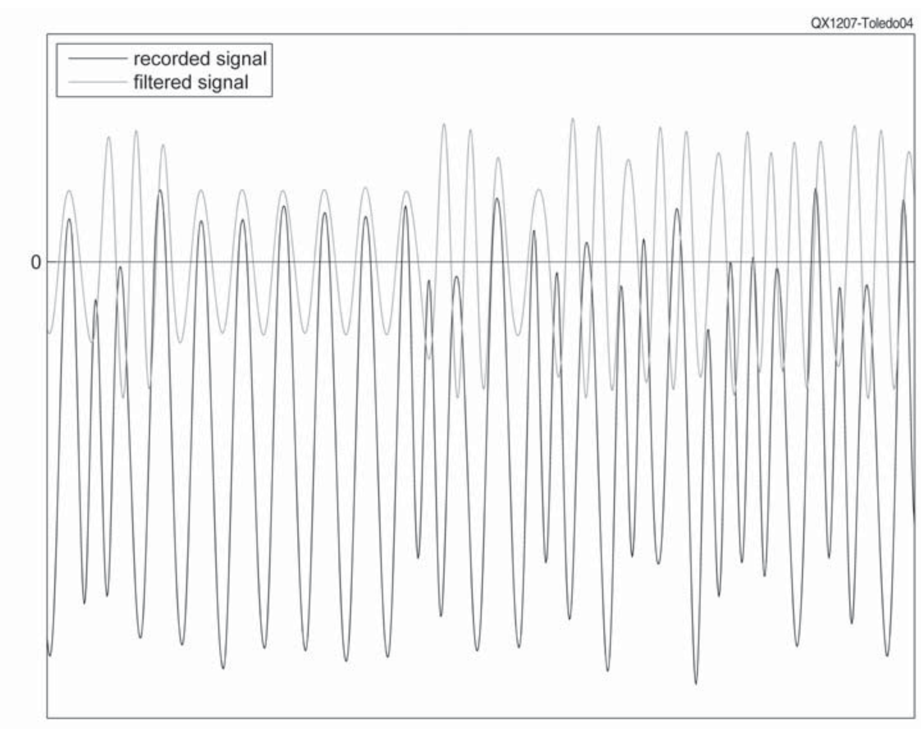

Figure 4 — Here is a graph of a signal recorded off the air, along with the filtered version after applying the bandpass filter of Figure 3. The filter has eliminated a dc component of the signal, but is a close representation of the original signal. You can also see that the filter has introduced a slight time delay.

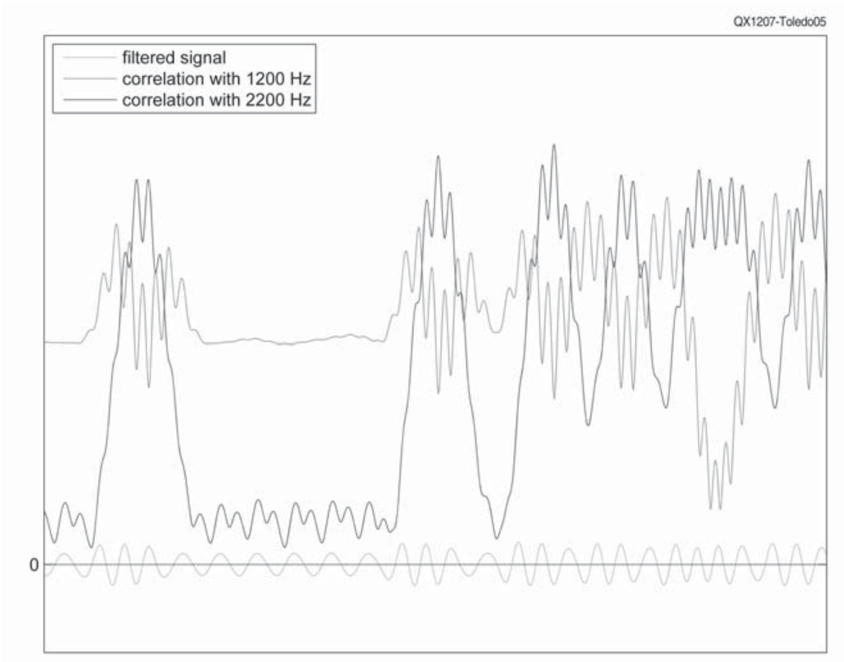

Figure 5 — Here we see the filtered signal, centered on the 0 line, along with the correlation signals for the 2200 Hz tone (highest when that tone is present and lowest when it is not) and the 1200 Hz tone (high when that tone is present, but not as low when it is not).

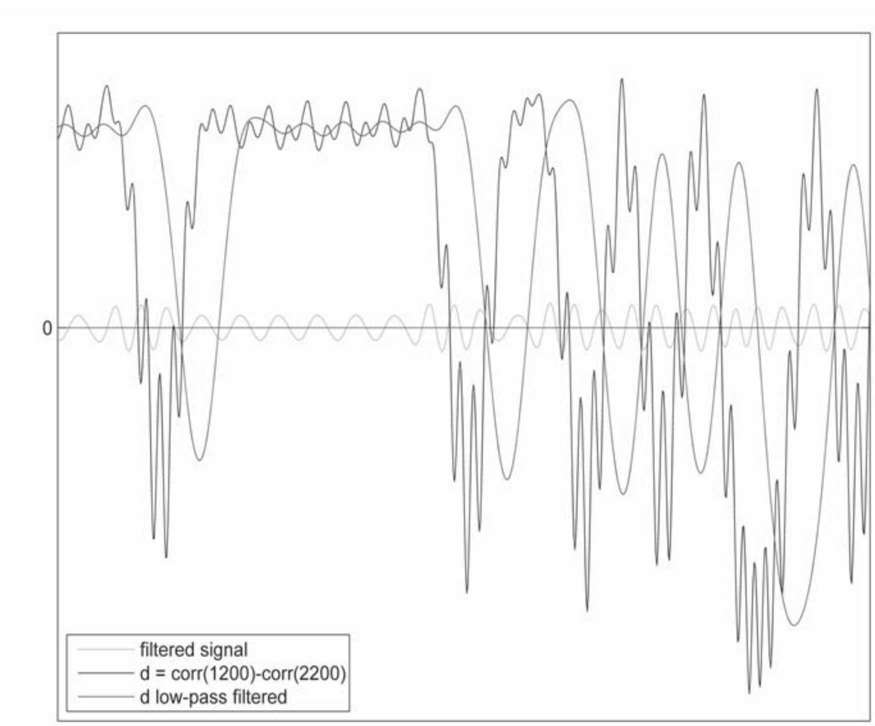

Figure 6 — This graph shows the filtered signal, centered on the 0 line, and the difference between the high and low tone correlation (the noisiest signal). After applying a low pass filter to the difference between tone correlations, we get the smoothed signal.

of the correlations is clearly evident in the 1200 Hz correlation; the 2200 Hz correlation is cleaner.) Deciding *which tone is stronger* is easier, however. We simply compare the two correlation signals and estimate which tone is present by selecting the stronger correlation. In the graph of Figure 6 we show the difference between the correlations; a positive value means that the 1200 Hz tone is stronger and a negative value means the 2200 Hz tone is stronger.

Like the correlation signals, the correlation-difference signal is also noisy. This makes it difficult to find the transitions between the two tones, because the high-frequency noise in the difference signal often causes several zero crossings to appear in quick succession. Fortunately, we know that tone transitions occur at most once every $^1/_{1200}$ of a second. Therefore, we can pass the correlation-difference signal through a 1200 Hz low-pass filter. The graph of Figure 6 shows that as expected, the low-pass filtering maintains the overall shape of the signal but removes the high-frequency noise and the spurious zero crossings that they generate.

The low pass filters that the demodulator uses have been constructed using the fir1 function in *Matlab*, which uses a Hamming window to construct the filter. The filter order is the same as that of the time-domain band-pass and emphasis filter, twice the number of samples in a symbol period.

Recovering the Bit Stream

At this point the demodulator can reliably determine the timing of transitions between the two tones. It is time to recover the AX.25 bit stream. The first step is to determine how many symbol periods separate consecutive transitions. The graph in Figure 7 shows the lengths of these periods in our signal.

Due to various potential sources of noise, the periods between estimated tone-transition times are not exactly integers, but they are close. The number of samples per symbol in this signal is 40, so an error of one sample is equivalent to an error of 0.025 symbol periods; we see that the errors in our processing of this signal are up to two samples.

At lower sample rates there are fewer samples per symbol. At 9600 samples per second, we have only 8 samples per symbol, but the method still works reliably. At 8000 samples per second, however, rounding errors become common and the method often fails. To avoid these errors at the 8000 samples/second rate, we interpolate the signal to 16000 samples/second and then decode it; this works reliably.

Detecting a transition 1 symbol period after another means that we have decoded a zero bit in the AX.25 bit stream; the modu-

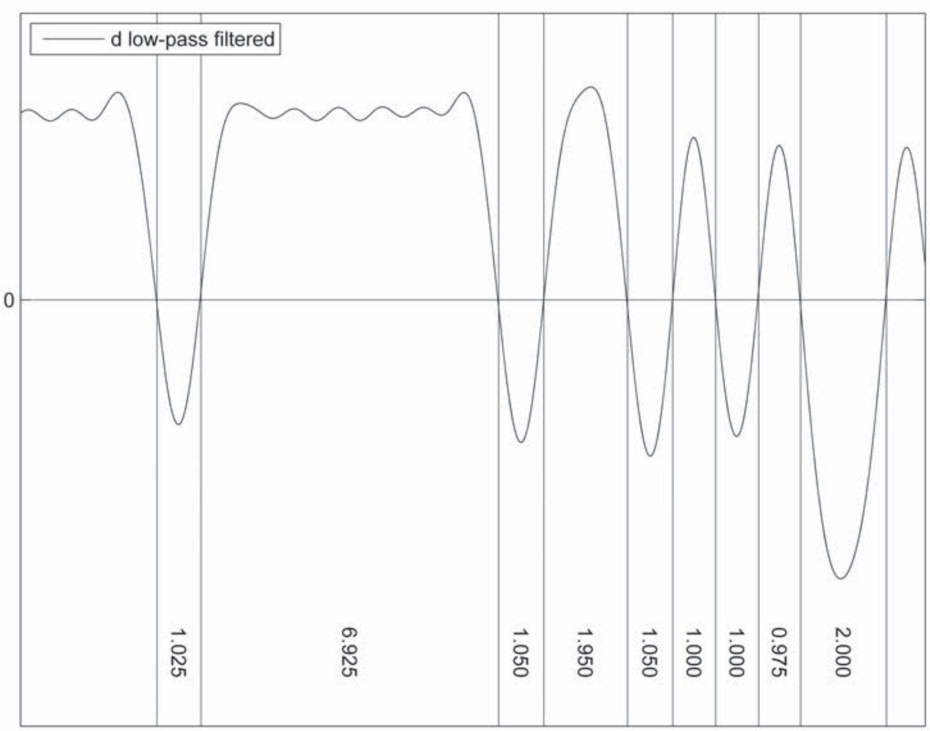

Figure 7 — Here is the low pass filtered signal from Figure 6. The symbol periods can easily be identified, so we can begin decoding the packet. Note that the longest time between transitions corresponds to 7 symbol periods, which represents a flag byte.

Table 1

		Track 1 (No De-emphasis)					*Track 2 (6 dB De-emphasis)*				
		8	*16*	*32*	*64*	*128*	*8*	*16*	*32*	*64*	*128*
Flat	11025	946	941	943	948	948	824	859	716	809	657
Filter	44100	436	937	967	961	961	77	418	891	856	760
Emphasis	11025	949	728	504	528	555	844	951	958	957	955
Filter	44100	439	938	966	927	524	76	539	895	945	959

lator sent a symbol for one period and then switched tones to indicate the zero. A transition after 2 periods means that we have decoded a one followed by a zero. Three periods decode into 2 ones and a zero, and so on up to 5 periods. When we detect a transition after 6 periods, we have decoded 5 ones but without a zero after them; a zero was stuffed into the bit stream to generate a transition so that the demodulator can stay synchronized with the modulator; the zero is not part of the AX.25 bit stream. When we detect a transition after 7 periods, we have decoded a flag byte, which might delineate a packet but is not part of a packet; we see such a flag in Figure 7 (the 6.925 periods get rounded to 7). A transition after more than 7.5 periods or less than half a period indicates a decoding error and causes the decoder to abort the current packet and to search for the flag that delineates the next packet.

Once we have decoded a supposed packet delineated by two flag bytes, the decoder checks the checksum value that is transmitted as the last two bytes of the packet. If the checksum is correct (it should be a specific function of the rest of the packet), the packet is considered valid and is passed to the client of the modem (typically an APRS program); otherwise the packet is discarded.

Optimizing the Demodulator

The demodulator's performance, both in terms of the amount of computation required and the ability to decode noisy and/or de-emphasized packets depends on the design of its two filters and on the sampling rate. The filters can be designed in many different ways: different filter orders, different cutoff and transition frequencies, and different filter-design algorithms. Understanding how all of these parameters affect the demodulator and how they interact is not easy, certainly not to people with limited background in DSP.

To address this issue, I performed many systematic experiments in which I tested different parameters on the first two tracks in the test CD. Table 1 shows some of the results of these experiments (it does not reflect exactly the performance of the final demodulator). The table shows the number of packets decoded from each track in two sample rates (11025 and 44100), with two types of time-domain filters (one with the same magnitude response at 1200 and 2200 Hz and the other with 6 dB emphasis), and at 5 filter orders (8 to 128).

We learn a lot from this table and from others like it. We see that filter orders that are much shorter than the number of samples per symbol lead to very poor performance. Filters of order 8 are fine for 11,025 samples/second but are terrible for 44,100. We see that a filter that is matched to the emphasis in the radio helps, but we also see that this is particularly true for filters of very high order; shorter filters often deliver good results in both tracks (for example, filter order 32 or 64 at 44100 samples/second).

Striking Twice to Hit Once

The realization that a flat filter is best on some signals and that an emphasized filter is best on others caused me some worries. I tried to come up with strategies to choose the correct filter; some of them were quite complex.

I eventually realized that I can avoid the choice altogether. I can feed the audio samples to two demodulator algorithms running in parallel. Sometimes both of them will decode a packet (and then a simple duplicate removal algorithm discards one of them). At other times only one will be able to decode a packet.

Running each audio sample through two copies of the demodulator is twice as expensive as running only one demodulator. On very weak computers (such as smart phones) this may be significant, but on desktops, laptops, and servers — even weak ones — the demodulator is cheap enough to run two copies in parallel. On a 1.6 GHz Intel Atom 330 computer (a relatively weak and slow CPU) running two demodulators in parallel on 11,025 samples / second audio uses only 8% of the CPU power.

Table 2 shows how many test-CD packets are decoded by the strike-twice-hit-once demodulator and by the two single-filter demodulators. We can see that using two demodulators with different filters is beneficial even compared to using a filter that matches the de-emphasis setting in the receiver; when there is a mismatch, the benefit is dramatic.

Software Design, Status, and Availability

One of the first choices that I made early

Table 2

	Track 1 (No De-emphasis)			Track 2 (6 dB De-emphasis)		
	Flat Filter	*Emphasized Filter*	*Both Filters*	*Flat Filter*	*Emphasized Filter*	*Both Filters*
8000	960	939	966	854	950	954
9600	964	686	966	854	957	958
44100	961	917	962	881	959	964

in this project was to completely decouple the signal-processing routines from the interface routines, mainly so that the modem could be used in different operating systems and environments. By interface routine I mean both the interface to the sound card and the interface to the modem client, typically an APRS program. The decision was partially based on an earlier experience trying to port parts of soundmodem from the *Linux*/*Windows* environment for which it was written to a microcontroller-based tracker. It was hard. Soundmodem does use a modular architecture, but still the separation between the modules was not clean enough to make separation easy.

The separation between the DSP routines and all the other software routine in the new modem is clean, which makes porting the DSP routines to new Java platforms and client environments easy.

The DSP routines are currently integrated into four different software environments. Three of these environments were written by me and I did the integration; somebody else authored the forth and integrated the modem into it. These environments are:

1) A command-line program to test the modem and to measure its performance. This program can generate packets into a sound card and can decode packets from either a sound card or a wav file.

2) *javAPRS*, an APRS iGate and digipeater software written by Pete Loveall.[15] *javAPRS* comes with interfaces to various types of hardware and software modems (serial TNCs, *Linux* kernel AX.25 support and AGWPE). I added support for my new modem, which can now run as an integral part of *javAPRS*.

3) An AGWPE emulator. This program does not implement the entire AGWPE TCP/IP protocol (which is not publicly documented, to the best of my knowledge), but it implements enough of it to support APRS client programs like APRSISCE.[16]

4) APRSdroid, an APRS client for Android phones and tablets written by Georg Lucas.[17] Georg integrated my modem into APRSdroid, reporting that the initial integration effort was easy and that the interface code (which did not include error checking at that point) consisted of only 50 lines. The audio processing mechanism in Android is completely different from the mechanism in *Java* running under *Windows*, *Linux*, and *Mac OS*; therefore, the ease of integration shows that the DSP routines in the modem are indeed well separated from the audio processing routines.

The modem has been running under *javAPRS* around the clock for a few months now as both an iGate and as a SatGate; both copies of *javAPRS* and the modem run on the same computer using two different sound cards (the internal one and an inexpensive USB sound card) and two radios. The iGate gates packets to and from RF; the SatGate only gates packets from RF to the internet. The modem has been tested under *Linux*, *Windows*, and *Android*.

The new modem is freely available along with a user manual under an open-source license.[18]

Sivan Toledo is Professor of Computer Science at Tel-Aviv University. He holds BSc and MSc degrees from Tel-Aviv University and a PhD from the Massachusetts Institute of Technology, where he was also Visiting Associate Professor in 2007-2009. He was licensed in 1982.

Notes

1 You can find more information and download this software at **www.baycom.org/~tom/ham/soundmodem/**.

2 James A. Mitrenga, N9ART, "An MX614 Packet Modem," *QST*, Jan 2000, pp 44-46.

3 Bob Ball, WB8WGA, "An Inexpensive Terminal Node Controller for Packet Radio," *QEX*, Mar/Apr 2005, pp 16-25.

4 See the Byonics website for more information about Byon Garrabrant's TinyTrak modems: **www.byonics.com**.

5 Scott Miller's OpenTracker series of modems are available from Argent Data Systems: **https://www.argentdata.com/**.

6 You can download Thomas Sailer's soundmodem software at: **www.baycom.org/~tom/ham/soundmodem/**.

7 Thomas Sailer's multimon modem software is available at: **www.baycom.org/~tom/ham/linux/multimon.html**.

8 You can find Georg Rossopoylos' AGWPE modem software at: **www.sv2agw.com/ham/agwpe.htm**.

9 Frank Perkins, WB5IPM. "DSP Programming using DirectSound and MFC/VC++," Proceedings of the 22nd ARRL and TAPR Digital Communications Conference, Hartford, Connecticut, September 2003, pp 140-149.

10 Andrei Kopanchuk's software modem is available for download at: **http://uz7.ho.ua**.

11 For more information about Pete Loveall's javAPRSSrvr software modem see: **groups.yahoo.com/group/javaprssrvr/**.

12 You can download *Audacity* for free at **audacity.sourceforge.net/**

13 For more information about Stephen Smith's test CD, see his website: **wa8lmf.net/TNCtest/index.htm**.

14 There is more information about Robert Marshall's microntroller-based modem on his website. **http://sites.google.com/site/ki4mcw/Home/arduino-tnc**.

15 For more information about Pete Loveall's software modem see: **http://groups.yahoo.com/group/javaprssrvr/**.

16 For more information about the APRSISCE APRS client program, see: **http://groups.yahoo.com/group/APRSISCE/**.

17 Georg Lucas has written an APRS client for Android smart phones: **http://aprsdroid.org/**.

18 You can download the software for the modem described in this article from my website: **https://github.com/sivantoledo**. The software version as of the publication date of this article is also available for download from the ARRL QEX files website. Go to **www.arrl.org/qexfiles** and look for the file **7x12_Toledo.zip**.

QEX

Dr. Christoph Kunze, DK6ED

Bildstrasse 44, 97903 Collenberg, Germany: **DK6ED@darc.de**

New Results on Shortening Beverage Antennas

You've wanted a better receive antenna for 80 m and maybe even 160 m, but just don't have the space. Perhaps you can have a Beverage antenna, after all.

How short can a Beverage antenna be? That question was raised by K9AY on the Internet recently. Using a coil is not as useful as it is with other antennas. So, I want to show a new way of building a more effective Beverage antenna.

Basics

A Beverage antenna is a highly directive receive antenna. It is mounted close to the ground, so the amount of noise picked up from the surroundings is reduced. You need a very long wire, however, normally 1 up to 2 λ. The one side of the wire is terminated by a resistor, and on the other end a transformer is used to match the receiver feed line. This antenna does not resonate, as it is a travelling wave antenna.

For modelling, the antenna is divided into a large number of small sections. First you look at a signal coming from the front or back of the antenna, as shown in Figure 1. If wave 1 reaches the front end of the antenna, its horizontal component will induce a current in this section. From that section, there will be a current along the wire to the transformer, and further to the receiver. If wave 2 reaches the opposite end, a current will also be induced, but this current is directed to the one end, terminated by the resistor. This resistor bypasses the signal to ground.

Of course a wave will not reach only one single segment of the antenna, it will induce currents on all the segments and all horizontal components will travel towards the specified end of the wire. On the wire there will be resistive influences and the current will also

[1]Notes appear on page 32.

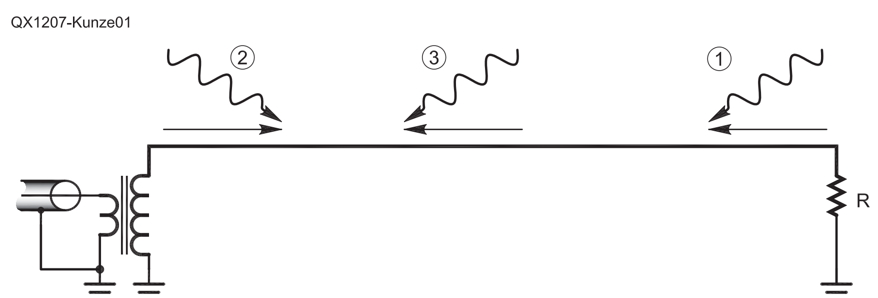

Figure 1 — This drawing illustrates a traditional Beverage antenna receiving signals from the front or back.

Table 1
Data Simulating a Conventional Design. Height = 3.5 ft

1 λ = 532 ft for 160 m

v = 0.97	*R (Ω)*	*1.85 MHz* Gain (dBi)	*F/B (dB)*	*3 dB Beamwidth (°)*	*Elevation (°)*	*3.65 MHz* Gain (dBi)	*F/B (dB)*	*3 dB Beamwidth (°)*	*Elevation (°)*
0.3 λ	200	– 18.5	4.2	127	62	– 10.7	6.5	93	41
0.4 λ	250	– 17.5	14.2	106	48	– 8.8	10.8	97	42
0.5 λ	250	– 15.1	13.5	93	40	– 7.6	14.6	82	35
0.75 λ	350	– 11.5	10.7	93	40	– 4.4	20.4	75	30
1 λ	270	– 9.3	15.5	79	33	– 2.2	16.3	57	27

Table 2
Data Simulating the New Design Versus a Conventional Design. Height = 3.5 ft

1 λ = 530 ft for 160 m

v = 0.97	*R (Ω)*	*1.85 MHz Gain (dBi)*	*F/B (dB)*	*3 dB Beamwidth (°)*	*Elevation (°)*	*3.65 MHz Gain (dBi)*	*F/B (dB)*	*3 dB Beamwidth (°)*	*Elevation (°)*
2 × 0.15 λ	45	– 21.1	9.9	92	42	– 15.8	9.6	87	33
0.5 λ	250	– 15.1	13.5	93	40	– 7.6	14.6	82	35
2 × 0.2 λ	45	– 18.0	11.0	87	35	– 13.4	15.9	75	30
0.75 λ	350	– 11.5	10.7	93	40	– 4.4	20.4	68	30

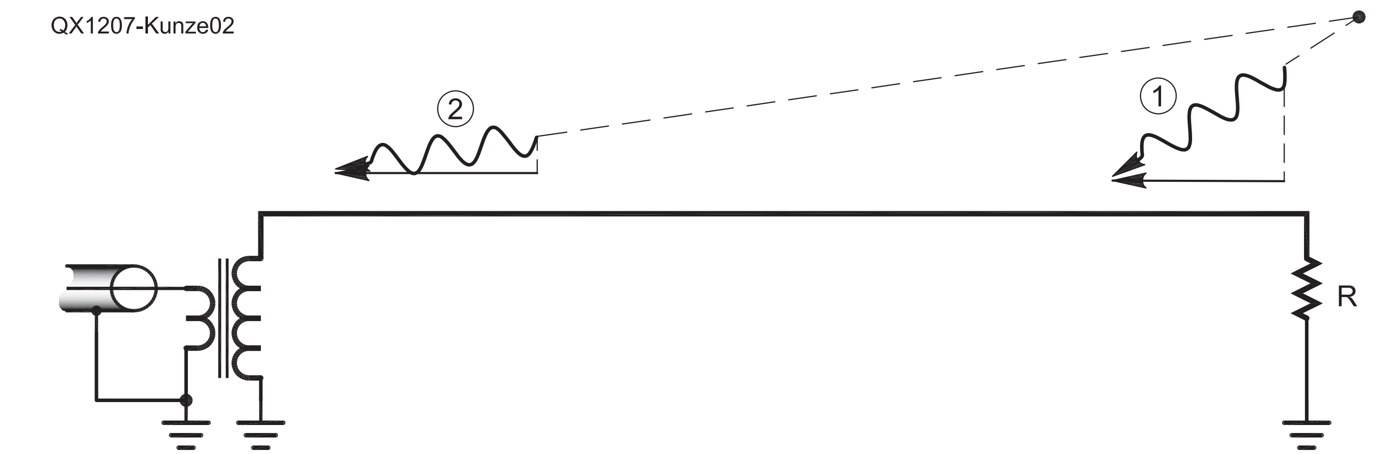

Figure 2 — This drawing illustrates a traditional Beverage antenna receiving signals coming in from the sides of the antenna.

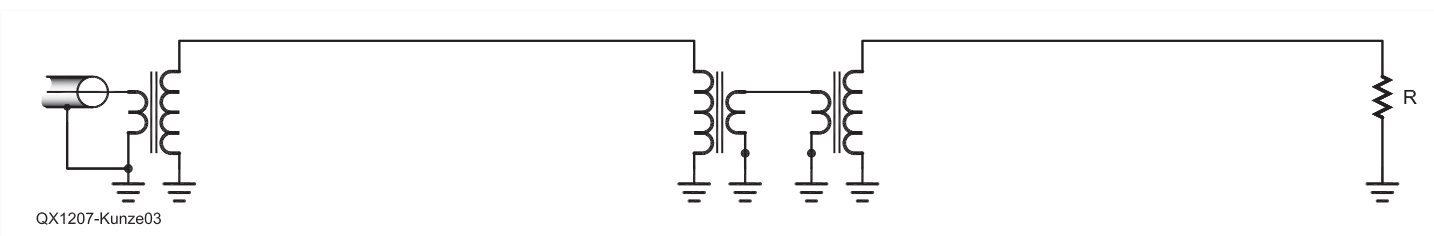

Figure 3 — Here we see the coupling two Beverage antennas to produce a bidirectional pattern.

be delayed. It means that the current induced by wave 1 will be reaching the transformer later than the one induced by wave 3.[1] If a signal is coming from the side of the antenna, as shown in Figure 2, it will induce a smaller current on the front end than at the receiver end. Also, the current from the front end is delayed when it is travelling along the wire. Because of this, the Beverage antenna becomes directive. The directivity increases as the wire gets longer. This is the reason why you should prefer a longer antenna. My experience modelling Beverage antennas with *EZNEC* shows that the system should be at least 0.4 λ long.[2] That is about 200 ft for 160 m. You should keep in mind that a 0.4 λ long antenna for top band is a 0.8 λ long antenna for 80 m, so the system improves quickly in directivity and front to back ratio. The resulting data is shown in Table 1.

Coupling Beverages

Now I did some experiments coupling two Beverage antennas in line, one behind the other, each having a length of 0.2 λ. See Figure 3. The results prove that it is possible to have two Beverages aligned this way. The *EZNEC* model results for one Beverage behind the other are shown in Figures 4 and 5. The data shows that you get the same results from this system as from a conventional Beverage of the same length. Of course the losses in the transformer are not simulated. Coupling is possible because the Beverage is a travelling wave antenna system.

Beverage Using a Phasing Line

Keep in mind the way a Beverage antenna works, and that a longer antenna creates a bigger signal and has more directivity by phase shifting. Why not create the same effect by arranging two smaller Beverages one behind the other, and coupling them by a coax line to get more phase shift? See Figure 6. Figure 7 shows the influence of the phasing line, comparing a conventional Beverage antenna with the newly designed one. In this case, we look at a wave coming sideways, inducing a lower current in the front end increasing step by step towards the receiver end of the system. That λ/8 piece of

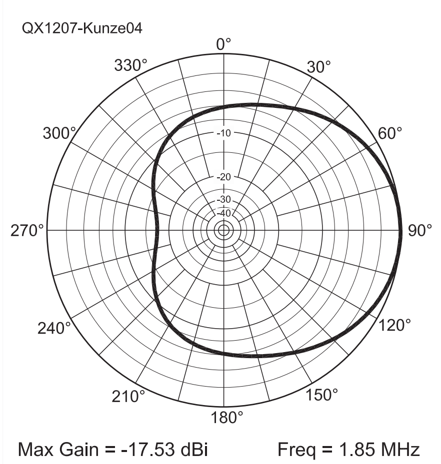

Figure 4 — Here is the horizontal (azimuthal) radiation pattern plot for two coupled Beverage antennas.

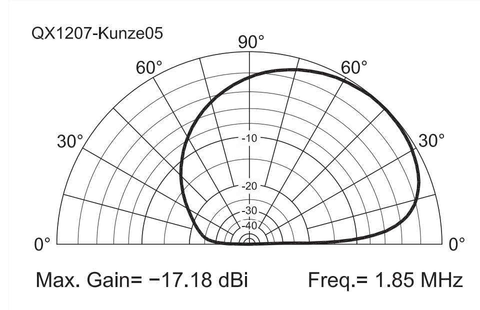

Figure 5 — This is the vertical radiation pattern plot for two coupled Beverage antennas.

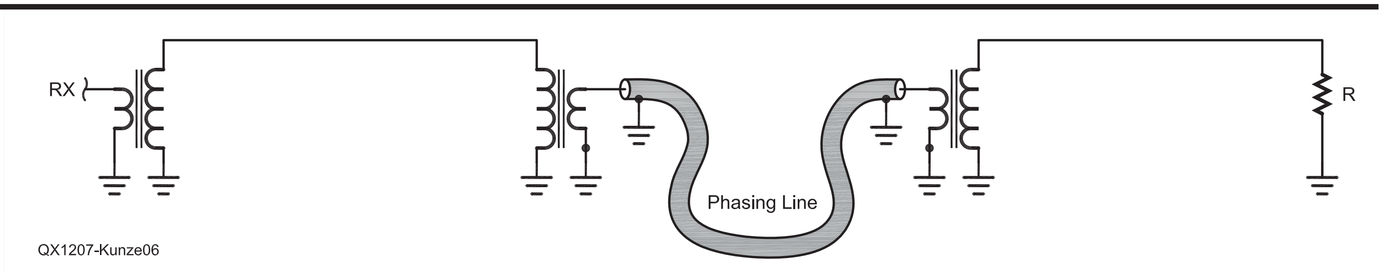

Figure 6 — In this drawing, two Beverage antennas are coupled through a phasing line.

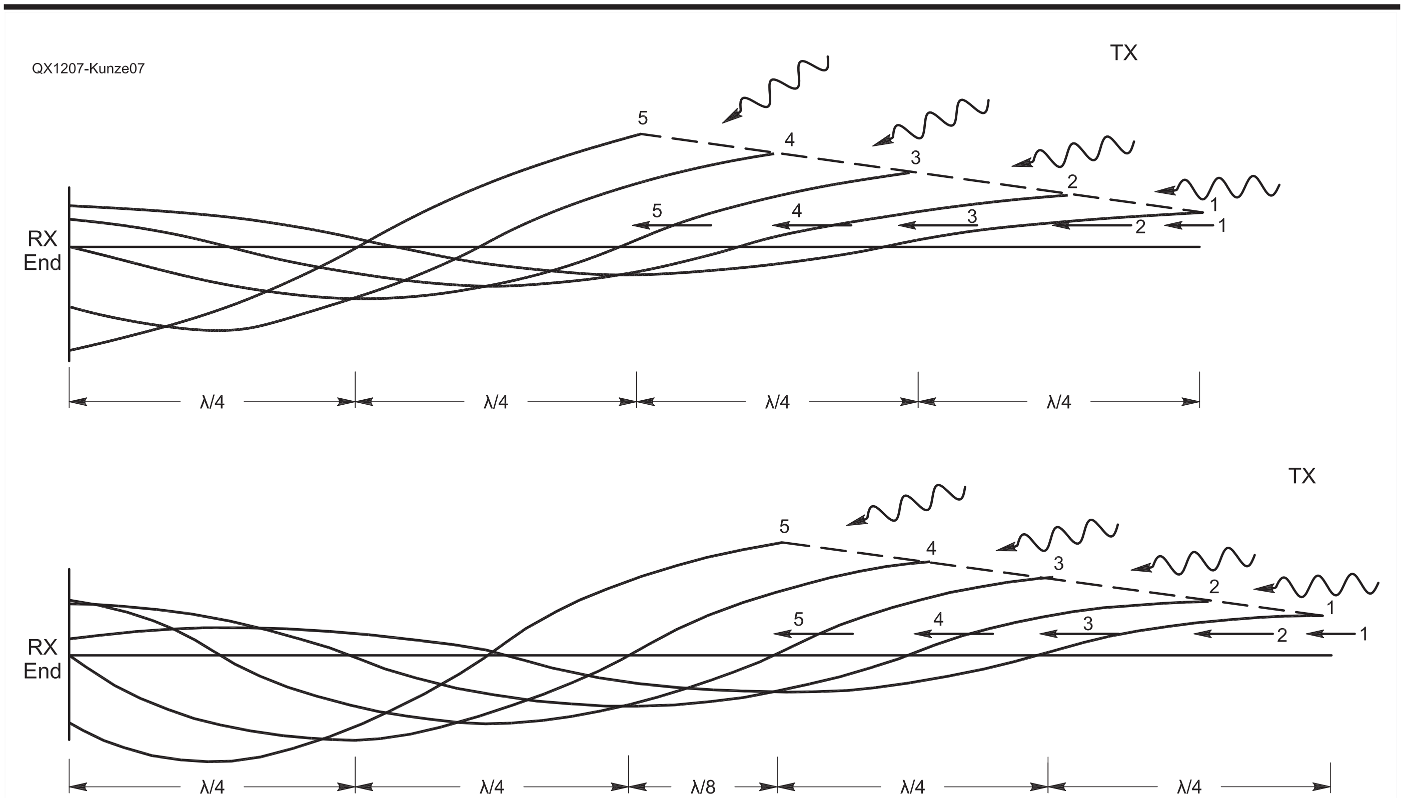

Figure 7 — Here we see the influence of a phasing line on the signals received from the sides by the coupled Beverage antennas.

coax line has a bigger influence on the directivity than would a longer antenna wire. On the one hand, it creates a phase shift, but on the other hand no more radiation is picked up, which would oppose directivity.

Changing Direction

A Beverage antenna like this will have good front to back ratio and good directivity, so you will need another antenna for the opposite direction. Jeffrey Parker, W1GJ, offers some good solutions in a paper he published on the Yankee Clipper Contest Club website, but he does not mention any data on directivity or front to back ratios.[3] Jeffrey cites *The Beverage Antenna Handbook* and *Low Band DXing* as sources for his design.[4, 5]

Since this new design is quite short, I decided to try another well known solution. You need a little more coax line, but you will have reliable results. See Figure 8. Switch 1A connects the receiver coax line to one end of the antenna. Switch 1B, selects the terminating resistor at the other end.

Additional Directions

So what about the other directions? Of course the best solution is to build another Beverage at a right angle to the first one, if you have the appropriate space. If that is not possible, you could make the following compromise.

A Beverage antenna not terminated by a resistor will lose its directivity, so you have all around reception. *The phasing line must be separated directly at the transformer, If you do it at the opposite end, the coax acts as a capacitor, bypassing the transformer and changing the radiation pattern. So, if you use the right side of the system for all around reception you need to open Switch 2B. For the left side, you open Switch 2A.* If both sides of Switch 2 are open, you will have reception from all directions. From my own experience reception is still better than what you get using your transmit antenna, with it being high in the air, picking up all kinds of noise from the surroundings.

Simulation by *EZNEC*

After proving that the idea of a phasing line works, it makes good sense to optimize its length and it is time to use *EZNEC* to simulate the antenna. I have to mention that these systems were simulated over real *MININEC* ground and there was not much done to simulate the radials. I just compared the different antennas with each other. This makes simulating quite easy and you can find the optimum performance for 160 and 80 m at the same time. I have tried two very short double Beverages (Figure 9) and compared their data to conventional Beverage antennas of double dimensions. The resulting data is shown in Table 2. The *EZNEC* plots for 1.85 and 3.65 MHz are shown in Figures 10 and 11 for the 2 × 0.15 λ antenna and in Figures 12 and 13 for the 2 × 0.2 λ system. So, the system almost compares to conventional Beverages of double length.

The plot and data of Figure 14 show the results of the second system with S2 in

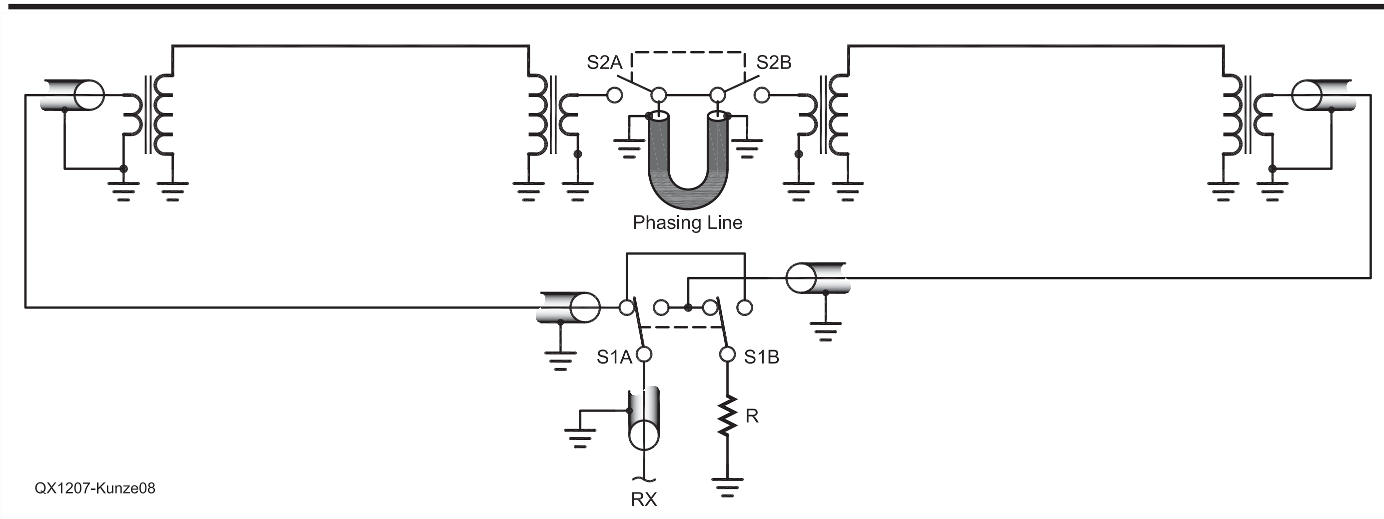

Figure 8 — This diagram shows how we can change the receive direction of a coupled Beverage antenna. Switch 1A connects either the left or right end of the antenna to the receiver and Switch 1B connects the opposite end to the terminating resistor. Switch 2 selects either the coupled Beverage or a single antenna for all-around reception. The selected single antenna depends upon which way S1A is set.

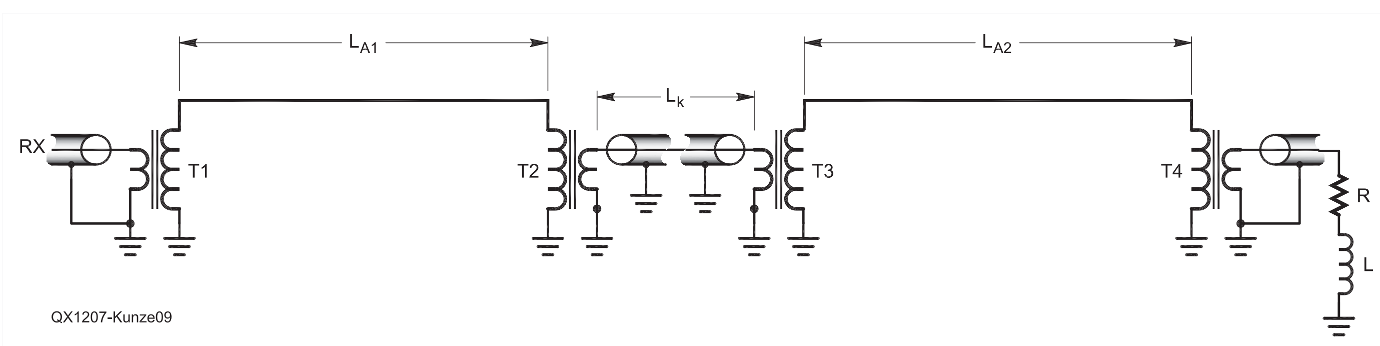

Figure 9 — This drawing illustrates how we can model the coupled Beverage antenna design to simulate the antenna in *EZNEC*.

Figure 8 being open for an all-round reception. *All systems are 3.5 ft above ground.*

Building the New Design

First you have to calculate the transformers. The impedances of the input and the output you can take from Table 3.

Minimum Inductance of the Transformer:

$$L = \frac{10\ Z}{2\pi f} \qquad \text{[Eq 1]}$$

where:
Z = maximum impedance (Ω)
L = minimum inductance (μH)
f = lowest frequency (MHz)

The equation looks unusual, but in this special case the inductance is doubled to minimize the influence of the transformer on the antenna system.

The transformers can be calculated as follows:

$$T = \sqrt{\frac{Z_1}{Z_2}} \qquad \text{[Eq 2]}$$

where:
T = transformation ratio
Z_1 = input impedance (Ω)
Z_2 = output impedance (Ω)

After choosing a ferrite toroid you can calculate the minimum number of turns for the side with the higher impedance. By applying the transformation ratio you then get the number of turns for the other side. All wires are twisted together.
Figure 15 shows the final circuit diagram. Depending on the length of the wires you can take the component values from Table 3. The Beverage is a directive antenna, so you will need a switching system. Since I still use the K9AY antenna control box, I decided on the following values:

North	East	South	West
AC	Ø	+	–

The level of the voltage is of course determined by the relays used.

For those using a transceiver without a separate receiver input I added a T/R switch, using the relay output from the transceiver, with the relay closed on transmit. If anything in the switch breaks, you might have full power output on your receive antenna, so there is some safety built-in. I use two antiparallel 1N4148 diodes in order to clamp the high power. (The diodes are connected in parallel, but the cathode ends are reversed.) If there is too much power flowing through the diodes the fuse will blow, protecting the diodes and the transformers of the antenna. In my experiences the diodes do not affect reception.

Since you can hardly see the antenna, you can just hide it even in a small garden. See Figure 16. You need three ground rods for the system, which can also be used to attach the cases for the electrical components, as Figure 17 shows. For the feed line, RG58 cable is sufficient, because the losses on the frequen-

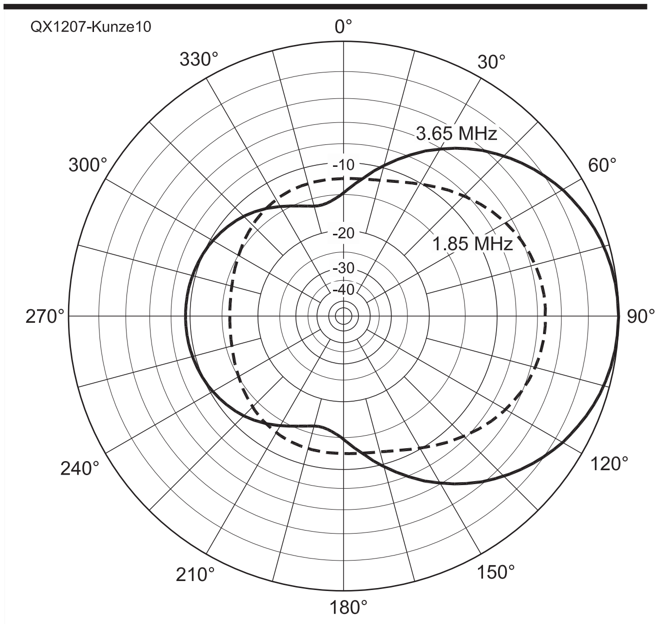

Figure 10 — The horizontal (azimuthal) plot of the new design with two coupled Beverages, each 77 feet long.

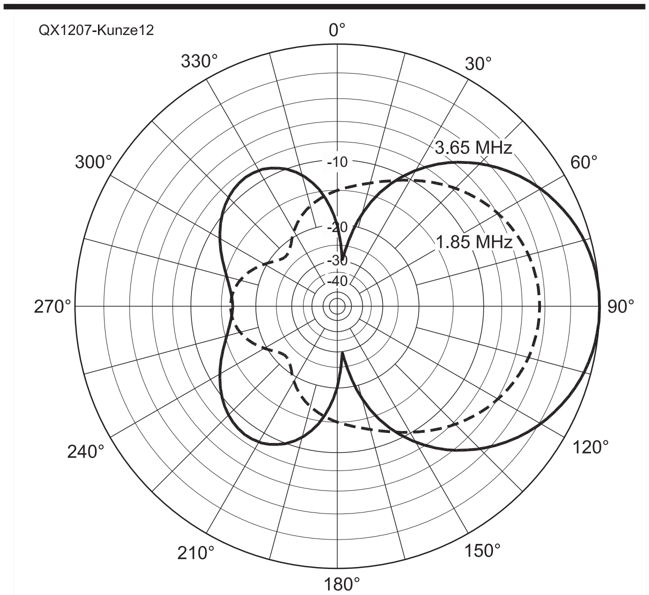

Figure 12 — Here is the horizontal plot of the new design with two coupled Beverages, each 105 feet long.

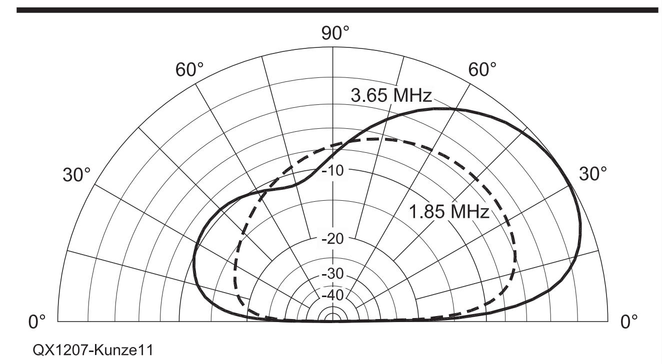

Figure 11 — The vertical radiation plot of the new design with two coupled Beverages, each 77 feet long.

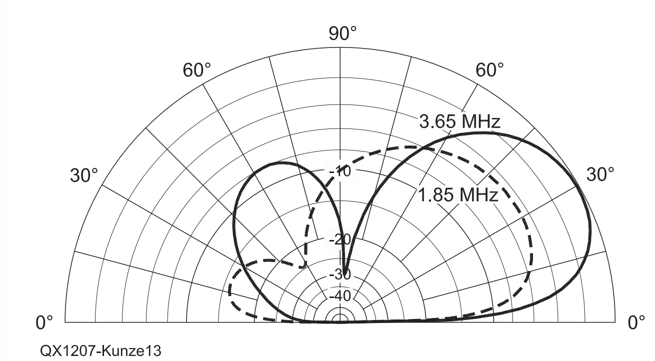

Figure 13 — The vertical plot of the new design with two coupled Beverages, each 105 feet long.

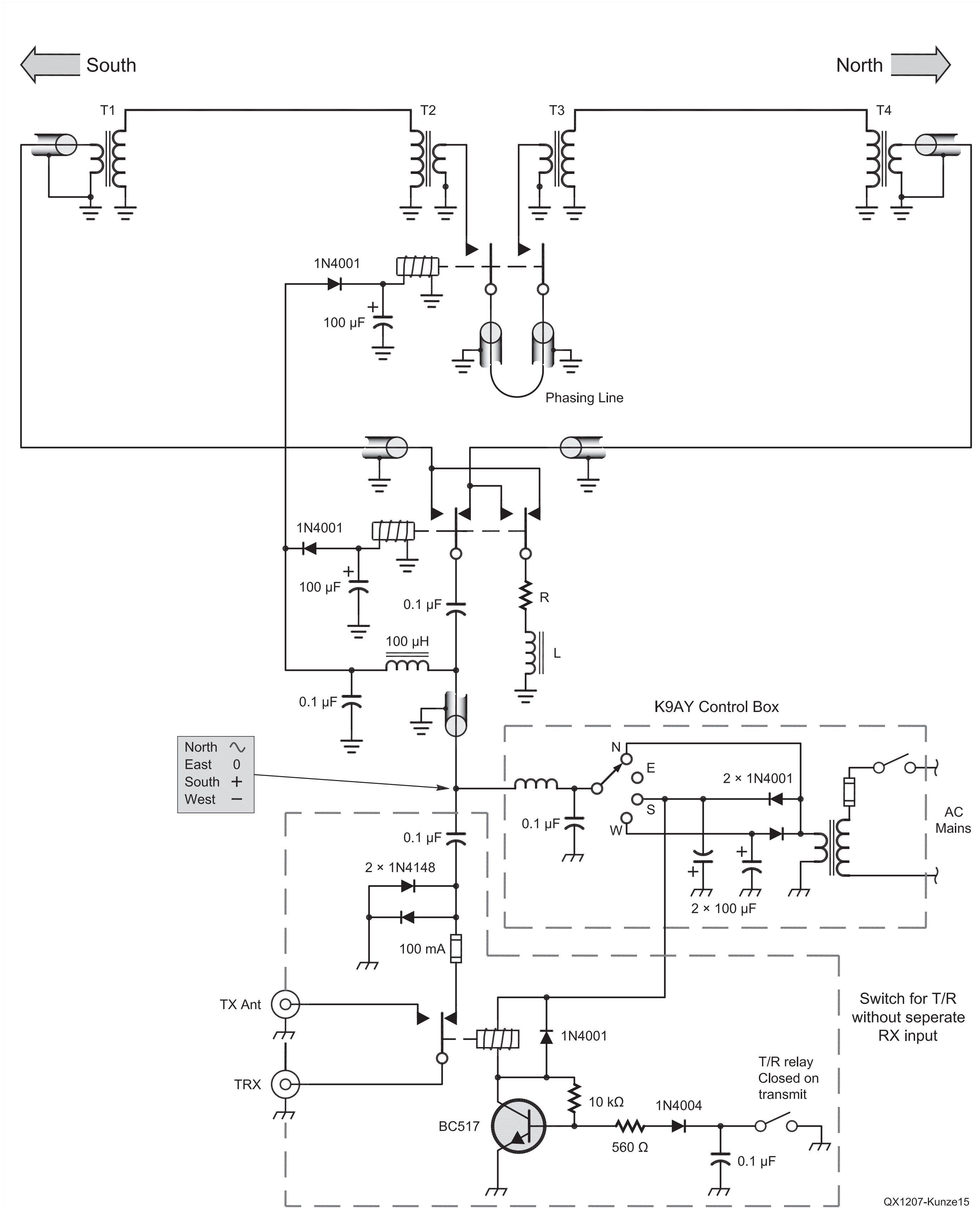

Figure 15 — This circuit diagram shows the complete coupled Beverage antenna system, including the K9AY switching control box.

Table 3
Values Of The Components

Antenna	*$L_{A1} = L_{A2}$ (ft) H = 3.5 ft*	*$T_1 = T_4$ (Ω)*	*$T_2 = T_3$ (Ω)*	*R (Ω)*	*L (μH)*	*L_k (ft) RG58*
2 × 0.15 λ	77	350/50	350/50	45	2.5	31
2 × 0.2 λ	105	350/80	350/50	45	0	26

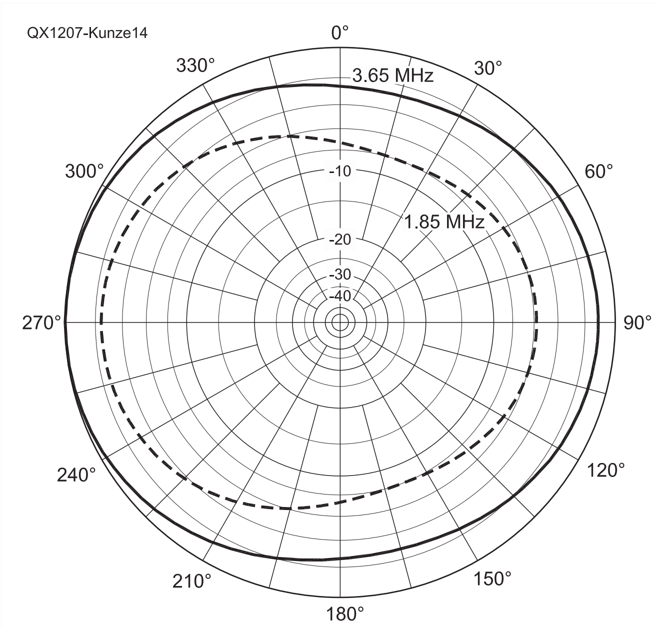

Figure 14 — The horizontal plot of the new design with two coupled Beverages, each 105 feet long, with S3 open.

Figure 16 — Beverage antennas are always mounted close to the ground. Here you can see one of the feed points of my antenna, which is installed along the fence of my garden.

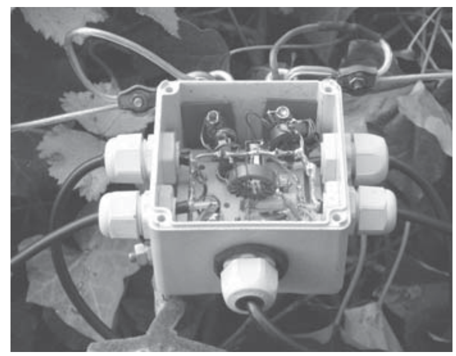

Figure 17 — This photo shows the control box of the new design, with the phasing lines and transformers.

cies used can be neglected. Make sure you use this type of cable because the velocity factor of other cables can be different and you have to recalculate at least the length of the phasing line.

Because the antenna is close to the ground it is highly directional, but of course the output is lower than what you get from a full size Beverage. You have to keep in mind that comparing a Beverage antenna to your transmit antenna, the noise level will be reduced so the output from the Beverage seems to be lower, but the DX-signal may even be stronger. If it is too low, you just use a Norton amplifier, as described by Todd Gale, VE7BPO, on the QRP/SWL Homebuilder website.[6]

Location of the Beverage

Locating the system is a major issue. Generally, the receive and the transmit antennas should be kept a major distance apart. In my experience, having a vertical and the Beverage at closer distance works out quite okay, but it does not work with a sloper or a dipole. These systems pick up the RF from the altitude and induce it into the receive antenna as they both run in parallel over a certain distance. My Beverage lost all directivity when the sloper was too close.

Results

When you have a good transmit antenna for the lower bands, you have to improve reception otherwise you lose a lot stations that are answering you. This implies not only DX stations, but also stations from shorter distances might be getting lost in the noise. A Beverage antenna is the best solution for this purpose, but not everybody has the space to erect one. In this article, I have shown a way to build a much shorter Beverage antenna; almost half the full size, while having the same front to back ratio and directivity. Of course signal strength is lower than what you can expect from a full size Beverage, but this only a minor problem. Now you can build a Beverage just having the dimensions of a half wave dipole. The results from the *EZNEC* simulation proved to be excellent and were matched by my experience on the bands. With this Beverage, I received the last new countries worked on 160 m.

Dr. Christoph Kunze, DK6ED, was born in 1956 and has been licensed since 1972. His Amateur Radio accomplishments include 5 Band DXCC in 1979 and DXCC Honor Roll Number 1 in 2002. He is a structural engineer with a doctorate in environmental engineering. Chris is Officer in Charge of a German municipal fire brigade, and is also busy in development aid.

Notes

[1]J. Litva, B.J. Rook, *Beverage Antennas for HF Communications*, direction finding and Over-The-Horizon Radars, p.2 ff, Department of Communications, Canada, 1976.

[2]Roy Lewallen, W7EL, *EZNEC* Demo, v.5.0.46, **www.eznec.com/demoinfo.htm**.

[3]Jeffrey Parker. W1GJ, Two Wire Beverage, **www.yccc.org/Articles/ka1gj_bev.htm**.

[4]Victor Misek, W1WCR, *The Beverage Antenna Handbook*, 1987, Misek Antenna Research, 1987, **http://exax.net/**.

[5]John Devoldere, ON4UN, *Antennas and Techniques for Low-Band DXing*, ARRL, 1994.

[6]Todd W. Gale, VE7BPO, "A Low Noise, High Dynamic Range Broadband RF Amp," *QRP/SWL Homebuilder*, RF Preamps, **www.qrp.pops.net/preamp.asp**.

QEX

Steve Whiteside, N2PON

RR 1 Box 138, Liberty, KS 67351; **stevewh2@cs.com**

A Linear Scale Milliohm Meter

There are many applications for an accurate, simple to use low-range ohm meter.

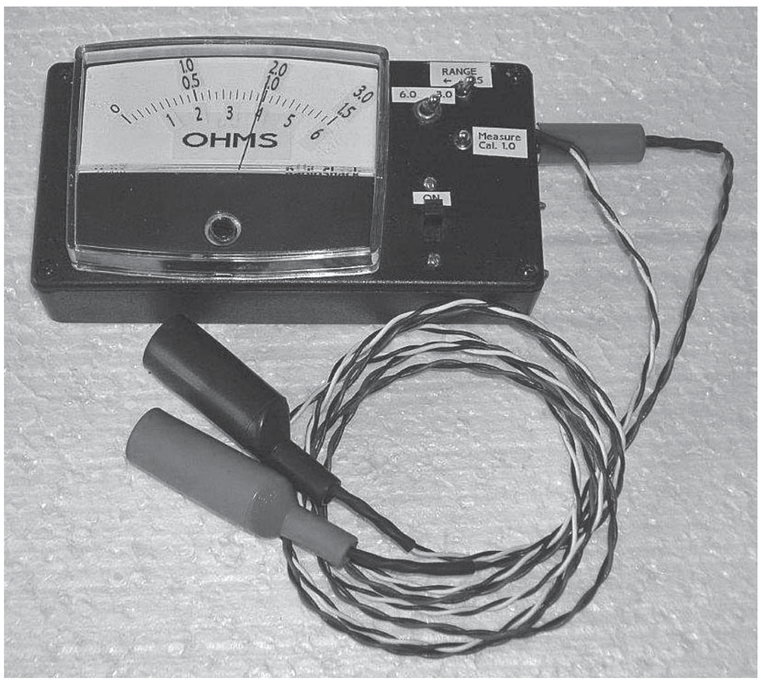

After encountering several bad connections at bolted ground cables on a friend's airplanes, I began to wish for a reasonable milliohm meter. The cables looked okay, but the bolts were not tight or the joints were corroded. Loose bolts on a Musketeer and a corroded joint on the master relay of a Mooney caused poor starting on both airplanes. A simple milliohm meter would have more quickly located these problems. My DVM does very well, but is a little uncertain below one ohm because of cable and connector resistances. Commercial milliohm/micro-ohm meters seem quite elaborate and too expensive for my occasional use.

RSGB's *Test Equipment for the Radio Amateur* by Henry Lou Gibson, G2BUP, includes an interesting adapter for VOMs to measure low ohms, but it uses a power rheostat.[1] Since those are now rare and expensive I decided to use a transistor current source instead.

I built two adaptors for my DVMs similar to the G2BUP approach. These used a 0.1 A test current. This results in a resistance of 5.00 Ω being indicated as 0.500 on the DVM. Months later, this proved confusing when I used the adaptor. Disconnecting the DVM leads to connect the adaptors also seemed undesirable.

What I really wanted was a dedicated milliohm meter all ready to go when I picked it up. Figure 1 is the circuit that I worked out, and that I find very useful. The circuit is a stabilized constant current source driving the unknown resistance. This gives a linear scale ohmmeter.

The circuit measures 0 to 1.5 Ω and 0 to 3.0 Ω using a RadioShack dc panel meter. The 0 to 15 V meter scale divisions are used as is, but are relabeled to indicate resistance. The smallest scale division is now 0.050 Ω on the 1.5 Ω range. This gives a clear indication of resistances even down to 0.010 Ω. (The meter needle is about 0.010 Ω wide on the 1.5 Ω range.) On the 3.0 Ω range, the smallest scale division is 0.100 Ω. With a ×5 range expansion switch, the meter will also read 0.300 and 0.600 Ω full scale. This makes the smallest scale divisions 0.010 and 0.020 Ω. One foot of no. 20 AWG wire has a resistance of 0.010 Ω and causes a one-division indication on the 0.300 Ω range.

The circuit has three unusual features. First, the infrared diode of a 4N25 photo coupler is used as a 1.1 V Zener diode in this 1.5 V circuit. Second, the phototransistor is also used to provide additional voltage compensation. This almost perfectly corrects for about 10% of the battery voltage decay. Third, a double-sided circuit board is used as a heat sink and as a thermal coupler between the 2N4401 and 2N4403 transistor collectors. The thermal coupling results in very rapid circuit warm-up with very little turn-on drift.

Earlier versions of this circuit exhibited a slow (10 second) warm-up drift of as much as two meter divisions. This made me distrust the calibration setting. After considerable unsuccessful work, I remembered that the TO-92 transistor die is usually attached to the collector lead. This means that the collector lead is likely the best thermal connection to the transistor. So I added a heat sink soldered directly to the collector lead. The improvement was dramatic. Warm-up drift was almost totally eliminated. On the 1.5 Ω range in the calibration mode, the meter moves almost instantly to the 1.0 Ω calibration setting and remains there. Figure 2 shows the circuit board material heat sink, which thermally connects the collectors of Q1, Q2, and Q3. The collectors are still electrically isolated.

I think you might find this collector heat sink idea useful in other circuits. In trying to build a stable 123.00 MHz oscillator, I noticed that it became a lot more stable when I added a "gimmick" capacitor. I did

[1]Notes appear on page 38.

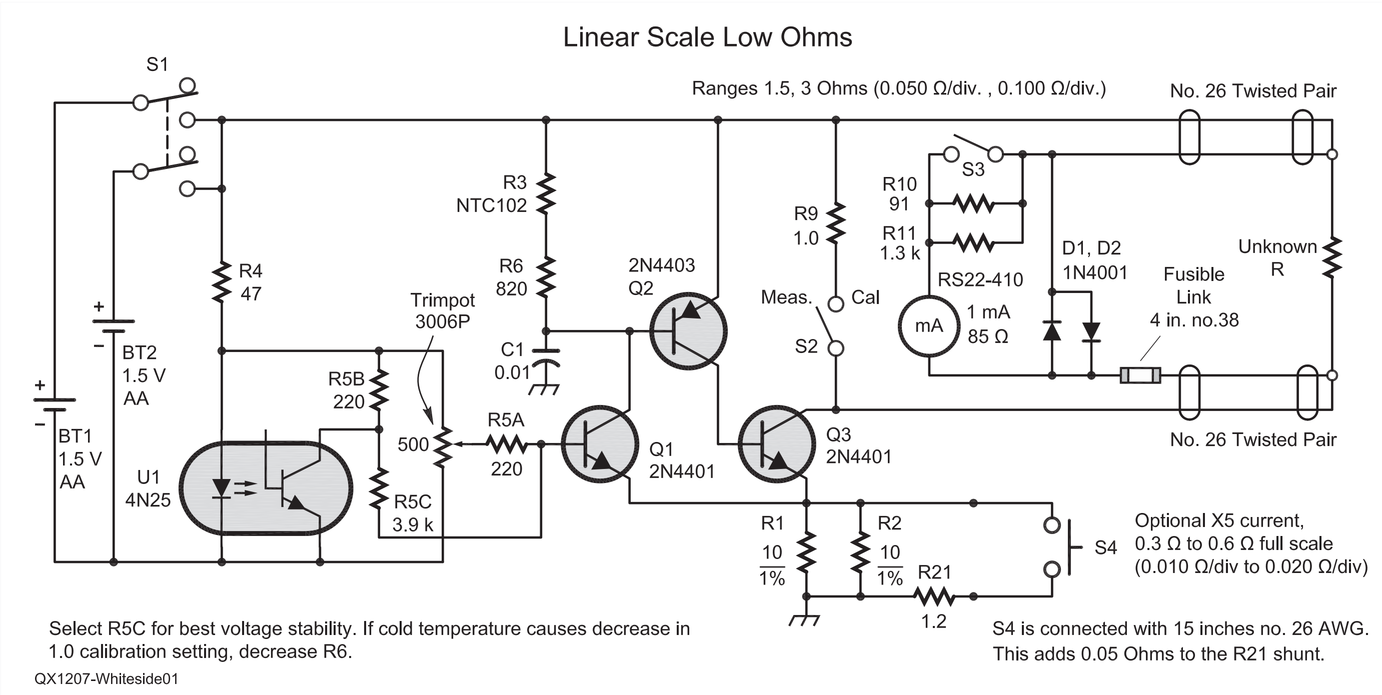

Figure 1 — This schematic diagram shows the final circuit that I built on the circuit board for a linear scale milliohm meter.

Battery	**1.5 V AA**	
Battery holder single AA		
C	**0.01 µF**	**Jameco 25507**
D1, D2	**1N4001**	**Jameco 35991 (1N4004)**
Fusible Link	**4 inches no. 38 AWG wire**	
Meter	**1 mA, 85 Ω**	**RS 22-410**
Or	**370 µA, 220 Ω**	**RS 22-036**
Q1, Q3	**2N4401**	**Jameco 38421**
Q2	**2N4403**	**Jameco 38447**
R1, R2	**10 Ω 1%**	
R3	**NTC102 Thermistor**	**Jameco 207483**
R4	**47 Ω**	
R5A, R5B	**220 Ω**	
R5C	**3.9 kΩ, selected for battery voltage stability**	
R6	**820 to 3.9 kΩ, selected for 65°F to 40°F stability**	
R9	**1.0 Ω**	
R10	**91 Ω**	
R11	**1.3 kΩ**	
R21	**1.2 Ω**	
SW1	**Power Switch**	**Jameco 2076210 DPDT slide switch**
SW2	**Cal/Meas. Toggle Switch**	**Jameco 75977 SubMini DPDT toggle**
SW3	**Range Toggle Switch**	**Jameco 75977**
SW4	**×5 range Momentary Switch**	**Jameco 154878 (Pins cut short and the smooth bushing is pressed into case hole.)**
Trimpot	**500 Ω**	**Jameco 41937, 3006P series**
U1	**4N25 Photo Coupler**	**Jameco 40985**
Case	**Eagle Plastics 400-1551-GR**	**Mouser 4.375 × 2.25 × 0.875 inches.**

5 feet no. 26 AWG twisted pair stranded wire.
2 solid copper alligator clips or RadioShack 270-356 2 inch Alligator Clips (5 amp)

not understand that at the time, but now think the increased stability came from the thermal heat sinking provided by the gimmick wire rather than thru the changed capacitance.

Highly accurate low ohms measurement really requires a four lead measurement. Two leads provide the test current and two more leads measure the voltage drop. This means four alligator clips must be attached to your part being measured or a special set of expensive probes is needed. The four connections eliminate the voltage drop in the current leads and the voltage drop at the connection points.

What I have found, however, is that the voltage drop at the connection is not so troublesome for measurements in the ranges provided by this meter. So I use a twisted pair for each test lead and just two alligator clips. The current source wire and voltage sense wire run separately until they are connected at the alligator clips. This seems to give me very solid measurements even with the no. 26 AWG twisted pair that I used for these wires. The lead photo shows my twisted pair test leads. The voltage drop in the current leads is eliminated from the measurement by running the two wires to each alligator clip. If the meter does indicate a higher than expected resistance, a wiggle of the alligator clips is enough to see if it will go lower. Of course, the lowest reading obtainable is the correct value.

On one unit, I made one probe interchangeable so that I can use a double-needle probe. This allows easier connection to large bolts. The needles are soldered on opposite sides of a strip of double sided circuit board material. A slight bend in the tips of the needles allows independent spring action for

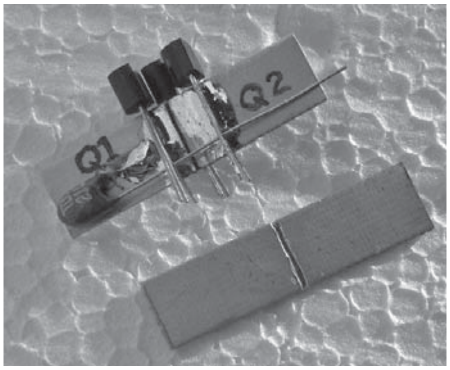

Figure 2 — This photo shows how I soldered the collector of the transistors to a piece of circuit board material for thermal stability.

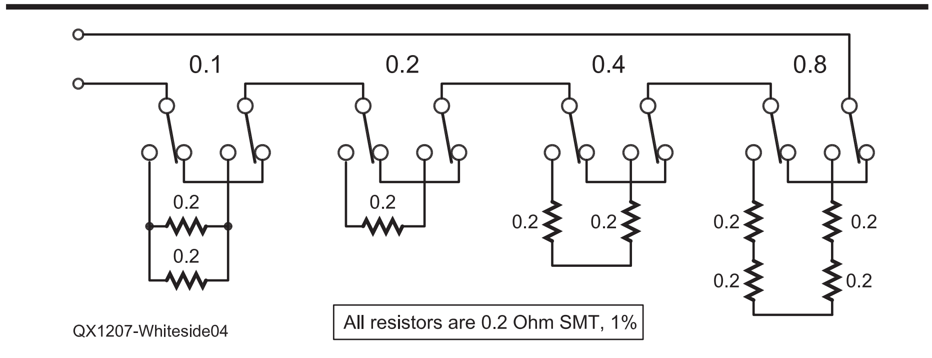

Figure 4 — This schematic diagram shows how you can wire series and parallel combinations of 0.2 Ω, 1% resistors to create a 0 to 1.5 Ω test fixture with 0.1 Ω steps. I used surface mount resistors for the one shown in the center of Figure 3.

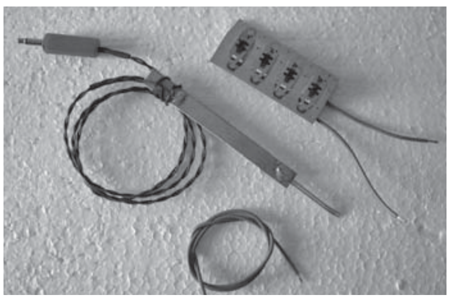

Figure 3 — This photo shows several test fixtures. At the center is the double needle test probe. The current source and voltage probe are on opposite sides of the double-sided circuit board material. Near the bottom of the photo there is a length of wire that can be used as a test resistance, to verify the operation of the meter. At the top right there is a test circuit that can be used to check the calibration of the meter. Switches select resistor combinations to provide steps of 0.1 Ω resistance values.

easier connection. You can see this probe in the center of Figure 3.

Two such double-needle probes would give you true 4-wire measurement, but I find the alligator clips much more convenient. It is best to use solid copper alligator clips, but if you use steel clips, you should extend the meter leads (VR and CR) down into the clips. Solder each between the teeth near the nose of the clip. This avoids the small (perhaps 0.004 Ω) resistance of the steel clips. The current supply lead can be soldered at the rear of the clip as is normally done. Steel clips connected in this way and clipped together move about one-half needle width (0.001 Ω) off of zero on the 0.300 Ω range. That is a very good zero.

In the top right corner of Figure 3 you can see a test fixture that I built from a piece of an old step attenuator. I used 0.2 Ω, 1% surface mount resistors in series and parallel combinations to produce 0.1 Ω steps from 0 to 1.5 Ω (see Figure 4). I use this fixture to verify the calibration of the meter. Also, at the bottom of Figure 3 there is a short length of wire that I use as a test resistor.

The RadioShack panel meter is about 85 Ω and needs 1 ma for a full scale deflection. Hence, the full scale (1.5 Ω) indication occurs with 85 mV across the tested resistance. To obtain a 0.085 V drop across 1.5 Ω requires a test current source of about 57 mA. Q3 supplies this constant current. The ×5 range expansion increases this current to about 285 mA. A single AA battery is adequate to supply the 57 mA load current, but Figure 1 shows the power switch wired to allow using two AA batteries in parallel to better handle the 285 mA load if you wish. My units are all built using just one AA cell.

The open circuit output voltage with the leads unconnected is about 0.76 V, and is determined by the 1N4001 meter protection diodes. The meter is very strongly pegged when the leads are not connected, but it seems to survive okay. To prevent this I usually turn the meter on with the Measure/Calibrate switch set to Calibrate, connect the leads to the test part and then switch to Measure. This avoids pegging the meter. The double-needle probe also eliminates pegging the meter.

I could not figure out a really good way to protect the meter. Fuses have too much resistance. So if you connect it to a live voltage source, it is likely to be damaged. I did add a series fusible link of 4 inches of no. 38 AWG wire. Wire tables show no. 38 wire will act as a fuse at 2.5 A, and this should provide some protection. Working with no. 38 wire is difficult. I think it is easiest to form a "U" from no. 22 bus wire, wrap and solder the no. 38 wire to the middle of each leg of the "U," solder the "U" into the circuit board and then cut off the loop of the "U." This leaves the two legs and the no. 38 wire attached to the circuit board.

R3 is a negative temperature coefficient (NTC) 102 thermistor (1 kΩ at 60°F). This is used with R6 to correct for ambient temperature changes. Adjust R6 so the meter reads 1.0 Ω in the calibrate mode at 65°F, and then put it into the refrigerator at 40°F for 20 minutes. Now it should give a turn-on reading of about 1.01 Ω. That is about 1 needle width of change. A smaller R6 value causes a more positive correction to the calibration setting with cold temperatures. So you can adjust the thermal change by adjusting R6. Without R3 and R6, the 40°F turn-on reading is about 0.94 Ω. The value of R6 will be affected by the betas of the transistors used. The overall current gain of the three transistors is about 5 million. Capacitor C1 is intended to eliminate RF pickup and circuit oscillation.

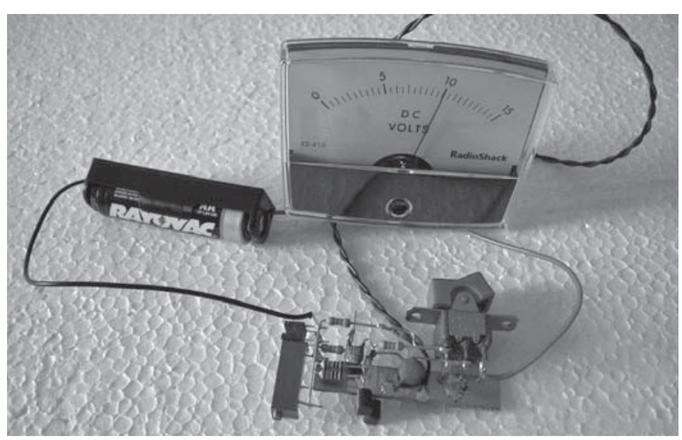

Figure 5 — Here is the point-to-point wiring of an early meter version.

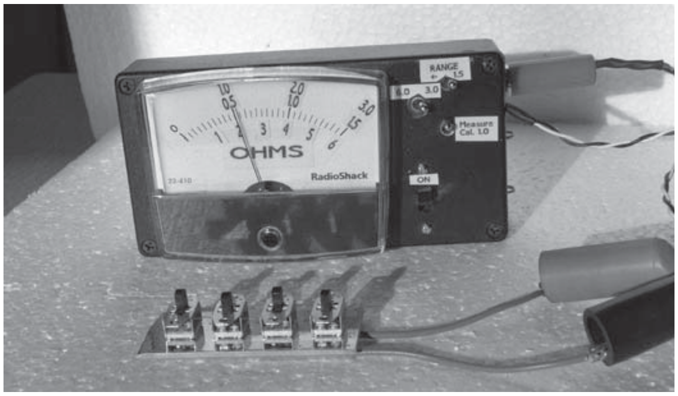

Figure 6 — In this photo the meter is being used to measure the resistance values selected by the switches.

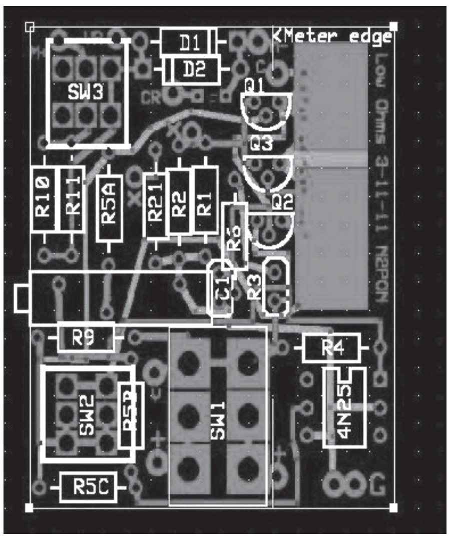

Figure 7 — The circuit board etching pattern created by using the *ExpressPCB* software.

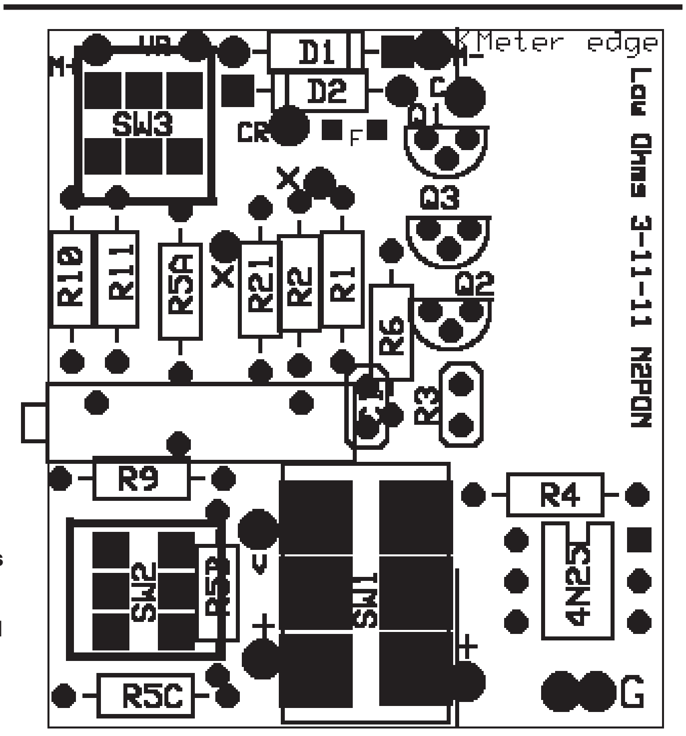

Figure 8 — This is the parts placement overlay created with the *ExpressPCB* software.

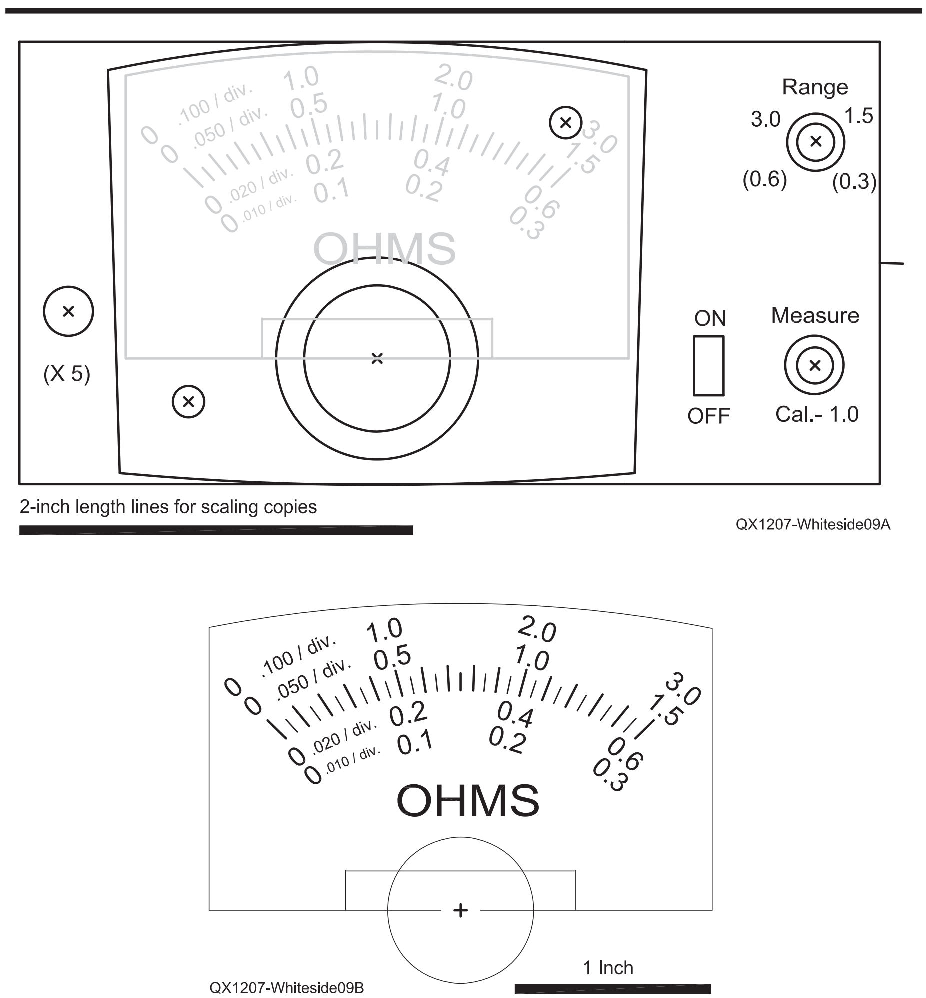

Figure 9 — This template gives a layout for the front of the box as well as a new meter scale for the meter, with direct readout in ohms.

As a test, I have carried one of these meters in my pickup for a year and turned it on to check the 1.0 calibrate reading with temperatures varying from 20°F to 100°F. The calibrate reading varied less than 1%.

I also wound about a foot of no. 30 AWG magnet wire around a 1 kΩ resistor and soldered it to the resistor leads. This gave me a 0.1 Ω test resistor so I can readily verify that the meter is reading correctly. The leads of this resistor poke out one end of the case so I can clip the leads to it when desired. This is especially important if I have accidentally abused the meter. On later units I used a 0.200 Ω, 1% current sensing resistor as a test resistor.

I wired the original circuit using point-to-point wiring, as shown in Figure 5. Later I installed the meter and switches into the lid of an Eagle 400-1551-GR plastic box. You might want to use a slightly larger box, because the meter just barely fits this one, and there is only room for one AA battery. I also had to cut the plastic nib off the back of the meter and bend the terminals down flat to fit this shallow box. It is convenient to position the trim pot so that it is available for adjustment with the box closed. Cutting small notches in the edge of the box bottom provides wire exits and some strain relief for the twisted pair leads. Figure 6 shows a finished meter, along with the 0 to 1.5 Ω test fixture.

As the battery voltage drops with age and use, the meter calibration will change. The 4N25 photo coupler helps to stabilize that variation. Since decreasing battery voltage reduces the LED current, this will also reduce the photo transistor current. Hence, the 4N25 collector voltage will increase and resistor R5C feeds this into the current source to achieve near perfect correction. To test this, I temporarily added a 3 Ω resistor in series with the battery. This gave a voltage change from 1.57 to 1.40 V at the circuit. Then I adjusted R5C until the meter did not change when I shorted and unshorted the 3 Ω resistor. You could also test this by using a new and an old battery. I have not tested this correction circuit over a wide range of voltages but it seems to do very well here. The current transfer ratio (I_C / I_{LED}) of the 4N25 will affect the optimum value of R5C.

Additionally, I did some testing of a 0.300 Ω full scale circuit. This gives a smallest meter scale division of 0.010 Ω. Hence, a 1 foot length of no. 20 wire now shows a full meter division above zero, where it showed only a single needle width above zero on the 1.5 Ω range. Some extra pads are placed on the circuit board to allow adding a shunt 1.25 Ω resistor (R21) to the existing 5.0 Ω Q3 emitter resistance (R1 and R2 in parallel) if you wish to include this ×5 range. Connecting these with a momentary switch increases the current source to about 285 mA, and gives the 0.3/0.6 Ω full scale ranges It is doubtful that the thermal corrections will be accurate with this big change from the 57 mA to 285 mA current source. That is the reason I decided a momentary switch would work best for me.

You will need a good quality switch to achieve stable readings. The usual mini push button switches seem to give a varying resistance connection over time. I used a 1.2 Ω resistor for the shunt (R21). Using 15 inches of no. 26 wire to connect the ×5 momentary range switch adds 0.05 Ω for a total of 1.25 Ω. This wire length is trimmed to calibrate the 0.3 Ω range, although on one unit I had to add a 12 Ω resistor in parallel with the 1.2 Ω component. This all seems to work very well.

Marissa Blevins, the daughter of a coworker, expressed interest in things engineering, so I helped her create a circuit board layout for the meter using the excellent *ExpressPCB* free software.[2] She seemed to really enjoy learning about this process. The circuit board layout is shown in Figure 7, with the parts placement diagram in Figure 8. Figure 9 is a template for a front panel layout with switch labels and a new meter face. The ExpressPCB circuit board files and a file for the panel template are available for download from the ARRL *QEX* files website.[3] You will likely have to adjust the size of your printout of that file, so 2 inch scaling lines are included. The switches fit the box I used. I attached the new meter face over the existing one with double-sided tape. I also attached the switch labels to the box with double sided tape. Clear shipping tape over them adds durability. Figure 10 shows the completed milliohm meter.

Only the resistors, diodes, capacitor, and thermistor are mounted on the top of the board and the switches, 4N25, transistors, and trim pot are all mounted on the bottom of the board. The resistor side has two heat sink pads, while the switch side has only one (larger) heat sink pad.

Using the Meter

This simple meter is very stable and works well. The analog indication is very useful in exploring varying connections such as a partially broken wire. It is difficult to see those variations with a digital meter.

Normally I use the 1.5 Ω range, and if it shows a very small value of resistance, then I push the button for a few seconds to expand to the 0.3 Ω range for a more accurate reading. This conserves the battery and the single AA I use works okay this way.

Many switches list maximum resistances of about 20 mΩ, and you can clearly see this on the meter. Often they will show about 0.010 Ω on first use, and then the wiping action cleans them to a near zero resistance. Bad switches usually show erratic resistances when operated, and don't improve with operation.

Also, bad test leads or coaxial cables are clearly indicated by this meter. You can test those partially corroded circuit board traces for integrity. Air conditioning Freon compressor windings often have a resistance of 0.6 to 1.5 Ω, which is easily readable on this meter. This low dc resistance is used by service technicians to help determine the condition of the compressor windings.

The gauge of copper wire can easily be estimated if you remember that no. 10 AWG wire has 0.001 Ω/ft. Also, if you change by 3 gauge sizes, the resistance is doubled or halved. Hence, each gauge shows a resistance change of 1.26, the cube root of 2. Additionally, you might remember that changing 10 gauges gives a factor of 10 in resistance change. So no. 20 AWG wire has a resistance of 0.010 Ω/ft and no. 30 AWG wire has a resistance of 0.103 Ω/ft. These values are specified at 68°F (20°C) and increase with higher temperature, but that

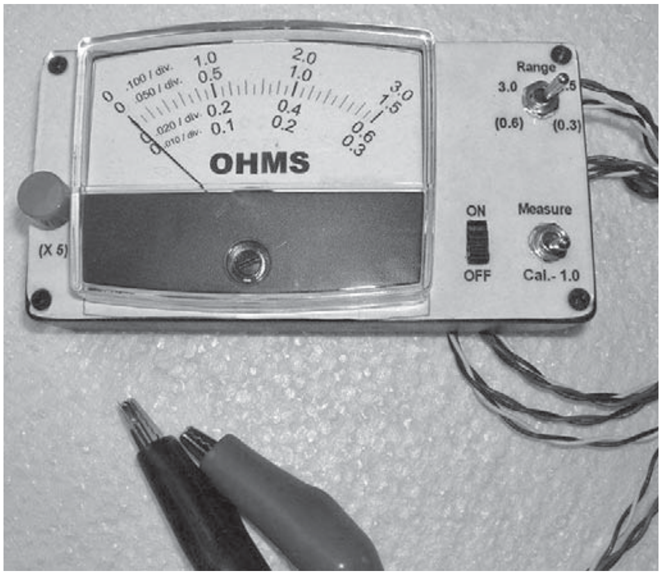

Figure 10 — This meter uses the circuit board and the front cover template. The new meter scale is attached using double sided tape.

RadioShack Meters

RadioShack seems to have discontinued the 22-410 15 V dc Panel meter that I used in this and other projects. They have a 22-036 15 V dc Panel meter that has the same face, but is much larger in the rear section. Also the 22-036 meter has the scaling resistors built inside.

It is a simple matter to convert the 22-036 meter for this project, however. Simply take a hot knife and cut off the top half of the rear 1.77 inch diameter cover. This exposes the meter connections and makes the meter movement available for use. Just unsolder or cut off the scaling resistors and discard the cutoff plastic part as well. Now solder wires for the meter, and cover the exposed section with tape to keep dirt out.

The meter movement in this new unit is 370 μA full scale and 220 Ω resistance. The full scale voltage is 370 μA × 220 Ω = 0.081 V. This full scale voltage is almost the same as the 22-410 meter (0.085 V). The calibration adjustment will easily handle that.

Figure A1 shows the part cut off of the 22-036 meter, a 22-036 meter with the rear cut made and a 22-410 meter along with the hot knife I used. The hot knife is from the craft section of Walmart. You could use a saw but it will create a lot of debris to clean out of the meter.

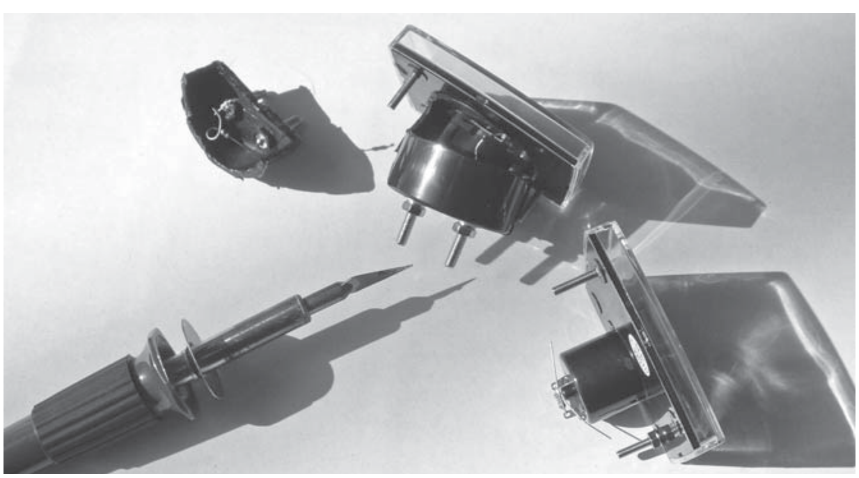

Figure A1 — Here, two of the newer RadioShack 22-036 15 V dc panel meters are being prepared for use in milliohm meters. The hot knife is used to cut part of the plastic dome that covers the back of the meter, to provide access to the meter connections.

temperature change is only about 0.4% per degree Celsius.

Of course, these values do not seem to apply to Chinese wire. My "super 6 gauge" jumper cables were made in China and actually measure to be no. 11 AWG. Do you suppose almost half of the copper just evaporated during the long boat trip to get to the US? See the Technical Correspondence from Mal Eiselman, NC4L, in the March, 2011 issue of *QST* for similar information.

This meter is also useful in timing the magneto on a small engine. The points-closed reading from the "P" lead is usually 0.05 to 0.1 Ω. When the points are open, the reading is about 0.4 to 0.6 Ω. This change is clearly visible on the 1.5 Ω scale. Bad contact points in the magneto are also readily seen.

This milliohm meter proved very useful recently when the starter on my pickup refused to pull in. The starter solenoid proved to be the culprit. It is made with two coils. One coil is a pull-in coil and it measured 0.15 Ω. The other is a hold-in coil and it measured 0.65 Ω. Tapping on the solenoid produced erratic changes in the pull-in coil resistance. More tapping led to one terminal, and unsoldering that showed a broken coil end about ⅛ inch from the soldered terminal. I was able to solder on an extension wire to the existing coil end and rescue the solenoid. Now it measures 0.12 Ω and exhibits no change with vibration. It is really neat to be able to clearly see such small changes in resistance.

The brushes in my 7¼ inch Skilsaw recently burned out. I ordered replacements from **www.ereplacement.com**. They quickly burned out as well. So I measured from segment to segment of the commutator using this milliohm meter. The typical measurement was 0.1 Ω, but one segment showed about 1.2 Ω. The folded-over heat-staked commutator tab was not well connected to the armature wire. Cleaning and soldering repaired that. A good solder to use for that is 95-5, because it has a higher melting temperature. I think the saw will be okay now.

Steve Whiteside, N2PON, holds a Technician class license and is an ARRL member. He is a retired EE, pilot, and aircraft owner. His primary interests are RDF antenna design, RF measurements and aircraft.

Notes

[1]Henry Lou Gibson, G2BUP, *Test Equipment for the Radio Amateur,* RSGB, 2nd Edition, 1978.

[2]The *ExpressPCB* software is available for free download from **www.expresspcb.com**.

[3]The *ExpressPCB* circuit board files, the front panel template and revised meter scale template are available for download from the ARRL *QEX* files website. Go to **www.arrl.org/qexfiles** and look for the file **Whiteside_7x12.zip**.

Upcoming Conferences

46th Annual Central States VHF Society Conference

July 26 – 28, 2012
Clarion Hotel and Convention Center
525 33rd Avenue, SW
Cedar Rapids, IA, 52404

The Central States VHF Society, Inc (CSVHFS) invites you to attend the 46th annual conference in Cedar Rapids, IA, July 26 - 28, 2012. The Planning Committee has a fun-filled, educational event in store for you! The on-line registration form is now active. For more details, visit the Society website at **www.csvhfs.org**.

The 31st Annual ARRL and TAPR Digital Communications Conference

September 21 – 23, 2012
Sheraton Gateway Hotel Atlanta Airport
1900 Sullivan Road
Atlanta, Georgia 30337
www.sheraton.com/atlantaairport

Mark your calendar now and make plans to attend the premier technical conference of the year, the 31st Annual ARRL and TAPR Digital Communications Conference to be held September 21 - 23, 2012, in Atlanta, GA. The conference location is the Sheraton Gateway Hotel Atlanta Airport, Atlanta, GA. To book your room, use the link on the TAPR website under Conferences (**www.tapr.org/dcc.htm**) or call the hotel directly (Reservations: 1-800-325-3535) and mention the group code “ARRL and TAPR Digital Communications Conference” when making reservations. Be sure to book your rooms early!

This is a three-Day Conference (Friday, Saturday, Sunday). Technical sessions will be presented all day Friday and Saturday. In addition there will be introductory sessions on various topics on Saturday. Join others at the conference for a Friday evening social get together. A Saturday evening banquet features an invited speaker and concludes with award presentations and prize drawings. The ever-popular Sunday Seminar will feature Tom Rondeau, N1YXZ, teaching “How to Use GNU Radio, Quick and Easy.” This is an in-depth four-hour presentation, where attendees learn from the experts.

Microwave Update 2012

October 18 – 21, 2012
Biltmore Hotel Santa Clara
2151 Laurelwood Road
Santa Clara, California 95054

Microwave Update (MUD) is an annual event held since 1985. The 50 MHz and Up Group of Northern California is pleased to host the 2012 event. MUD is a conference dedicated to microwave equipment design, construction, and operation. It is focused on, but not limited to, amateur radio on the microwave bands. There are technical presentations all day Friday and Saturday, with an antenna measurement range and outdoor flea market Sunday morning.

Call for Papers

The Microwave Update 2012 program committee is soliciting papers and presentations on the technical and operational aspects of microwave Amateur Radio communications or related subjects. Papers will be published in the conference proceedings (print and CD). Many will also be selected for presentation at the conference. The deadline for paper submissions is August 18, 2012, but please contact the technical program chair with your ideas now. Detailed formatting information for authors (margins, photos, other files) is provided on the conference website at **http://microwaveupdate.org.**

2012 AMSAT Space Symposium and Annual Meeting

October 26 – 28, 2012
Holiday Inn Orlando-International Airport
5750 T. G. Lee Blvd,
Orlando, FL 32822
1-407-851-6400

AMSAT announces the 2012 AMSAT Space Symposium will be held on Friday, October 26th through Sunday, October 28th, 2012.

Call for Papers

Proposals for papers, symposium presentations and poster presentations are invited on any topic of interest to the amateur satellite community. See the AMSAT website for more details: www.amsat.org.

Send a tentative title of your presentation as soon as possible, with final copy to be submitted by October 1 for inclusion in the printed proceedings. Abstracts and papers should be sent to Dan Schultz, N8FGV, at **n8fgv@amsat.org**.

A Monday trip to Kennedy Space Center is planned. Please call or e-mail Office Manager, Martha Saragovitz (martha@amsat.org) and let her know if you are interested.

Reunion

Jim George, N3BB

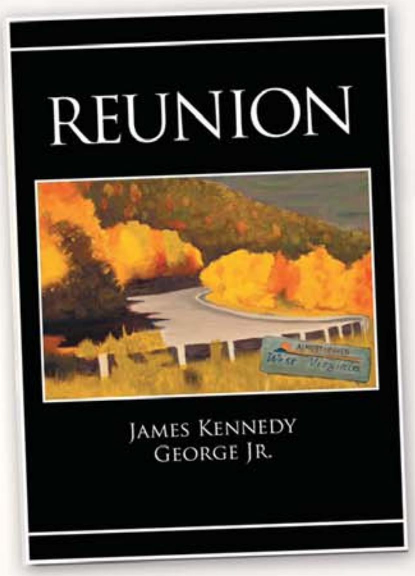

About the Book

Reunion begins and ends with the 45th reunion of the 1960 class of Princeton, West Virginia, high school. Set in a small town on the southern edge of the state, it deals with usual themes of coming-of-age and high school, as well as the once-in-a-lifetime experience of desegregation and its impact on a group of friends. In addition, the debut novel, written in the first person in an engaging style, probes the relationship, or lack of it, between an emotionally-distant father and his son, who much later in life begins to understand what it means to grow up as the adult child of an alcoholic.

The characters are rich and varied, with the very essence of Americana: high school, football, and social interactions on multiple levels; the music of the 50's; the thrill of short-wave ham radio; a unique peer group, including an emerging high school rock band; and of course the family of origin, a complex mix of stately Virginians and more informal Kentuckians.

* **Generations of radio amateurs will relate to how the sights and sounds that Jimmy encounters on his first visit to a ham radio station set him on a path out of his small town and into a career.**

– David Sumner, K1ZZ Chief Executive Officer American Radio Relay League

* **We all have reflected on our own lives, but how many of us could remember them as vividly and could express ourselves so eloquently? This is a wonderful book, written with great sensitivity, and is deserving of a very wide readership.**

– William F. Stephenson, Dean Emeritus, College of Engineering, Virginia Tech

* **Jim George's *Reunion* is a beautifully written story of innocence, loss, and reconciliation. George's finely crafted prose and compelling voice make this debut novel a memorable read.**

– Diane Umstead, Author, The Wisdom Tree: A Mother's Journey Into Israel and the Palestinian Territories

* ***Reunion* is a deeply personal journey of discovery. It lays bare the angst and confusion of coming-of-age on the edges of America's moral awakening to civil rights. There are familiar themes of hot rods, heart throbs, and early rock and roll—and darkness as well, of family secrets and silent suffering. *Reunion* may inspire you to do just that, to reunite with family, friends, or even a buried past.**

– Stewart Vanderwilt, Director & General Manager, KUT FM, Austin, Texas

***

Reunion is available worldwide in Hardcover, Softcover, and eBook from all Internet retailers and any independent book store.

Create Your Own Microprocessor Devices!

ARRL's PIC Programming For Beginners

Revised First Edition. Now for use with ARRL's PIC Programming Kit.
(book and kit sold separately)

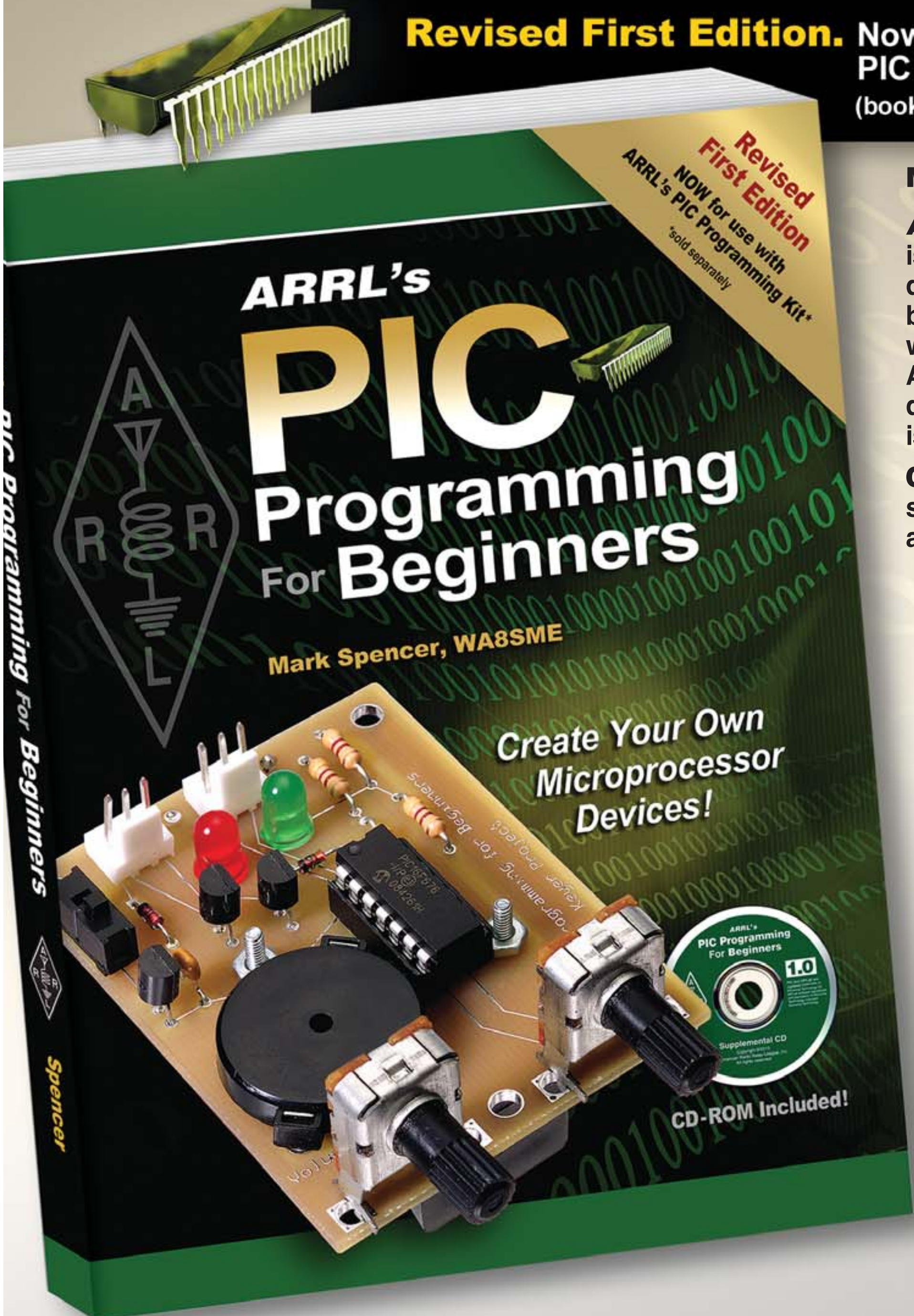

Mark Spencer, WA8SME

ARRL's PIC Programming for Beginners is an introductory guide to understanding PIC® design and development. Written in a building block approach, this book provides readers with a strong foundation on the subject. As you explore the potential of these powerful devices, you'll find that working with PICs is easy, educational and most importantly fun.

CD-ROM included with programming resources, supplementary reading, short video clips and other helpful data.

Contents:

- Inside the PIC16F676
- Software and Hardware Setup
- Program Architecture
- Program Development
- Working With Registers —The Most Important Chapter
- Instruction Set Overview
- Device Setup
- Delay Subroutines
- Basic Input/Output
- Analog to Digital Converters
- Comparators
- Interrupts
- Timer 0 and Timer 1 Resources
- Asynchronous Serial Communications
- Serial Peripheral Interface Communications
- Working With Data
- Putting It All Together

…and more!

ARRL The national association for AMATEUR RADIO®
225 Main Street, Newington, CT 06111-1494 USA
SHOP DIRECT *or call for a dealer near you.*
ONLINE WWW.ARRL.ORG/SHOP
ORDER TOLL-FREE 888/277-5289 (US)

ARRL's PIC Programming Book	ARRL's PIC Programming Kit
ARRL Order No. 0892 **Special ARRL Member Price!** **Only $39.95*** (regular $44.95)	ARRL Order No. 0030 **Build the Kit Yourself!** **Only $149.95***

*Plus shipping and handling. Book and Kit sold separately.